Nonlinear First Ply and Progressive Failure of Laminated Composite Skewed Plates and Shells

Thesis Submitted

by

Dona Chatterjee

Doctor of Philosophy

(Engineering)

Civil Engineering Department
Faculty Council of Engineering & Technology
Jadavpur University
Kolkata, India
June 2024

INDEX NO. 139/19/E of 2019

1. **Title of the Thesis:** Nonlinear first ply and progressive failure of laminated composite skewed plates and shells.

2. **Name, Designation & Institution of the Supervisor/s:** Dr. Dipankar Chakravorty, Professor, Jadavpur University, Kolkata. Dr. Arghya Ghosh, Assistant Professor, Netaji Subhas University of Technology, New Delhi.

3. **List of Publication**:

International Journal Publications:

a) D. Chatterjee, A. Ghosh, D. Chakravorty, Nonlinear First Ply Failure Study of Laminated Composite Skew Plates, *Materials Today: Proceedings*, 2021, Vol. 45(P6), pp. 4925-4930. https://doi.org/10.1016/j.matpr.2021.01.370.

b) D. Chatterjee, A. Ghosh, D. Chakravorty, Finite Element Prediction of First-Ply Failure Loads of Composite Thin Skewed Hypar Shells Using Nonlinear Strains, *Thin Walled Structures*, 2021, Vol. 167(108159), pp. 1-13. https://doi.org/10.1016/j.tws.2021.108159.

c) D. Chatterjee, A. Ghosh, D. Chakravorty, First Ply Failure Behaviour of Laminated Composite Skew Plates of Various Edge Conditions, *Mechanics of Composite Materials*, 2021, Vol. 57(5), pp. 699-716. https://doi.org/10.1007/s11029-021-09989-4.

d) D. Chatterjee, A. Ghosh, D. Chakravorty, Progressive failure prediction of laminated composite thin skew plates under transverse loading using nonlinear strains, *The Journal of Strain Analysis for Engineering Design*, 2024, Vol. 59(5), pp. 337-350. https://doi.org/10.1177/03093247241240821.

e) D. Chatterjee, A. Ghosh, D. Chakravorty, Application of FEM in Nonlinear Progressive Failure of Composite Skew Plates with Practical Non-Uniform Edge Conditions, *Structural Engineering and Mechanics*, 2024, Vol. 90(3), pp. 287-299. https://doi.org/10.12989/sem.2024.90.3.287.

International Conference Publications:

a) D. Chatterjee, N. Modak, D. Chakravorty, Experimental and Finite Element Failure Investigation of Carbon Fiber Reinforced Composites, 64th Congress of Indian Society of Theoretical and Applied Mechanics, ISTAM, IIT, Bhubaneswar, December 9-12, 2019.

b) D. Chatterjee, A. Ghosh, D. Chakravorty, First Ply Failure Analysis of Laminated Composite Skew Plates Using ANSYS, 64th Congress of Indian Society of Theoretical and Applied Mechanics, ISTAM, IIT, Bhubaneswar, December 9-12, 2019.

c) D. Chatterjee, A. Ghosh, D. Chakravorty, Effect of stacking sequence variation on first ply failure load of laminated composite skew plate, 12th Structural Engineering Convention – SEC 2022, ASPS Conference Proceedings 1:13-18. https://doi.org/10.38208/acp.v1.465.

Book Chapters:

a) D. Chatterjee, A. Ghosh, D. Chakravorty, First ply failure behaviour of corner point supported laminated composite skew plate, Recent Advances in Computational and Experimental Mechanics, Vol I, pp 1-10, 2022. Springer, Singapore. https://doi.org/10.1007/978-981-16-6738-1_1.

b) D. Chatterjee, A. Ghosh, D. Chakravorty, On nonlinear first ply failure behaviour of angle ply composite thin skew plates using FEM, Advances in Structural Mechanics and Applications, Vol 19, pp 419-435, 2022. Springer, Cham. https://doi.org/10.1007/978-3-030-98335-2_28.

4. **List of Patents:** No.

5. **List of Presentations in International Conferences:**

a) D. Chatterjee, N. Modak, D. Chakravorty, Experimental and Finite Element Failure Investigation of Carbon Fiber Reinforced Composites, Indian Society of Theoretical and Applied Mechanics, ISTAM, IIT, Bhubaneswar, December 9-12, 2019.

b) D. Chatterjee, A. Ghosh, D. Chakravorty, First Ply Failure Analysis of Laminated Composite Skew Plates Using ANSYS, Indian Society of Theoretical and Applied Mechanics, ISTAM, IIT, Bhubaneswar, December 9-12, 2019.

c) D. Chatterjee, A. Ghosh, D. Chakravorty, First ply failure behaviour of corner point supported laminated composite skew plate, 1st Online International Conference on Recent Advances in Computational and Experimental Mechanics 2020, IIT, Kharagpur, September 4-6, 2020.

d) D. Chatterjee, A. Ghosh, D. Chakravorty, On nonlinear first ply failure behaviour of angle ply composite thin skew plates using FEM, Advances in Structural Mechanics and Applications (ASMA 2021), NIT Silchar, October 6-8, 2021.

6. List of Presentations in National Conferences:

a) D. Chatterjee, A. Ghosh, D. Chakravorty, Static bending response of laminated composite plates with cut-out using ANSYS, National Conference on Sustainable Development and Circular Economy in Civil Engineering (SDCE 2021), HIT Kolkata, December 16-17, 2021.

7. List of Workshops:

a) Workshop on writing quality research article for publication, Jadavpur University, 13^{th}-14^{th} January 2020.

b) Paper presentation on "First ply failure study of clamped composite skew plates", in Web-based Exposition on Engineering and Technology Research at Jadavpur University WEBINAR-FET-JU R&D Expo 2021, Sponsor: TEQIP-III, R&D Committee, TEQIP-III, Jadavpur University during February 26-27, 2021.

PROFORMA -1
"Statement of Originality"

I Dona Chatterjee registered on 17.06.2019 do hereby declare that this thesis entitled "Nonlinear first ply and progressive failure of laminated composite skewed plates and shells" contains literature survey and original research work done by the undersigned candidate as part of Doctoral studies.

All information in this thesis have been obtained and presented in accordance with existing academic rules and ethical conduct. I declare that, as required by these rules and conduct, I have fully cited and referred all materials and results that are not original to this work.

I also declare that I have checked this thesis as per the "policy on Anti Plagiarism, Jadavpur University, 2019", and the level of similarity as checked by iThenticate software is …2…%.

Signature of Candidate: Dona Chatterjee
Date: 18.06.2024

Certified by Supervisor(s):
(Signature with date, seal)

1. Dipankar Chakravorty 18/06/2024

Dr. Dipankar Chakravorty
Professor, Civil Engineering Department
Jadavpur University, Kolkata.

Dr. Dipankar Chakravorty
Professor, Structural Engineering Division
Civil Engineering Department
Jadavpur University
Kolkata-700032
Mob: 9830188502, 8240145761

2. Arghya Ghosh 18/06/2024

Dr. Arghya Ghosh
Assistant Professor, Civil Engineering Department
Netaji Subhas University of Technology, New Delhi.

DR. ARGHYA GHOSH
B.E. (Civil), M.E. (Structures), Ph.D
Assistant Professor
Civil Engineering Department
Netaji Subhas University of Technology
(Govt. of NCT of Delhi)

PROFORMA – 2
CERTIFICATE FROM THE SUPERVISOR/S

This is to certify that the thesis entitled "**Nonlinear First Ply and Progressive Failure of Laminated Composite Skewed Plates and Shells**" submitted by Smt. Dona Chatterjee, who got her name registered on 17.06.2019 for the award of Ph.D. (Engineering.) degree of Jadavpur University is absolutely based upon her own work under the supervision of Prof. Dr. Dipankar Chakravorty and Dr. Arghya Ghosh and that neither her thesis nor any part of the thesis has been submitted for any degree/diploma or any other academic award anywhere before.

Dipankar Chakravorty 18/06/2024.

Dr. Dipankar Chakravorty
Professor, Civil Engineering Department
Jadavpur University, Kolkata.
(Signature and date with office seal)

Dr. Dipankar Chakravorty
Professor, Structural Engineering Division
Civil Engineering Department
Jadavpur University
Kolkata-700032
Mob: 9830188502, 8240145761

Arghya Ghosh 18/06/2024

Dr. Arghya Ghosh
Assistant Professor, Civil Engineering Department
Netaji Subhas University of Technology, New Delhi.
(Signature and date with office seal)

DR. ARGHYA GHOSH
B.E. (Civil), M.E. (Structures), Ph.D.
Assistant Professor
Civil Engineering Department
Netaji Subhas University of Technology
(Govt. of NCT of Delhi)

ACKNOWLEDGEMENT

The author owes her most sincere thanks and profound gratitude to her supervisors, Prof. Dr. Dipankar Chakravorty and Dr. Arghya Ghosh for their indispensable advices and inspiration rendered at each phase of the research work. Their valuable suggestions, constructive criticism and critical evaluation throughout the research work are thankfully acknowledged.

The author is grateful to the Head of the Department and to all the faculty members of Civil Engineering Department for their cooperation. The author also expresses her gratitude to staff members of the departmental library and the central library of Jadavpur University.

The excellent cooperation and support of the co-researchers are thankfully acknowledged.

It would not have been possible for the author to pursue the research work without the constant effort, sacrifices and encouragement of her family from the very first day of her student life till date. The author is thankful to all those, whose efforts either directly or indirectly have contributed substantially during the course of this thesis work.

Signature of the Candidate: Dona Chatterjee

Date: 18.06.2024

Place: Kolkata

TABLE OF CONTENTS

LIST OF FIGURES

LIST OF TABLES

NOTATIONS

The following notations are used in the text of the thesis. The symbols which are not listed in the following are explained where they appear for the first time.

1. VARIABLES IN MATRIX FORM

$[B_l]$	Linear part of strain-displacement matrix.
$[B_{nl}]$	Nonlinear part of strain-displacement matrix.
$[D]$	Laminate stiffness matrix.
$[J]$	The Jacobian matrix.
$[k]_T$	Tangent stiffness matrix.
$[k]_s$	Secant stiffness matrix.

2. VARIABLES AS VECTORS

$\{\delta\}$	Element nodal displacement vector.
$\{d_{judm}\}$	Nodal displacement of undamaged plate or shell.
$\{d_{jdm}\}$	Nodal displacement of damaged plate or shell.
$\{F\}$	Generalized internal stress resultant vector.
$\{P\}$	External generalized forces.
$\{r\}$	Resultant of internal forces and external generalized forces.

3. OTHER VARIABLES

x, y, z	Global coordinate axes.
L, T, T'	Local coordinate axes.
a, b	Length and width of shell or plate in plan.
c	Rise of skewed hypar shell.
h	Shell or plate thickness.
A	Area of shell.
FPF	First ply failure.
FL, UFL	First ply and Ultimate ply failure load or pressure respectively.
$(\overline{\text{FPFL}})$	Nondimensional first ply failure pressure value.
$(\overline{\text{UPFL}})$	Nondimensional ultimate ply failure pressure value.
f_y	Intensity of uniformly distributed load.
R_{xy}	Radius of cross curvature of hypar shell.

$\varepsilon_x, \varepsilon_y$	In-plane strains along *X* and *Y* axes of the shell.
$\gamma_{xy}, \gamma_{xz}, \gamma_{yz}$	In-plane and transverse shear strains, respectively.
${\kappa_x}^0, {\kappa_y}^0, {\kappa_{xy}}^0$	Mid-surface curvatures of the shell or plate due to loading.
N_x, N_y, N_{xy}	In-plane normal and shear force resultants.
Mx, My, Mxy	Bending moment and torsional moment resultants.
Q_x, Q_y	Transverse shear resultants.
n	Total number of ply.
h_k, h_{k-1}	Top and bottom distances of the k^{th} ply from mid-plane of a laminate.
N_1 to N_8	Shape functions for first to eight nodes of the element.
$P_0 - P_7$	Constant terms of displacement polynomial.
$\sigma_L, \sigma_T, \tau_{LT}$	Normal stresses along L and T axes and shear stress acting on $L-T$ surface of a lamina, respectively.
$\varepsilon_L, \varepsilon_T, \gamma_{LT}$	In-plane normal strains along L and T axes and shear strain acting on $L-T$ surface of a lamina, respectively.
$E_L, E_T, E_{T'}$	Modulus of elasticity along the directions L, T and T'.
$G_{LT}, G_{LT'}, E_{TT'}$	Shear modulus of a lamina in $L-T$, $L-T'$ and $T-T'$ planes corresponding to the local axes of that lamina, respectively.
υ_{LT}	Poisson's ratio.
${\sigma_{L_{Ten}}}^u, {\sigma_{T_{Ten}}}^u$	Ultimate normal tensile stresses along L and T direction, respectively.
$\sigma^u_{L_{Comp}}, \sigma^u_{T_{Comp}}$	Ultimate normal compressive stresses along L and T direction, respectively.
${\varepsilon_{L_{Ten}}}^u, {\varepsilon_{T_{Ten}}}^u$	Ultimate normal tensile strains along L and T direction, respectively
$\varepsilon^u_{L_{Comp}}, \varepsilon^u_{T_{Comp}}$	Ultimate normal compressive strains along L and T direction, respectively.
${\tau_{LT}}^u, {\tau_{LT'}}^u, {\tau_{TT'}}^u$	Ultimate shear stress values in $L-T$, $L-T'$ and $T-T'$ planes corresponding to the local axes of that lamina, respectively.
${\gamma_{LT}}^u, {\gamma_{LT'}}^u, {\gamma_{TT'}}^u$	Ultimate shear strain values in $L-T$, $L-T'$ and $T-T$ planes corresponding to the local axes of that lamina, respectively.
ρ	Material density.
λ	Skew angle.

φ	Orientation of fibers in a lamina with respect to the global *x*-axis of shell.
ipg	Failure progression number.

ABSTRACT

In civil engineering, plates and shells are used as cladding units and research on these structural units has found a good place in the volume of published literature. The focus of research started from bending analysis of isotropic plates and shells and in course of time, more advanced and complicated aspects started getting attention from researchers. Engineers went on trying fabricating these structural units with innovative options of advanced materials with high specific strength and stiffness properties like the laminated composites. Parallel development in the area of analysis with the introduction of finite element method and advent of high speed computers made it possible to analyze complicated shapes of plates and shells which are aesthetically appealing and may be subjected to complicated load functions. Non-conventional boundary conditions which suit to specific practical situation became possible to be modeled by finite element approach. Numerical models of plates and shells had continuously been compared with experimental results and advanced theories of shear deformation, geometric and material nonlinearity were introduced to take care of mismatches between theoretical and experimental results. Successful applications of plates and shells with advanced materials like laminated composites required appropriate characterization in terms of different performance parameters including failure characteristics – both at initiation and during progress up to ultimate load. A study of literature shows that failure of skewed plates and skewed hypar shells has not received due attention.

The finite element method is employed here to study the first ply and progressive failure behaviour of laminated composite skew plates and skewed hypar shells considering Sanders' geometrically linear strains and von Kármán's approach of nonlinear strains. An eight noded curved quadratic Serendipity element having five degrees of freedom at each

node is used to model the surface. The Newton – Raphson iteration is utilized to solve the nonlinear equation of static equilibrium. Different well-established failure criteria like maximum stress, maximum strain and those proposed by Hoffman, Tsai-Hill, Tsai-Wu, Hashin and Puck are used to obtain the linear and nonlinear first ply and ultimate ply failure load values.

The finite element code developed is validated through comparison of present results with published theoretical and experimental ones before applying the code to generate new results. The first ply and ultimate ply failure strength of thin skewed plate and skewed hypar shell geometry under uniformly distributed load for different boundary conditions and laminations are computed. Failure locations (such as failed element, failed Gauss point etc.) and failure mode or tendencies are also reported. The author further studies the first ply failure (FPF) and associated frequency reduction of composite skew plates considering practical parametric variations. The effects of skew angle on the first ply failure load are summarized in the form of charts and working equations. The engineers and researchers may use the charts and equations directly to predict the first ply failure load provided the geometry of the plate is known. Apart from reporting the failure load values, the failure zones and nature of damage progress on the skew plate surfaces are also presented which are expected to be valuable inputs for non-destructive health monitoring. Numerical experimentation with parametric variations of skewed hypar laminated composite shells are carried out and the results are post processed and interpreted to extract meaningful engineering conclusions. Further this investigation is aimed towards proposing design guidelines regarding failure characteristics of skewed hypar laminated composite shells with partially free boundaries considering both the aspects of collapse and serviceability using well-established failure criteria.

The literature review, mathematical formulation, details of investigations are presented chapter-wise in the thesis. Scope of future research work is also discussed about at the end of this thesis.

ORGANISATION OF THE THESIS

There are ten chapters and one appendix in this thesis. The basic introduction and some of the essential aspects of the current investigation are presented in Chapter 1. The review of the published literature is extensively detailed in Chapter 2. The published papers are carefully examined and critically evaluated. The precise scope of the current work is identified and presented in Chapter 3 based on the thorough review exercise.

After defining the scope, Chapter 4 presents the mathematical formulation used in the current investigation.

To check the validity of the current formulation, results are generated for a few benchmark problems that earlier researchers have solved and are presented in relevant portions of Chapters 5 to 9.

In Chapters 5 to 9, a variety of the author's own problems are taken up and the outputs are thoroughly studied from practical standpoints. Conclusions drawn from the interpretation of results are furnished at the end of the respective chapters.

Chapter 5 deals with the investigation of linear first ply failure of laminated composite skew plates of various edge conditions. In this chapter the damaged frequency post first ply failure is also computed. Chapter 6 contains first ply failure problems of clamped skewed plates using geometrically linear and nonlinear strains for seven different skew angles. The nonlinear first ply failure and ultimate ply failure aspects of laminated composite skew plates for clamped and irregular boundary conditions are reported in Chapters 7 and 8 respectively. In these chapters the author also studies failure loads from serviceability criterion and reports the load factors, nature of damaged area at ultimate failure and failure initiation zone. Ranks of different skewed plate options in terms of first and ultimate ply failure pressure and percentage of damaged area at ultimate stage of failure

are also reported. Chapter 9 furnishes the nonlinear first ply failure characteristics of skewed hypar shell roofs for clamped-free edge combination. Chapter 10 outlines the future course of research and possible extension of the present study. The references are presented in the Appendix.

KEYWORDS

- Skew plate
- Skewed hypar shell
- First ply failure
- Ultimate ply failure
- Geometric nonlinear analysis
- Finite element method
- Serviceability failure
- Failure zone
- Failure mode
- Damaged area
- Newton Raphson iteration

Chapter 1

INTRODUCTION

1.1. GENERAL

In civil engineering, plates and shells are used as cladding units and research on these structural units has found a good place in the volume of published literature. The focus of research started from bending analysis of isotropic plates and shells and in course of time more advanced and complicated aspects started getting attention from researchers. Engineers go on trying with innovative options of plates and shells depending on the area of their applications. As a result stiffened plates and shells, those with cutouts started being studied using conventional materials and advanced materials with high specific strength and stiffness like the laminated composites. Parallel development in the area of analysis with the introduction of finite element method and advent of high speed computers made it possible to analyze complicated shapes of plates and shells which are aesthetically appealing and are subjected to complicated load functions. Non-conventional boundary conditions which suit to specific practical situations became possible to be modelled by finite element approach. Numerical models of plates and shells had continuously been compared with experimental results and advanced theories of shear deformation, geometric and material nonlinearity were introduced to take care of mismatches between theoretical and experimental results. Successful applications of plates and shells with advanced materials like laminated composites required appropriate characterization in terms of dynamic behaviour and failure characteristics apart from

static bending response. The papers published recently on plates and shells reflect this trend and establish the fact that advanced analysis of plates and shells is an active area of research.

1.2. PRESENT PROBLEM- ITS IMPORTANCE IN RESEARCH

The flexibility of tailoring the properties of laminated composite plate and shell units by changing the fibre orientation in different lamina is one of the reasons for making this material very popular in the weight sensitive areas of engineering. However, the transverse shear weakness of the laminated composite may cause internal damage within the laminate due to static or dynamic overloading and such damage may remain undetected. Hence, it is very important for an engineer to know the first ply failure load of a composite structural unit and also the nature of progress of the damage. A laminated composite may fail at the fibre level or in the matrix when specific stresses and strains are exceeded. A laminate may also fail in interactive modes. Estimation of first ply failure load and study of progressive failure necessitate use of nonlinear components of strains which may be implemented combining the finite element approach with Newton Raphson iterative scheme. A study of literature shows that nonlinear first ply and progressive failure analyses of skewed plates and skewed hypar shells have not received adequate attention and this fact is the motivation behind the present study.

Chapter 2

LITERATURE REVIEW

2.1. GENERAL

In this chapter the volume of literature that has accumulated on research about plates and shells is presented in form of different sections for lucid understanding. The history of plate and shell research is presented in Section 2.2 including the very early publications while in Section 2.3 the focus is restricted only on the research carried out on the recent trend of failure studies of laminated composite plates and shells. In Section 2.4 the attention is further narrowed down to discuss the very recent papers published within the last decade to highlight the area of today's interest. Finally, Section 2.4 briefly but critically discusses the total volume of literature to identify the lacunae in the published volume and to indicate the broad area where research can be carried off. Based on Section 2.4 the pinpointed scope of the present research is presented in the next chapter.

2.2. HISTORICAL REVIEW ON PLATES AND SHELLS RESEARCH

Research on plates and shells dates back to as early as 19^{th} century and this section is about the course of development of this research area encompassing different aspects that were felt to be important from time to time. The very first text book on theory and analysis of plates and shells was due to Timoshenko and Krieger (1959). Thereafter several other books were published such as those of Novozhilov (1964), Kraus (1967), Dym (1974), Gould (1999), Reddy (1999), Chandrashekhar (2001) and Reddy (2004). The course of plates and shell research is discussed in this section. This section is further

divided into multiple subsections for clear understanding of the systematic and historical evolution of the various areas of plates and shell study.

2.2.1. Review on Plate Research

Petit and Waddoups (1969) were the first to present the nonlinear continuous stress strain curve for anisotropic laminate with mid-plane symmetry up to ultimate failure. The authors restricted the analysis to only biaxial membrane loading and validated their plots against the experimental results. Provan and Koeller (1970) developed the pure bending theory of isotropic elastic plates with Cosserat surfaces and it was observed that this method of analysis gives close results when compared with three dimensional theory of elasticity. A three dimensional linear elastic solution was suggested for solving vibration problem of isotropic thick laminates by Srinivas et al. (1970a) which was further extended for thick orthotropic plates undergoing flexure, vibration and buckling for simply supported edge condition by Srinivas and Rao (1970b). The inaccuracies in results were found to increase as the thickness of the laminate increases or as the order of the mode increases. Also it was found that in laminates, the modular ratios between the plies increase the errors mostly when the moduli of the outer plies increase. Srinivasan and Munaswamy (1975) used finite strip approach to examine the frequency and mode shapes of vibration for point supported isotropic skew plates using small deformation theory. The authors reported the variation in results with change in support positions and skew angles and compared it with other results available in the literature for regular rectangular plates. Benveniste and Aboudi (1975) employed effective stress theory to investigate the dynamic characteristics of laminated composite plate (LCP) for time varying area loading. Both small and large deflections effects were considered in this study. Hussainy and Srinivas (1974) studied the flexure behaviour of boron epoxy and glass epoxy rectangular plate using their own developed theory and compared the results

with those obtained by thin plate theory. The authors considered the transverse shear effect in computation of deflection and moments for plates having one pair of opposite edges simply supported and other pair of opposite sides with variable support conditions. The effects of fibre orientation, aspect ratio of plates and percentage of fibre by volume on flexural response were investigated and found to be complex functions of these parameters. Chandra and Raju (1975 a) investigated the free flexural vibration of fully clamped and simply supported cross ply laminates. Authors obtained the nonlinear frequencies for both carbon fibre reinforced and glass fibre reinforced plastics and compared the results with those of isotropic plates. A similar kind of study on angle ply laminates were also conducted by Chandra and Raju (1975 b). In this work the authors used von Kármán equations for large deflection and used perturbation technique. Sathyamoorthy and Chia (1980) analysed the nonlinear period of vibration for anisotropic plates with all sides simply supported, clamped and with mixed edge conditions. The authors employed Galerkin method and numerical Runge-Kutta procedure to solve nonlinear dynamic von Kármán equations. Authors included the effect of transverse shear and rotary inertia to compute the nonlinear period and obtained the impacts of different parameters such as lamination, ratio of sides, width to thickness ratio and fibre angle on period of vibration. Pica et al. (1980) conducted the geometric nonlinear finite element analysis with small rotations using Mindlin plate theory. They checked the efficiency of linear, serendipity, Lagrangian and heterosis isoparametric element in prediction of displacement and stresses of circular, square, elliptical and skew plates under uniform and concentrated loading. Authors compared their results with analytical result and with results of thin plate analysis available in the literature. The serendipity elements which shows over stiffness ‘locking’ behaviour for very thin plates was overcome by use of nine noded Lagrangian elements. Witt and Sobczyk (1980) studied the dynamic response of

LCP using Mindlin formulation. The authors considered the transverse shear deformation and rotary inertia in their analysis. The response was studied for time varying random excitation. The correctness of this method of analysis was entrenched by contrasting the outcomes with those attained through Kirchhoff and Mindlin theory on elastic plates. Giri and Simitses (1980) examined the deflection response of simply supported anisotropic rectangular plate under uniform compressive, shear and transverse loading. The authors used modified Galerkin method to solve the nonlinear compatibility and transverse equilibrium equations. Reddy and Chao (1980) presented the finite element analysis of single and double layer cross ply thin to moderately thick rectangular simply supported plates. The authors performed the static analysis for sinusoidal and uniformly distributed normal pressure and compared the deflections obtained with those achieved through closed form solution. Singh and Rao (1987) proposed a finite element considering the large deflection, strains and rotation to analyze the response of thick and thin laminates. It is found that boundary condition and fibre orientation significantly influenced the nonlinear deflection of unidirectional laminates. Baharlou and Leissa (1987) suggested an analytical method proficient of producing precise computational solution of dynamic response and buckling characteristics of composite plates with random stacking order and boundary restraints. Polynomials were used to represent displacement functions and an algorithm for satisfying the geometric boundary requirements was described. To determine the correctness of the method, numerical results were compared to those of other researchers. Owen and Li (1987a and 1987b) published two papers where the authors reported the static bending, transverse vibration and buckling characteristics of anisotropic thick composite plates using refined approximate theory. By considering subsequent linear alteration of the extensional displacements and a fixed value of the transverse displacement in the thickness direction, the three-dimensional problem was

simplified to a two-dimensional one. This model produced accurate and acceptable results for all thickness and modular ratio ranges when compared to both precise three-dimensional evaluation and higher-order plate bending theory. Chen and Sun (1985a) used the finite element method to solve the nonlinear time dependent response of initially stressed composite plates. The authors used Mindlin plate theory and von Kármán nonlinearity combined with a nine noded isoparametric quadrilateral elements to analyse composite plates. The Newmark constant acceleration approach was employed in the time integration, together with an efficient and accurate iteration scheme. Static bending characteristics of isotropic and LCP were numerically studied. Chen and Sun (1985b) used the same formulation to explore the impact responses of composite laminates with and without commencing stress. The impact force was evaluated using a finite element model that incorporates an empirically determined contact law that is accountable for the permanent impression. The plate deflections, associated strains and contact forces all were obtained numerically. Mukherjee (1991) studied the dynamic behaviour of LCP applying finite element method. Authors employed a higher-order quadratic isoparametric element and compared the performance of both eight noded serendipity and nine noded Lagrangian elements. Various mass matrix generation strategies were addressed, and a correlative analysis of these theories was offered. The obtained results were compared to the closed form solutions and experimental observations of prior researchers. Librescu and Stein (1991) studied the post buckling behaviour of transversely isotropic symmetrically LCP using a higher-order, geometrically nonlinear theory. The equations derived were used to investigate the post-buckling behaviour of shear-deformable simply supported plates. Chang and Huang (1991) presented a geometric nonlinear finite element solution of static and transient vibration response of LCP. The analysis used a higher-order displacement theory that allows both transverse shear and normal strains. Also the

effects of laminate thickness, stacking sequences, and stacking orientations were investigated. Using a Levy-type solution, Chen and Liu (1990) studied the static response and natural modes of vibration of isotropic and anisotropic plates. The overall consequence of ratio of sides, width to thickness, fibre rotation angle, lamina stacking order and modulus ratio was summarized. Chen and Yang (1990) conducted the stability analysis of composite plates under time dependent axial load. Authors chose antisymmetric angle-ply lamination and considered combination of a periodic flexural stress and axial compressive stress and solved the problem using the Galerkin FE model including transverse shear effects and rotary inertia. The large deformation response of laminated composite circular plates was investigated by Sridhar and Rao (1995) employing four-noded anisotropic sector element having forty eight degrees of freedom. By inserting correct values for the geometric parameters, the strain-displacement relation for the sector element was deduced from quadrilateral shell element. Kermanidis and Labeas (1995) developed semi analytical method of static and stability analysis of thin anisotropic plates. The results obtained by them converged perfectly with the one obtained through exact solution and finite element analysis. Sadek (1998) made a comparative study on the performance of three different types of rectangular eight-noded serendipity elements in the prediction of bending response of LCP considering transverse shear deformation. The deflection across the plate thickness was considered constant for two types of elements where seven and nine degrees of freedom were considered per node respectively. The first ply failure (FPF) probability and buckling strength of LCP under inplane load were proposed by Lin et al. (1998) using stochastic finite element analysis. The lamination, fibre angles and ply thickness were chosen as random variables and the results were compared with those obtained through Monte-Carlo simulation. Wang (1997) conducted the dynamic analysis of fibre reinforced composite skew plates

employing the B spline Raleigh Ritz method. The coupling of inplane and bending strains was considered and the authors chose three translations and shear strains instead of rotations just to minimize the problem of shear locking. Kolli and Chandrashekhara (1997) conducted the nonlinear finite element analysis of laminated composite eccentrically stiffened plates. The plate was modelled using an isoparametric nine noded quadrilateral element and stiffeners were modelled with three- noded beam elements. The authors used direct iteration technique combined with Newmark constant acceleration scheme to solve the nonlinear dynamic equilibrium equations. The effect of rotary inertia on dynamic response of symmetric LCP was studied by Wang et al. (2000). Only symmetric rectangular LCP were considered for their study. It was seen that rotary inertia effects were more in case of thick plates compared to thin plates. Lin (2000) reported the buckling failure analysis of composite laminates under in plane loads using stochastic finite element approach. To validate the correctness of the results computed through the technique, those were compared with the one obtained using Monte Carlo method. Kouchakzadeh and Sekine (2000) conducted the buckling analysis of rectangular LCP with multiple instilled delamination. Buckling study of skew laminates was performed by Hu and Tzeng (2000) for inplane compression through finite element package ABAQUS. Buckling response for different skew angles, laminations, presence of concentric cut-out, aspect ratio, plate thickness and boundary conditions were investigated. Chen et al. (2000) adopted the semi-analytical finite strip method to conduct the nonlinear transient dynamic analysis of rectangular orthotropic and isotropic simply supported plates. The nonlinear transient dynamic equations were solved by Newmark's time integration method combined with Newton Raphson iterative approach. The basic idea of the created finite strip procedure and those of a finite element method were shown to be very similar.

A triangular element capable of including the effect of transverse shear deformation for investigating bending of LCP was proposed by Sheikh et al. (2002).

Based on a higher-order improved theory, Kant and Swaminathan (2002) reported detailed explanations and results of static analysis for composite and sandwich plates of simply supported boundary conditions. Higher-order theories and the first-order theory proposed previously published by other researchers were also considered. The authors employed Navier's approach to attain a closed-form solution for the boundary value problem.

Using a finite element technique, the large amplitude free flexural vibration behavior of thin skewed LCP was explored by Singha and Ganapathy (2004). The geometric nonlinearity was introduced using von Kármán’s assumptions. The direct iteration technique was used to solve the nonlinear governing equations produced, using Lagrange's equations of motion. Various parametric variations were used to investigate the fluctuation of nonlinear frequency ratios with amplitudes. Tanriover and Senocak (2004) investigated the large deflection analysis of plates of various edge conditions. The authors employed Newton Raphson iteration technique combined with the Galerkin method. Nonlinearity was introduced through von Kármán equations and the results obtained by them were compared with those computed through dynamic relaxation technique and finite element method. Dai et al. (2004) introduced the concept of mesh-free analysis of thick and thin LCP. The authors used the moving least square method and variational theorem to perform the analysis based on third-order shear deformation theory. The outcomes were finally compared with those derived through finite element and exact analyses. Aagaah et al. (2006) studied the natural frequencies of LCP for various support conditions and laminations based on third-order shear deformation theory (TSDT). The authors mainly reported the effect of ply numbers, stacking sequences and

support condition combinations on the natural frequencies using finite element analysis. Zhang et al. (2006) described the penalty function method to predict the damage inception and proliferation of LCP under low velocity impact. To develop the damage evolution law, a damage surface was created that included stress-based and fracture-mechanics-based failure criteria. The damage model was implemented in ABAQUS' user subroutine VUINTER, a commercial finite element tool. Hu et al. (2006) reported the nonlinear finite element buckling analysis of skewed LCP based on Tsai-Wu failure criterion under compressive load. The influences of plate skew angle, laminate layup and plate aspect ratio on composite laminate skew plate buckling resistance were discussed.

Considering the first-order shear deformation theory (FSDT) and the differential quadrature method, a nonlinear free vibration analysis of thin-to-moderately thick skewed LCP was described by Malekzadeh (2008). A detailed investigation by varying the skew angle, thickness-to-length ratio, aspect ratio and various types of boundary conditions was carried out. Bhar et al. (2010) furnished a comparative study between the performance of FSDT and HSDT in analysis of thin to thick stiffened LCP. It was seen that response of thin plates by FSDT matches very closely with those predicted by Pagano's 3D elasticity theory. But as the plate thickness increased or stiffeners were added then the solution diverges far from the exact solution if computed using FSDT. So, it was suggested to use HSDT instead of FSDT or classical plate theory for analysis of thick stiffened plates. Dash and Singh (2010) presented the bending deformation of LCP under transverse loading (based on HSDT). The authors established the geometric nonlinearity from Green-Lagrange theorem on MATLAB environment. The direct iteration approach was used to obtain nonlinear fundamental frequencies. Lee (2010) reported the dynamic stability analysis of skewed LCP based on HSDT. The numerical solution for square and skew plates with and without a central cut-out was found to be very similar to those

published by previous researchers. It was found that the skew laminates become increasingly dynamically unstable as plan dimension to thickness ratio decreases. Upadhyay and Shukla (2012) reported the flexural analysis of moderately thick skewed LCP under transverse load using von Kármán nonlinearity and TSDT. The nonlinear equations were reduced to linear ones by quadratic extrapolation technique. The authors furnished the effects of transverse shear, aspect ratio and skew angles on the bending response of the plates. Dash and Singh (2012) addressed the buckling and post buckling behaviour of LCP using C^0 isoparametric element combining HSDT and Green–Lagrange nonlinear strain–displacement equations. The formulation included all higher-order terms that arise from nonlinear strain–displacement relation. The free vibration of differently arranged point supported skewed LCP were studied by Naghsh and Azhari (2014) using element free Galerkin method. The nonlinear governing equations were used and the direct iteration procedure and weighted residual method. Pavan and Nanjunda Rao (2017) proposed the isogeometric collocation method for solving the linear static bending analysis of LCP and sandwich plates governed by Reissner-Mindlin theory. For the assessment of LCP, a locking-free primeval and a mixed formulation were offered in addition to the normal primal formulation. In the case of thin LCP, both locking-free and blended formulations were found to be beneficial in reducing shear locking.

Thakur et al. (2020) proposed the non-polynomial shear deformation theory (NPSDT) based on C^0 isoparametric element for vibration analysis of folded LCP. The conjectural formulations were based on inverse hyperbolic shear deformation theory (IHSDT) and nine-noded Lagrange isoparametric finite element as NPSDT. The governing equation of the system was derived using Hamilton's concept. The pressure load and vertical load transient analysis was performed using Newmark's direct integration scheme. The consequence of different parametric variations such as crank

angle, fibre angle, plies stacking, fold position, and edge conditions on the natural frequency and transient response of LCP was investigated. Sinha et al. (2020) investigated the free vibration of woven fibre stiffened LCP numerically and experimentally. Thirty-four stiffened plates were tested in an FFT analyzer to determine their natural frequencies by varying lamination, boundary condition and geometry.

2.2.2. Review on Shell Research

The thickness of the shell is one of the most popular means of classifying shell theories. A thin shell is one whose thickness is minimal in comparison to its other dimensions and curvature radii. The thin shells from the first half of the nineteenth century picked the interest of a number of researchers. Lame and Clapeyron (1833) studied shells of revolution under symmetric loading. Aron (1874) was the first to apply the general theory of elasticity to the shell problem, to get bending and twist components that were independent of tangential displacements using Kirchhoff's (1876) assumption for plates. When Love (1888) developed his theory of shells, he discovered that Kirchhoff's postulate that stated mid surface normal before and after deformation remains straight and normal, was not precisely correct. Based on the classical theory of elasticity, Love was the one who proposed first a reasonable model for bending behaviour of thin shell. All moment expressions were ignored in Lame and Clapeyron's (1833) membrane theory and bending strains were neglected in comparison to longitudinal strains. The general form of solution using this theory was proposed by Beltrami (1881). The limitations of established membrane theories prompted Marguerre (1938), Vlasov (1947), and Reissner (1955) to develop a comprehensive theory of shell bending. Following that, it was realized that both the membrane and bending theories may be used to solve various problems depending on the nature of the shell geometry. Reissner (1946, 1955), Johnson and Reissner (1958), Kalnins and Naghdi (1960), Hoppmann (1961) employed analytic

techniques to investigate the vibration properties of shallow spherical shells. Nazarov (1949) and Wang (1953) focused on shell bending theories, while Vlasov (1964) continued working on the membrane theory. Flügge and Conrad (1956) refined Marguerre's (1938) bending theory by proposing more appropriate forms for the set of differential equations. Parme (1956) expanded the membrane theory of hyperbolic and elliptic paraboloids to get the stresses representing the shell surface in Cartesian coordinates. Sanders (1959), Koiter (1960), Naghdi (1963), and Goldenveizer (1968) developed different hypotheses as shell research progressed. The ideas of Koiter (1960) and Budiansky and Sanders (1963) were consistent with the core of Love-Kirchhoff assumptions. Among the numerous theories offered, those proposed by Flügge and Geyling (1957), Fischer (1960), Ramaswamy and Rao (1961), Soare (1966) were membrane theories, wheareas bending theories were put forward by Bongard (1959) and Chetty and Tottenham (1964). Iyengar and Srinivasan (1968) investigated the bending theory of shells using Bongard (1959) equations to define the boundary condition, satisfying displacement functions while Ramaswamy (1971) used three coupled differential equations to explain the problem.

Marguerre (1938), Reissner (1946), Donnell (1933) and Vlasov (1958) were credited with the creation of shallow shell theory. Vlasov (1964) defined a shallow shell as one whose rise is less than one-fifth of its smallest plan dimension. Munro (1961) devised a generalized heterogeneous expression for solving shallow thin second order shells in linear form with Gaussian curvature of positive, zero, or negative values. Apeland and Popov (1961) published on the flexural solution of rectangular planforms and hypar shells. Russel and Gerstle (1967, 1968) expanded on Brebbia's (1966) theoretical and experimental research on umbrella-like hyperbolic paraboloid shells. Reisman and Culowski (1968) described forced vibrations of axisymmetric shallow

spherical shells. Bandyopadhyay and Ray (1971, 1972) investigated the behaviour of hypar shells. Abel and Billington (1972) investigated the buckling criterion of various shell forms whereas Gergely (1972) estimated the buckling load using the energy concept. Dong (1968) and Dulaska (1969) investigated the frequency and stability of laminated composite cylindrical and other shallow shell forms. Olson and Lindberg (1968) investigated the dynamic properties using triangular finite elements to model doubly curved shells, while Brebbia and Hadid (1971) used rectangular finite elements to tackle conoidal shell problems. The Ritz approach was used by Leissa and his colleagues to calculate the free vibration characteristics of shallow shells [Leissa et al. (1981, 1983), Narita and Leissa (1984), and Qatu and Leissa (1991a)]. The vibrations of simply supported elliptic planform shells were reported by Coleby and Majumdar (1982). The forced vibrations of elastic shallow shells under moving loads was investigated by Xiang-Sheng (1985). Ghosh and Bandyopadhyay (1989) studied the static flexural response of isotropic conoidal shells, while Qatu (1989) reported both the bending response and free vibrations of laminated shallow shells. Chao and Tung (1989) reported the response of orthotropic hemispherical shells under step pressure and blast loads for fully fixed edges. By expanding Sanders' approach, Chandrashekhara (1989) employed a nine noded isoparametric Lagrangian element for frequency response study of cylindrical and spherical composite shells.

While many academicians worked to simplify and improve the theory of shell structures, another set of researchers began inventing exotic materials with exceptional strength and stiffness capabilities. As a result, from the second part of the twentieth century, laminated composites were introduced in engineering applications. Laminated composites have high stiffness/strength to weight ratio, superior fatigue resistance, reduced susceptibility to weathering damage, and, most importantly, offer flexibility of

tailoring stiffness and strength properties by changing fibre orientations and lamina stacking sequences. As a result, laminated composite materials started getting applied in shell fabrication. Subsequently, examining the bending behaviour of laminated composite shells emerged as a research subject. Hildebrand et al. (1949) applied the shell equations to an anisotropic material for the first time. Ambartsumyan (1953) was the first to combine bending and stretching coupling in his study on laminated orthotropic shells. Thereafter, Dong et al. (1962) provided a postulate for thin anisotropic shells and Stavsky (1963) proposed the same theory for anisotropic material plates. Vlasov (1964) reported on a discussion on orthotropic shell theory. By asymptotically integrating the elastic equations, Widera and his associates (1970, 1980) computed the unsymmetrical deflection of anisotropic, elastic cylindrical shells using the simplest first-approximation hypothesis. The theory was reduced to that of Donnell (1933) for a homogeneous, isotropic material. The transverse shear deformation effects in composites were incorporated by Gulati and Essenberg (1967) and Zukas and Vinson (1971). Whitney and Sun (1973, 1974) proposed a shear deformation theory that takes into account transverse shear deformation and transverse normal strain, as well as extensional strains.

Closed form solutions for laminated composite shells were reported by a number of researchers, including Reddy and Chao (1981), Bert and Reddy (1982), Bert and Kumar (1982) and Reddy (1984). Bert and Kumar (1982) studied the behaviour of simply supported cylindrical and spherical shells with sinusoidal transverse load distributions, while Reddy (1984) presented accurate bending and vibration solutions for moderately thick laminated composite cylindrical and spherical shells. Anisotropic laminated composite shell structures, including transverse shear deformation theories, were studied by Reddy (1984) and Vinson and Sierakowski (1986). Comprehensive review articles on

composite laminated plates and shells was published by Noor and Burton (1989, 1990), Kapania and Raciti (1989 a, 1989 b).

Lim et al. (1995) used HSDT to evaluate the vibration characteristics of thick cylindrical shallow rectangular planform shells for various boundary conditions and shell geometries. Xiao-ping (1996) devised a simplified HSDT for laminated composite shells. He established the governing equations of shallow shells using Love's first-order geometric approximation and Donnell's simplification. Khatri and Asnani (1996) published a damped vibration study for axisymmetric vibrations of laminated composite and fibre reinforced composite conical shells based on individual layer deformation. Wang and Schweizerhof (1997) conducted a free vibration analysis of laminated anisotropic shallow shells using FSDT. The boundary domain element technique was employed. Gendy et al. (1997) used a recently developed mixed finite element formulation for stability analysis of laminated plates and shells including the influence of significant spatial rotations on geometric stiffness and inertia operators for vibration. Simultaneously, Aksu (1997) proposed a finite element method for undamped frequency response analysis of shell with curved isoparametric trapezoidal element, which included the transverse shear strains and did not ignore z/R ratio. Both thin and moderately thick shells could be analysed using shell element with eight nodes and forty degrees of freedom. Shin (1997) revealed that doubly curved shallow open shells with simply supported edges exhibit large amplitude free vibration. Gautham and Ganesan (1997) investigated the free vibration properties of isotropic and orthotropic spherical caps. Simultaneously, Sivasubramonian et al. (1997) reported finite element free vibration of curved stiffened panels with symmetric square cutout and on the other hand Crossland and Dickinson (1997) studied effect of presence of slits parallel to an edge on the free vibration characteristics of thin shallow shells. For different boundary conditions, aspect

ratios, thicknesses and laminations, Chakravorty et al. (1995a, 1995b and 1996) investigated free vibrations of laminated composite conoidal, hyperbolic paraboloid and elliptic paraboloidal shells.

Researchers working on shells presented a variety of solution techniques to handle shell analysis, including variational methods such as Ritz, Collocation, subdomain (Biezeno-Koch), least squares, Galerkin, Kantorovich, Trefftz method and finite element methods. When Greene et al. (1961) proposed the finite element method with flat elements; it gave the field of shell study a whole new dimension. Subsequently, Grafton and Strome (1963) proposed a singly curved element. Since then, the finite element approach became a popular and powerful analytical tool in the field of shell research.

Lakshminarayana and Viswanath (1976) and Rao (1978) suggested a highly accurate shallow triangular, cylindrical and rectangular finite element capable of modelling any arbitrary geometry. The researchers focused on developing refined theories and better finite elements at the same time. For dynamic analysis of shells, Greene et al. (1961) used a doubly curved finite element. Connor and Brebbia (1967) presented the convergence study for shallow hyperbolic paraboloid shell using displacement based finite element and finite difference methods. Isoparametric curved elements were developed by Ergatoudis et al. (1968), in which the displacement and co-ordinates are approximated from the nodal coordinates using the same set of interpolation functions and Gallagher (1969) reported finite element implementation for solving plates and shells problems. The concept of analysing shell elements as a specific case of three-dimensional analysis was first suggested by Ahmad et al. (1970). Dhatt (1970) used discrete mathematics to solve thin shell problems with curved triangular elements. Choi and Schnobrich (1970) used the finite element method to investigate Kirchhoff's hypothesis applied to translational shells. The Ritz approach was used by Qatu and Leissa (1991a)

who studied the free vibration characteristics of LC double curved cantilevered shells for various material properties, stacking orders, fibre directions and curvatures. The vibrations of twisted composite cantilever plates with radius of cross curvature were examined by Qatu and Leissa (1991b). The study revealed that when the fibres were perpendicular to the clamped edge, the largest fundamental frequencies were obtained. The findings provide a solid platform for further research on mode forms. Tsai and Palazotto (1991) investigated nonlinear free and forced vibrations of isotropic and composite shells using a curved quadrilateral finite element. The approach of harmonic balance was used by Chia and Chia (1992) to handle nonlinear frequency analysis of moderately thick spherical composite shells. Dey et al. (1994) examined the bending analysis of laminated composite elliptic paraboloids and conoids. Sheinman and Reichman (1992) used the Ritz approach to investigate the buckling and vibration characteristics of shallow composite shell panels. Touratier (1992) extended the theory of composite shallow shells by including the cosine variation of transverse shear strains and tangential stress in a simple shear deformation theory. Some isotropic and composite shells were studied for bending and vibration. Qatu (1992) provided an outstanding summary of the developments on shallow shell vibration research. Frequency response of an axisymmetric shallow spherical shell with a circular cutout was presented by Hwang and Foster (1992). The results of both analytical and finite element solutions were compared. Mohd and Dawe (1993) performed a finite strip analysis of diaphragm-supported composite shells. Qatu and Leissa (1993) investigated the effect of change in curvature on frequency response of thin isotropic shallow shells with two adjacent edges clamped and the others free applying Ritz approach. Bhaskar and Varadan (1993) studied the interlaminar stresses in laminated composite cylindrical shells subjected to dynamic loading based on FSDT. The authors used Navier's approach combined with Laplace

transform to solve the dynamic equilibrium equations, while Liew and Lim (1994) used the Ritz minimization procedure to investigate vibrations of perforated isotropic shallow shells. With three-dimensional degraded finite elements, Kant et al. (1994) examined shell dynamics. Problems of cylindrical and spherical caps were solved. Using the Galerkin approach, Sathyamoorthy (1994) demonstrated significant amplitude vibrations of fairly thick spherical shells. Response of spherical shells to periodic load was reported by Ganapathi et al. (1994) applying a shear flexible element. Jing et al. (1995) examined bending behaviour, while Ye and Soldatos (1995) focused on buckling characteristics. The vibrations of laminated composite shells were the focus of Piskunov et al. (1994), Sathyamoorthy (1995), Mizusawa and Kito (1995) and Tessler et al. (1995). Ye and Han (1995) employed semi-analytical technique to investigate the nonlinear static bending and buckling characteristics of orthotropic shallow shells. Noor and Burton (1989, 1990) and Burton and Noor (1995) published exceptional reviews of computational models employed by many researchers and compared the accuracy of the results obtained by six different approaches of analysis. One of their studies focused on the topic of shear deformation in particular. Qatu (1996) used the Ritz approach with algebraic polynomials to find the natural frequencies of cantilevered shallow shells with triangular and trapezoidal planforms. Suzuki, Shikanai, and Leissa (1996) solved the displacement and rotations of free supported cross ply laminates. The frequencies of a set of elliptical cylindrical shells with varied stacking sequences were presented. By comparing the conclusions deduced from the new theory with those obtained from the classical laminated shell theory, the effect of shear deformation and rotary inertia was appreciated. Schokker et al. (1996) focused on dynamic buckling response of composite shells.

2.3. LITERATURES ON FAILURE STUDIES OF LAMINATED COMPOSITE PLATES AND SHELLS

The historical review establishes the fact that plates and shells being fabricated by laminated composites started gaining popularity from the second half of the last century and the truth that the failure behaviour of these materials weak in transverse shear needs to be studied in depth was realized by the researchers. Failure in composite begins with the yielding of the weakest lamina and can spread throughout the structure, leading to progressive failure. The reliability and performance of a composite structural component throughout its design life can be predicted only if the process of failure initiation, progression and the ultimate collapse characteristics can be correctly assessed. The collapse of a lamina in a laminate does not indicate total failure, as the failure of the laminate is progressive in nature. Each lamina in a laminate is presumed to be in a state of plane stress. Stresses in each lamina are evaluated separately by transforming the stresses in the principal material axis direction and applying suitable failure criteria. The load deflection behaviour of such thin laminates under transverse loads exhibits large deflection and hence demands for geometric nonlinear analysis involving complex numerical computation. Many factors like orientation of fibres, stacking pattern of laminas, manufacturing process and others decide the overall strength and performance of a laminate.

Tolson and Zabaras (1991) used an eight-noded serendipity and a nine-noded heterosis element to analyse the FPF and last ply failure (LPF) of a laminated composite simply supported square plate. The authors developed a computer code for performing the failure analysis using HSDT. A total of seven degrees of freedom were considered at each node (three translations, two rotations of normal to the mid plane about x and y axis and two warps of normal along x and y axes). The load increments and stiffness reductions

were repeated until element stiffness matrices of all layers were decreased to zero at a specific place.

Reddy et al. (1995) investigated the FPF and ultimate ply failure (UPF) of tensile test coupon and three-point bend test specimens of different span to depth ratios. The authors introduced the concept of 3D theory known as generalized layer wise plate theory (GLPT) as one of the alternative option to equivalent-single layer theory such as FSDT. GLPT assumes the piecewise continuity of displacement field and thus is capable of capturing the interlaminar stresses near the free edges and supports. For progressive failure analysis, stresses evaluated at Gauss points were extrapolated to nodes which were then put in to different failure criteria. Further, the stiffness properties were reduced at nodes based upon the failure modes. Authors used reduced integration for analysis based on FSDT and full integration was employed for GLPT. The significance of the effect of geometric nonlinearity on composite structure subjected to bending load was already explained by Reddy and Reddy (1992). The authors reported both linear and geometric nonlinear FPF and UPF loads for a simply supported three-point bend test sample under uniformly distributed central line load. Cheung et al. (1995) carried out the progressive failure analysis of anisotropic laminated composite plate developed from HSDT and failure criterion as proposed by Lee (1982). To calculate the central deflection, bending stresses, and maximum transverse shear stresses of a simply supported square LCP, the authors presented a finite strip approach. They noted that increasing the number of plies keeping total thickness constant significantly enhances the ultimate failure load of thick plates but similar characteristics were not found in case of thin plates. Padhi et al. (1998) reported FPF and progressive failure of LC structures for simple load cases like purely tensile, compressive or shear. At and post FPF, LC structures mostly shows both material and geometric nonlinearity. So authors attempted to develop the nonlinear load versus

deflection plot of LC plate for uniformly distributed normal pressure employing finite element program ABAQUS developed with FSDT. Both large strain and large deflection were taken in to consideration in their formulation. For progressive failure analysis, stiffness reduction was done at the integration points. Further, the numerical outcomes were compared against the previously published experimental results. Gummadi and Palazotto (1998) proposed a nonlinear finite element progressive damage model for LC plates and cylindrical shells using large displacement, rotation, and strain. Material nonlinearity was accommodated through various failure theories and geometric nonlinearity was incorporated by modifying the constitutive laws to account for large displacements, stresses, and rotations. Spottswood and Palazotto (2001) developed the finite element progressive damage model of a composite cylindrical shell panel established on third-order shear deformation theory, taking transverse shear and strain continuity into account. The finite element program developed, termed as simplified large displacement and rotation theory (SLR), considered the through thickness flexibility and reduced the shell problem from three dimension to two dimension. Kumar and Srivastava (2003) investigated the FPF strength of stiffened cross ply plates under evenly distributed and sinusoidal loads with varied stiffener geometry. Prusty (2005) investigated the linear FPF and progressive failure load of LC stiffened and unstiffened panels under transverse loading. An eight noded isoparametric quadratic element was employed to model the plate or shell element. The stiffener was modelled with a curved three-noded beam element. A total ply discount approach was adopted for progressive failure analysis where stiffness contribution of failed plies were totally discarded and the stiffness was recomputed with the available unaffected plies. Ganeshan and Liu (2008) determined the nonlinear FPF, UPF and buckling loads with failure modes and failed location for LC tapered plate under uniaxial compressive load. The authors developed the finite element

formulation using FSDT and von Kármán nonlinearity. The influence of different tapering angles, stacking patterns, and fibre angles on FPF, UPF and buckling loads were studied. Lopes et al. (2007) studied the post buckling progressive damage behaviour of LC panels made of straight fibres and tow steered fibres. Authors found that use of variable stiffened laminates and curvilinear fibres instead of straight fibres proved a marked improvement in the load carrying capacity. The damage initiation and stiffness degradation of continuum damage model was simulated by inserting a user defined finite element code in ABAQUS. Pal and Bhattacharyya (2007) studied the linear progressive failure analysis of simply supported laminated composite cross ply plate. The authors employed FSDT to add shear flexibility parameters throughout the thickness. Researchers like Nanda et al. (2009) performed geometric nonlinear transient analysis and reported the nonlinear displacements of geometrically flawed doubly curved laminated composite shells with and without cutouts. Zhang et al. (2010) devised a layerwise B spline finite strip method on stress and progressive failure analysis of composite laminates. The method was found to be efficient enough to predict both local and global stresses of both thick and thin laminates. Adali and Cagdas (2011) reported the first ply failure and buckling of simply supported and clamped cylindrical shell panels. The authors investigated the effects of fibre orientation, aspect ratio and panel thickness on failure and buckling stresses. They used eight node finite elements to analyse the stability and stress of symmetrically laminated angle ply laminates subjected to uniaxial compression. The minimum of buckling and first ply failure loads was defined as the governing failure mode. The authors found that first ply failure was the most common failure mechanism for thick panels, while buckling was the most common failure form for thin panels. Anyfantis and Tsouvalis (2012) developed nonlinear finite element formulation using ANSYS to estimate the LC stiffened panels' failure initiation and final failure

characteristics. Under compressive load, the developed progressive failure model was able to appropriately forecast the buckling and post buckling failure behaviour of the LC structural units. Ellul et al. (2014) presented the ultimate load and load deflection response of LC as a function of type of failure algorithm chosen for progressive failure analysis. In this work, the authors attempted to compute the UPF load of LCP for out of plane loads by three different approaches of stiffness degradation. These approaches were based upon total ply discount and failure mode dependent method. Besides, effects of different types of support conditions and mesh density on ultimate failure load were also investigated. Bakshi and Chakravorty (2012, 2013, 2014a, 2015) investigated the first ply failure analysis of laminated composite conoidal shells using geometric linear strains. The failure loads for clamped and simply supported boundary conditions were explored by the authors. In these investigations, different parametric variations were tested, such as lamina sequences (cross and angle ply), angle of laminations and number of repetitions of symmetric and anti-symmetric units. The authors (2014b) also looked into the first ply failure behaviour of composite cylindrical shells when geometric nonlinearity was taken into account and made some recommendations relevant to practising engineers. Gupta et al. (2012, 2013) used the FSDT to investigate the effect of evolving damage on the static response characteristics of laminated composite cylindrical and conical panels (Gupta et al., 2012) and plates (Gupta et al., 2013) subjected to uniformly distributed transverse loading. Later, the authors (2015) conducted a detailed parametric study to investigate the effects of evolving damage, span-to-thickness ratio, lamination scheme, boundary conditions and semi-cone angle on the post buckling response and failure load of laminated cylindrical and conical panels under meridional compression, taking geometric nonlinearity and evolving material damage into account. Namdar and Darendeliler (2017) studied the buckling, post buckling and progressive failure behavior of LC plates under

compressive loading. Hashin's failure criterion was used to compute the failure load and stiffness degradation were carried out for progressive damage analysis. The authors presented the experimental and numerical plots for load versus out of plane displacements.

Sabik (2018) presented the progressive failure of laminates based on 6-field shell theory. Modified Hashin hypothesis was adopted where elastic brittle material behavior was included to develop the constitutive model. The proposed method was found to be effective in analysis of regular and irregular shells. Xu et al. (2019) developed the nonlinear cohesive zone models (CZMs) based on recently developed augmented finite element method (A-FEM). Authors investigated the effects of complex stress conditions on crack growth and initiation of notched and un-notched composite laminates under tensile and compressive loads. The A-FEM tool was used to estimate damage at each load level. Joshi and Duggal (2020) computed the natural frequencies of LC plate under uniformly distributed load during progressive failure analysis using Jacobi iterative method. The finite element codes were developed in FORTRAN environment considering seven degrees of freedom at each node. The authors studied the effect of material and geometrical properties on natural frequencies of LC plate. The failure mode and the failed ply was identified using the Hashin failure criterion. Bishay et al. (2021) used the Monte Carlo Simulation to study the randomness effect of various input parameters including material and geometrical uncertainties on FPF load, failure probability and failed ply. The authors conducted failure investigation on LC plate under tensile loading based upon two limit theories (maximum stress and maximum strain) and two interaction theories (Tsai-Hill and Tsai-Wu).

Ghannadpour et al. (2021) carried out the progressive failure and buckling analysis of LC simply supported square plates under compressive load using semi

analytical method. This method for failure analysis of moderately thick to thick laminates was developed using HSDT and geometric nonlinearity. Ritz approximation was employed to simplify the formulation and Hashin-Rotem failure criterion was used to predict the failure loads. Gohari et al. (2015) studied the FPF characteristics of internally pressurized LC ellipsoidal shells made of woven glass fibre reinforced composite. Linear interpolation technique was used to interpolate the FPF pressure based upon Tsai-Wu failure criterion. The analytical outcomes were verified with the experimental results.

Hochard et al. (2006) developed the continuum damage model for LC made of woven fibres based nonlinear mechanics. Behaviour of both normal and perforated plates under static and fatigue tensile loads were investigated. Karsh et al. (2018) investigated the deterministic and stochastic behaviour of LC plates for spatially variable loading positions, taking into account the serviceability feature of delamination. The authors chose Monte Carlo Simulation (MCS) for the probabilistic analysis and finite element analysis for deterministic solution. The effect of ply stacking pattern, thickness, orientation of fibres and degree of orthotropy on failure strength were studied using different failure criteria. The results were validated against those published in literature.

Kelly et al. (2005) presented the failure investigation of LC plate under transverse concentrated loading both numerically and experimentally. The authors discussed the nonlinear load displacement behaviour of various laminations and specimens of various sizes, taking into account both intralaminar and interlaminar damage buildup. Knight et al. (2002) reported the geometric nonlinear progressive failure analysis of laminated composites under tensile and compressive load. Anish et al. (2019) employed IHSDT (intermediate HSDT) with C0 continuity to investigate the non-dimensional FPFL, failure mode and failure location of LC sandwich plate. A 2D finite element code was developed based on FORTRAN environment using nine-noded elements with seven degrees of

freedom at each node. Results were verified with those obtained through exact analysis available in literature. New results with uniform transverse and bisinusoidal loads for various boundary conditions, laminations and thicknesses, valuable to designers, were also published. Lal et al. (2012) examined the stochastic geometric nonlinear failure response of LC plate using C0 finite element based on HSDT employing von Kármán nonlinearity. The mean of nondimensional failure load and covariance of failure index of a geometric nonlinear composite plate were computed. In this computation, randomness in material properties and loading variation were considered for uniformly distributed transverse and sinusoidal loading. Hoffamn's and Tsai-Wu failure criterion were used in in probabilistic prediction of failure load and indices in which Hoffman's criterion was found to be more sensitive as compared to Tsai-Wu criterion. Lopes et al. (2008) presented ABAQUS subroutines to numerically compare the FPF and buckling characteristics of straight and curved fibres for evaluating the tailoring benefits in composites. A remarkable improvement in FPFL and buckling response was found when curvilinear fibres were used instead of straight fibres under compressive load. Moreno et al. (2016) reported the FPF mode of cross ply laminates using three-point bend test using standard fixture in a universal testing machine. The experimental results were compared against the analytical ones. Nagaraj et al. (2020) developed the Carrera Unified Formulation to study the impact induced progressive damage analysis of LC structure based on higher- order structural theories. The results obtained were compared with those available in literature and experimental outcomes. Onkar et al. (2007) studied the FPFL based on analytical and stochastic finite element methods. Effects of various thickness, ply sequences, plate aspect ratios and boundary conditions on FPF indices were investigated and reported.

Ray et al. (2019) investigated the experimental FPF of hybrid fibre and glass fibre reinforced plastic laminates. The derivative of the strain-displacement matrix was used to calculate transverse shear stresses. With C0 continuity, the warping effect was integrated through refined higher-order zigzag theory. Taetragool et al. (2017) employed the Nest-Site Selection optimization algorithm to find the rotation of fibre in every ply of a rectangular laminate physically distorted by loads perpendicular to the main face that optimised the FPFL using the Tsai-Wu criterion for failure. A third order shear deformation and normal deformable plate theory (TSNDT) were used to examine the laminate deformations. In the progressive failure analysis, the material elasticities of a failed material point were lowered by a factor of 10e-06 until the laminate collapsed at the ultimate load. Mondal et al. (2018) explored the thermodynamic buckling and post buckling analyses of composite plates subjected to non-uniform heating. The delamainated plate was modelled based on Reddy's layerwise plate theory. The Tsai-Wu criterion identified the FPF of a composite plate as a result of localised heating. It was revealed from the study that the essential location of the heating area for a simply supported edge was closer to the boundary but for a clamped boundary condition, it is at the central. The failure temperature was found to be lower for increasing percentages of delamination. Yuan et al. (2017) experimentally studied the cracking strength and collapse mechanisms of thin ply carbon fiber-reinforced polymer (CFRP) angle-ply laminates and subsequently a finite element method (FEM) and theoretical mode were used to anticipate the results. Both analytical and FEM models were developed to predict the strength and failure modes of thin ply CFRP angle-ply laminates with different ply thicknesses and fibre volume fractions. Eventually, the failure of thin ply angle-ply laminates under tensile load was depicted pictorially, illustrating the various failure mechanisms (fibre breaking, delamination, and transverse matrix failure). Zahari et al.

(2009) developed the nonlinear analysis based on finite strip approach implementing the latest polynomial finite strip elements and Mindlin's theory. Applying the Tsai–Wu stress-based failure criterion, a progressive failure algorithm for composite laminates was effectively designed for the new finite strip approaches. With the Mindlin plate-bending element, a finite strip analysis programming package was created that was capable to execute progressive nonlinear failure analysis of stiffened composite plates and shells. By comparing the findings with ABAQUS based finite element analysis, the new finite strip package was successfully validated. Kharghani et al. (2019) used HSDT integrated with fracture analysis to anticipate the ultimate strength of laminated composite with delamination under compressive load. A close agreement between analytical and experimental outcome confirmed the capability of this improved analytical method in correct prediction of load and displacement at the delamination site. Kumar et al. (2015) presented the failure analysis of laminated composite and sandwich cylindrical shells using 2D C0 finite element model employing higher-order zig zag theory. Non dimensional uniformly distributed and sinusoidal FPFL were reported for laminated composite and sandwich cylindrical shells with different parametric variations. Hu et al. (2006) performed the buckling analysis of composite skew laminates using finite element for uniaxial compressive loads considering material nonlinearity based on Tsai-Wu failure theory with nonlinear in-plane shear. The effect of stacking sequence, skew angle and plate aspect ratio on the buckling characteristics of composite skew plates were reported. Prusty (2005) studied the linear progressive failure behaviour of unstiffened and stiffened composite panels under transverse static loading with eight noded isoparametric quadratic elements in association with three-noded curved beam elements using FSDT and Tsai-Wu failure criteria. Post FPF, the stiffness of the failed lamina was totally discarded from the laminate and the remaining laminae were considered for further

analysis. Kumar and Srivastava (2003) developed a finite element formulation to predict the sinusoidal and uniformly distributed FPF load of stiffened cross-ply plates with I, Hat and blade sections and varying fibre angles ranging from 15˚ to 75˚ using various distinguished failure theories. The plates stiffened with blade stiffener were found to show higher failure loads than the I-sectioned stiffened plates for fiber angles below 45˚. Prusty et al. (2001a) studied the FPF analysis of laminated composite shallow and deep shell roof panels under transverse static load using various prominent failure theories including the Yeh-Stratton theory. Prusty et al. (2001b) reported the FPF load of laminated composite stiffened and unstiffened panels for various loading conditions such as central concentrated load, uniformly distributed load and sinusoidal load. Various failure theories were used such as maximum stress, maximum strain and those of Hoffman, Tsai-Wu and Yeh-Stratton. Chang (2000) studied the experimental and analytical FPF strength of symmetrically laminated composite pressure vessels for various material properties, radius to thickness ratios and different number of layers considering uniform internal pressure loads. Maximum strain, Hoffman, Tsai-Hill and Tsai-Wu failure criteria were used to predict the FPF load of clamped vessel. Kam and Lai (1999) presented the experimental and theoretical FPF strength of LCP under different loading conditions and aspect ratios. Bogetti et al. (2015) conducted the nonlinear progressive failure analysis to study the through thickness response of laminated composite plates based on maximum strain criterion. The authors also reported the limitation of their method in predicting the overall growth of damage due to its post failure capacity. Kumar and Chakrabarty (2017) used a finite element (FE) model with nine nodes per element and seven degrees of freedom per node to investigate the FPFL of laminated composite skew plates. For simply supported and clamped boundary edges, failure loads were furnished using several failure theories.

Xie, Liu and Wang (2019) have studied the free vibration characteristics of parallelogram laminated thin plates under multi-points supported elastic boundary conditions using improved Fourier series method. To simulate the various boundary constraints, artificial virtual springs were introduced. Classical thin plate elasticity theory was used to establish the energy equations which were solved by Rayleigh-Ritz method. The authors obtained the natural frequencies and mode shapes of parallelogram laminated thin plates and the numerical results were compared with finite element outputs.

Srinivasa et al. (2014) presented the experimental and finite element investigation on free vibration characteristics of isotropic and composite skew plates. The free vibration response were analysed using CQUAD8 and compared with the experimental and finite element solution. The effects of skew angle, aspect ratio, fiber orientation angle and laminate stacking sequence on the natural frequencies of antisymmteric laminated composite skew plates were studied. Srinivasa et al. (2012) examined the fundamental flexural frequencies of isotropic and laminated composite skew plates with simply supported and clamped boundary conditions. Lee (2010) studied the dynamic stability analysis of laminated composite skew plates based on HSDT. Numerical results were obtained for square and skew plates with and without cutouts. Effects of various parameters such as skew angle, cutout size, fiber angle, thickness-to-length ratio were reported. Gurses et al. (2009) studied the free vibration of laminated skew plate using discrete singular convolution (DSC) method. Singha and Daripa (2007) examined the large amplitude free vibrations of skew plates using four noded shear flexible quadrilateral high precision plate bending element for both clamped and simply supported boundary conditions. The authors reported that the nonlinear frequency ratio increases with the increase in thickness and skew angle. Bakshi et al. (2020) studied the geometric nonlinear FPF of thin laminated composite conoidal shell roofs. For varied curvature and

aspect ratio of the shell, the study gives the failure loads, locations on the shell surface where the failure begins and the lamina stress that regulates failure onset. Bakshi et al. (2014b) conducted the geometric nonlinear FPF investigation of laminated composite cylindrical shells. The authors tabulated the failure loads, the failure modes and tendencies and location of failure initiation on the shell surface. Cagdas et al. (2013) investigated the influence of fibre orientation on the uniaxial compressive failure load of curved composite panels for mixed boundary conditions. Among the buckling and first ply failure analysis, the failure load was defined as the lesser of the two. The failure load was investigated for different laminations, fibre orientations, thickness and aspect ratios.

Chang et al. (2010) employed both experimental and theoretical methodologies to study the FPF strength of antisymmetrically laminated composite elevated floor plate with varied length-to-depth ratios, aspect ratios and ideal fibre orientations. An acoustic emission (AE) technique was used to conduct an experimental assessment of first ply failure strength of a composite plate subjected to static transverse load. The numerical analysis on the other hand was performed using the ANSYS linear finite-element programme. Das et al. (2008) presented the results of a large-amplitude free vibration analysis of thin isotropic skew plates. Backbone curves in a non-dimensional frequency–amplitude field were used to depict the dynamic behaviour of skew plates. The impact of various types of loadings, as well as the combination of clamped and simply supported boundary conditions, was examined. Ghosh and Chakravorty (2014) studied and reported the linear FPF and UPF load of simply supported laminated composite skewed hypar shells. The initial and progressive failure of simply supported hypar shells under transverse distributed pressure were studied. Post FPF, the stiffness of the failed element was completely neglected and subsequent analysis were carried out with the remaining laminate. Das et al. (2010) solved the bending problem of a composite stiffened conoidal

shell subjected to central concentrated load using a combination of an eight-noded shell element and a three-noded beam element. Static deflections as well as force and moment resultants were extensively investigated. The relative performances of the various shell options were investigated by ranking them and using a typical relative performance matrix.

Huang et al. (2005) used double Chebyshev series for analytical computation of post buckling response of LCP with random short spatial fibres. First-order shear deformation theory and von Kármán nonlinearity were used in the mathematical formulation. For various boundary conditions and the number of layers in the composite, numerical results for E-glass/Epoxy fibre reinforced laminates were reported. It was concluded that composites with fibres in perfect random dispersion found to be stronger in buckling and post buckling strength. Lai et al. (2011) studied the effectiveness and reliability of the DSC-Element approach for oblique plates with big skew angles. Frequency response analysis of skew plates was conducted for varied skew angles, thickness and aspect ratios. Narwariya et al. (2019) presented the harmonic behaviour of laminated composite skew plates using symmetric and anti-symmetric layer configurations. The impacts of different skew angles, lamination schemes and layer counts were demonstrated. The largest resonance amplitude occurred at the first fundamental mode of vibration for various skew angles. The plates were analysed using the ANSYS finite element programme. Reddy et al. (1987) presented the finite element computational procedure of FPF of composite laminates under inplane and transverse loads considering several failure theories. It was found that all theories of failure were equally efficient to predict the FPF of composite laminates for inplane loads, whereas for transverse load, maximum strain and Tsai-hill criteria were governing. Iyengar and Srinivasan (1967) presented the double series method to compute the deflection and

bending moments for isotropic skew plates under uniformly distributed loading for various aspect ratios and skew angles.

2.4. RECENT RESEARCH ON LAMINATED COMPOSITE PLATES AND SHELLS

In this section, some of the very recently published papers within the last decade are discussed to highlight the recent trend of research in areas of laminated composite plates and shells. Coelho et al. (2015) used the Hashin's failure criterion to forecast damage onset in punctured laminated composites under in-plane tensile strain. The authors used the brick elements that behaved like shell elements in terms of kinematics and constitutive behaviour. The Newton – Raphson approach was used to solve the nonlinear governing equation. The authors used Hashin's failure theory to determine the failure of the composite laminates. Chrócielewski et al. (2016) used a nonlinear finite element approach to study the FPF stresses of LCP and cylindrical shell panels with updated Tsai Wu's and Hashin's failure criteria. Reinoso and Blázquez (2016) used geometric nonlinearity to study post-buckling failure of a composite cylindrical stiffened panel subjected to uniform pressure load. Using Hashin failure criteria, Laxminarayana et al. (2016) investigated the progressive failure of a symmetrically LCP with circular and elliptical cutout subjected to uniaxial compressive force. The authors showed how the magnitude of FPF strength is affected by the size, shape and orientation of cutouts together with plate thickness. Using the finite element approach, Priyadharshani et al. (2017) investigated glass fibre reinforced polymer (GFRP) stiffened composite plates with and without rectangular cutout under axial, lateral, and combined axial and lateral loadings. Bakshi (2021) studied the free vibration behavior of laminated composite stiffened cylindrical shell using C^0 finite elements for various boundary conditions, laminations and stiffeners positions. The author modeled the curved surface with

geometric nonlinear strains but for stiffener modeling, the author considered both linear and nonlinear strains. Polturi and Rao (2019) investigated the effects of circular cutouts on the buckling behaviour of thin composite laminated plates. With the increase in cut-out dimension, the buckling load factor at higher modes was shown to have decreased. Ferreira et al. (2022) studied the progressive damage behavior of LCP subjected to three point bending using Carrera's unified simulation combined with the principles of continuum damage mechanics written as a user element subroutine in FORTRAN. The authors further made an experimental validation of their reported work. The method was found to be computationally efficient enough to predict out of plane stresses to predict delamination. Ge et al. (2022) studied the low velocity impact response of woven carbon fibre reinforced thick laminate. The authors examined the dynamic characteristcs such as peak force and displacement both numerically using ABAQUS and experimentally by extracting the load displacement curve of drop weight testing machine. Damage morphology was further investigated using ultrasonic C scan and digital microscope where various modes of failure were identified including indentation, delamination, fibre breakage and matrix cracking. Hu et al. (2022) determined the flexural failure characteristics of carbon fibre reinforced epoxy/ aluminum laminates under three point bend test. The addition of layers of composite laminated sheets with metallic sheets showed a significant improvement in strength and stiffness. Further a good consistence was found between experimental numerical results computed using Linde failure criterion. Wang et al. (2022) reported the progressive damage behavior of glass fibre reinforced composite open-hole plate at room temperature in dry and hygrothermal state. It was found by the authors the presence of hygrothermal environment significantly reduce the ultimate tensile and compressive strength by 39% and 35% respectively. Although the time of damage progression was shortened under tensile loading but same

was not much affected for compressive loading. The numerical model was developed in ABAQUS using user subroutine and the experimental verification of the same was also performed. Falcó et al. (2022) performed the experimental and numerical investigations of low velocity impact damage on laminated composite starting from damage initiation to full penetration through the laminates. The virtual laboratory was integrated with ABAQUS/Explicit, a commercially available explicit FE solver programme. The stability, load carrying capacity and failure analysis of CFRP LCP with cutout under compressive load were investigated by Falkowicz et al. (2021). The study comprised of both experimental tests on genuine samples and numerical computations utilizing the ABAQUS® program's finite element approach. The effect of compressive loads on the buckling and post-buckling behaviour of thin-walled composite plates, as well as the loss of load capacity was examined. Acoustic emissions were employed in the experiments to determine the state of the composite material's deterioration. Numerical calculations were performed for progressive failure analysis, which was based on the commencement of the failure using Hashin's theory and the subsequent progression of the failure using the energy criterion. Experimental outputs were compared with numerical results of critical and post critical states to show locations prone to material failure. Mahdy et al. (2021) presented a competitive framework for failure analysis of composite laminated cylindrical shell. For buckling failure analysis, the linear buckling interacting curve approach was utilized and for stress failure analysis, the strength ratio based on the Tsai-Wu failure criterion was applied. It was found that buckling failure was more likely in composite materials with higher longitudinal compressive strength to longitudinal modulus and shear strength to longitudinal modulus ratios; otherwise, stress failure occurred. Gupta and Pradymna (2022) studied the free and forced vibration characteristics of variable stiffness laminated composite and sandwich shells with curvilinear fibres using

Newmark's time integration technique. The authors employed C^0 nine noded isoparametric element with thirteen degrees of freedom at each node and TSDT and geometrical nonlinearity was included by using von Kármán nonlinear strain–displacement relations. Liu et al. (2021) introduced a new rectangular element for doubly curved LC shells based on new set of strain based shape functions that considered the effect of shear stress based of Mindlin plate theory. For the purpose of validating the proposed method, numerical results of linear static bending, dynamic vibration and nonlinear bending of flat plate, cylindrical shell and doubly-curved laminated shell were compared with results in published literatures and with those obtained by ABAQUS simulation. Mohammadrezazadeh and Jafari (2021) analysed and reported the nonlinear vibration of LC cylindrical and conical shells considering the rotary inertia and shear deformation. While the geometrical nonlinearity was addressed using the von Kármán technique, the basic equations of the system were obtained using the Hamilton principle. The Ritz method was used to turn these equations into nonlinear ordinary differential equations based on the time variable. Lu and Guo (2022) developed the continuum damage model for accurate failure prediction of laminated composite. Fracture behaviour of each lamina was modelled presuming homogenous properties and the interlaminar delamination were predicted deploying cohesive element. Liu et al. (2023) investigated the low velocity impact induced damage and fracture behavior of carbon/glass fibre hybridised composite plate with varying mass proportion of carbon and glass fibres. The failure modes found were fibre matrix debonding and fibre failure. The authors reported the experimental load deformation behavior and also conducted the numerical simulation of the impact induced damage models using LS DYNA solver and found that glass fibres showed better impact resistance than carbon fibres. Li et al. (2023) studied the low velocity impact induced damage for different impact energies and reported the impact

force versus displacement curves. Further, the damage was inspected both visually as well as using ultrasonic and computed tomography scan. Falcowicz (2023) presented the failure and stability analysis of thin carbon fibre reinforced LCP with cut out under axial compressive load. Both experimental and numerical experimentation were performed and a good agreement was found among the results.

In the following subsection, the volume of literature presented above is critically examined in order to determine the main areas where research activities may be carried forward.

2.5 CRITICAL DISCUSSIONS

An in-depth analysis of the research publications related to laminated composite plates and shells establishes the fact that the researchers are focusing on failure analysis of these structural elements in recent times. The journey on failure analysis started in the last decade of the last century when Reddy et al. (1995), Padhi et el. (1998) and Gummadi and Palazotto (1998) reported nonlinear failure analysis of composite plates and cylindrical shells. Thereafter, Knight et al. (2002) carried out similar work on composite curved and flat panels followed by researchers like Ganeshan and Liu (2008), Ellul et al. (2014), Ghannadpour and Abdollazadeh (2021) and then by Kharghani and Soares (2019) very recently who worked on composite plates under different loading conditions. Gupta et al. (2015) reported progressive damage of cylindrical and conical composite panels under meridional compression. Linear and nonlinear first ply failure of composite skew plates and skewed hypar shells were studied and reported by Ghosh and Chakravorty (2014, 2018 a, 2018 b) and Kumar and Chakrabarty (2017).

Kumar and Chakrabarty (2017) carried out a limited study of FPF of skew plates but the aspect of nonlinear analysis of first and progressive failure was not addressed. Ghosh and Chakravorty (2014, 2018 a and 2018 b) carried out some study on nonlinear

failure of skewed hypar shells but this area needs to be studied in greater details for other practical boundary and loading conditions. Based on the above observations the actual scope of present work is presented in the next chapter.

Chapter 3

SCOPE OF PRESENT STUDY

3.1. GENERAL

The in-depth analysis of the literature that is presented in Chapter 2 and the critical evaluation of it, point to a number of possible directions for further research. The purpose of the present thesis is to focus on a specific area within the comprehensive scope of future research possibilities. The scope of this thesis is methodically provided in Section 3.2.

3.2. PRESENT SCOPE

For the first and progressive ply failure analyses of industrially significant skew plates and anticlastic skewed hypar shells, a generalized finite element formulation using eight noded isoparametric curved quadratic Serendipity finite elements is described in Chapter 4.

In order to establish the applicability of the current approach, a significant number of benchmark problems are solved. Various well established failure criteria such as maximum stress, maximum strain and that of Tsai-Wu, Tsai-Hill, Hoffman, Hashin and Puck are used to study various important aspects of failure behaviour which are reported in Chapters 5 to 9. The failure load values obtained by linear and nonlinear approaches are studied using both linear strains as proposed by Sanders and nonlinear components of strains as recommended by von Kármán. The major outcomes of the numerical experiments are the values for the first ply failure loads, the failure modes or tendencies,

governing failure criteria, zone of failure initiation and propagation, ultimate ply failure load, percentage and nature of damaged area at ultimate failure load. A variety of other pertinent data that describe the failure behaviour of skew plate and skewed hypar laminated composite shells are obtained from the results after post-processing.

Chapter 5 deals with study of linear first ply failure behaviour of laminated composite skew plates for various edge conditions.

The linear and nonlinear failure loads of laminated composite skew plate roofs for clamped boundary condition are reported in Chapter 6.

The first and ultimate ply failure characteristics, considering geometrically linear and nonlinear strains of fully clamped and irregularly supported skew plate roofs with varying skew angles and laminations, are furnished in Chapter 7 and 8 respectively. Specific guidelines regarding areas on the plate surface where non-destructive testing procedure may be carried out are also indicated.

Chapter 9 presents the nonlinear first ply failure study of skewed hypar shell for (clamped-free) mixed boundary condition. All the results are meticulously analyzed to arrive at conclusions of engineering significance.

The scope of future research in line with the area addressed in this thesis is described in Chapter 10.

Chapter 4

MATHEMATICAL FORMULATION

4.1. GENERAL

This chapter presents the mathematical formulation to address the scope of the present research. A finite element code based on user based subroutines is developed in FORTRAN environment which can successfully compute geometric linear and nonlinear strains of thin laminated composite skewed plates and skewed hypar shell roofs. The present computer code further can evaluate the first and ultimate ply failure strength of the above mentioned structural units subjected to uniformly distributed load for different boundary conditions and laminations. Besides, the present code is capable to predict the failure location (such as failed element, failed Gauss point etc.) and failure mode or tendencies. The present code implements eight noded isoparametric serendipity plate and curved shell elements to develop the structural models. The displacement field, strain-displacement relations, finite element formulation, constitutive relations of composite materials, governing nonlinear equilibrium equation and its solution procedure, lamina stress computations, failure theories used to explore the first and progressive ply failure characteristics are covered in details in several sections of this chapter. The symbols used to describe the formulation are explained either where they appear initially or in the list of 'Notations' at the beginning of the thesis.

4.2. COMPOSITE PLATE AND SHELL ELEMENT

4.2.1. Mid-Surface Equation of Skew Plate Geometry

A skew plate (Fig. 4.1) of plan dimension $a \times b$ is considered such that the total thickness of the laminate is h (consisting of n number of layers with each of equal thickness, h/n). The laminas are numbered sequentially from top to bottom in order of their stacking. The skew angle is measured in terms of angle λ (shown in Fig. 4.1). x, y and z represent the global coordinate system of the skew plate surface (Malekzadeh 2008). The equation of plate mid-surface in global Cartesian system x, y, z can be written as,

$$x = x' + y' \, sin\lambda; y = y' cos\lambda; z = z' \tag{4.1}$$

where, x' and y' are non-orthogonal axes parallel to the edges of the skew plate and z'axis is perpendicular to $x' - y'$plane. This means that x' and z' axes coincide with x and z axes respectively.

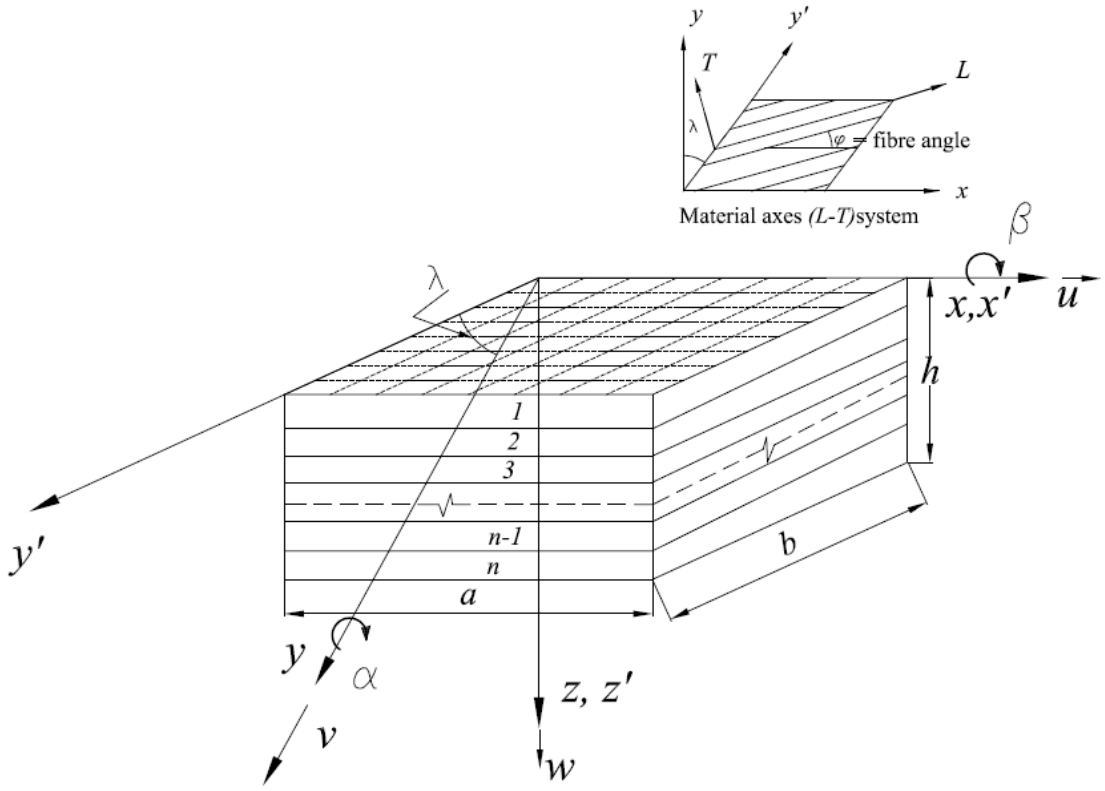

Fig. 4.1 Schematic representation of skew laminated composite panel

4.2.2. Mid-Surface Equation of Skewed Hypar Shell

A skewed hypar shell with its projection on *x*-*y* plane, having dimensions $a \times b$ is shown in Fig. 4.2. The total thickness is $'h'$(consisting of n number of layers of equal thickness, h/n) and a twist radius of curvature R_{xy} is considered. The expression of cross curvature $(1/R_{xy})$ is given as,

$$C_{xy} = 1/R_{xy} = \frac{\partial^2 z}{\partial x \partial y} = \frac{4c}{ab} \tag{4.2}$$

The equation of shell mid-surface in the global Cartesian (x, y, z)system can be expressed as,

$$z = (4c/ab)(x - a/2)(y - b/2) \tag{4.3}$$

The height of each ply $(1, 2, \ldots n)$ is measured from the midsurface in terms of $h_0, h_1, h_2 \ldots\ldots, h_n$. The fibres in each lamina may be oriented at an arbitrary angle φ with respect to global x axis.The material axes are represented by means of L, T and T' axes where T' axis is perpendicular to the L, T plane.

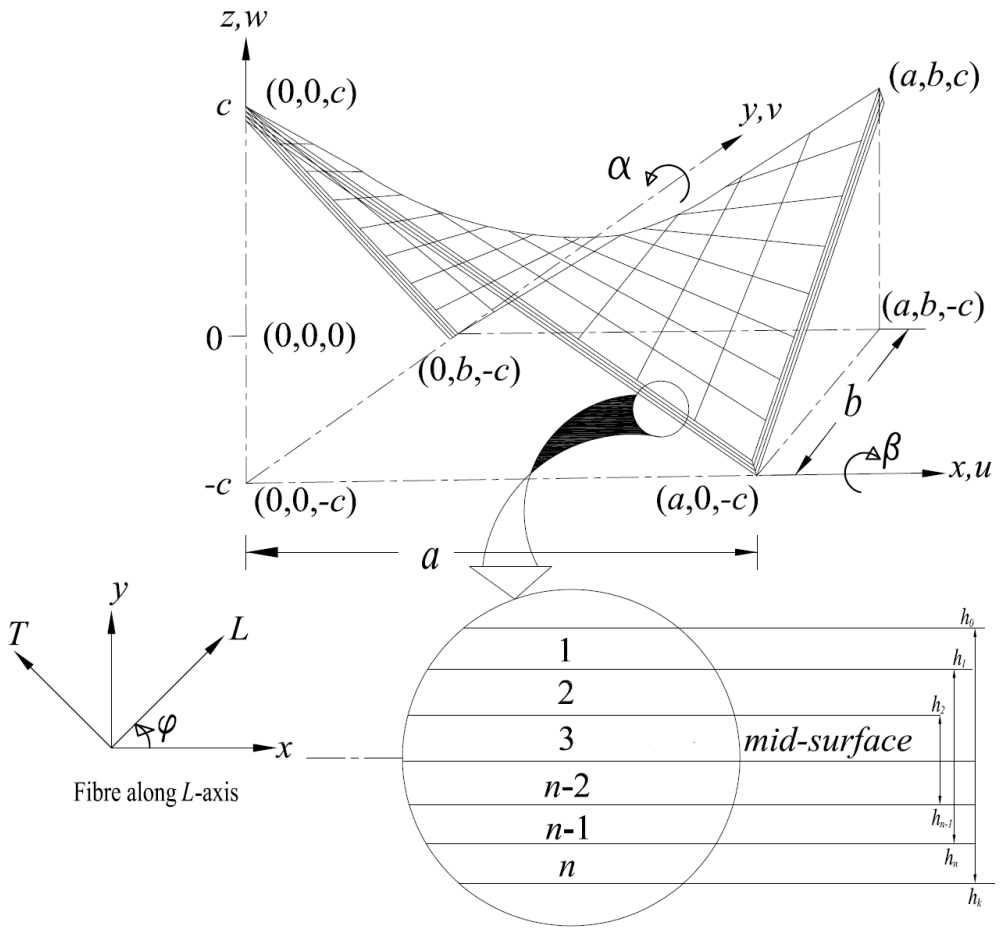

Fig. 4.2 Schematic representation of laminated composite skewed hypar shell geometry

4.3. DISPLACEMENT FIELD

The translational displacement at any node along x, y and z directions are given by u, v and w respectively and the rotations about x and y axes are indicated by β and α respectively. The displacement field is obtained based on the following assumptions:

1. Total thickness h of the laminate is equal to the sum of the thickness of each ply and the bond between the plies is assumed to be of zero thickness.
2. In Fig.4.3, line AB is the transverse normal which is straight and perpendicular to the mid-surface before bending remains straight but not necessarily perpendicular to the mid-surface after bending (thus, $\varepsilon_z = 0, \gamma_{xz} \neq 0, \gamma_{yz} \neq 0$).

3. Also point B moves by a distance u_0 in the x direction, v_0 in the y direction and w_0 in the z direction and line AB is rotated to $A'B'$ by an angle α along y direction as depicted in the Fig.4.3.

   Thus, the displacement of any point C at a distance z from point B in the deformed configuration is given as:

$$u(x,y,z) = u_0(x,y) + z\alpha = u_0(x,y) + z\left(-\frac{\partial w_0(x,y)}{\partial x}\right)$$
$$v(x,y,z) = v_0(x,y) + z\beta = v_0(x,y) + z\left(-\frac{\partial w_0(x,y)}{\partial y}\right) \quad (4.4)$$
$$w(x,y,z) = w_0(x,y)$$

Here u_0, v_0 and w_0 are the mid plane or mid-surface displacements and α and β are the rotations along x and y axes respectively.

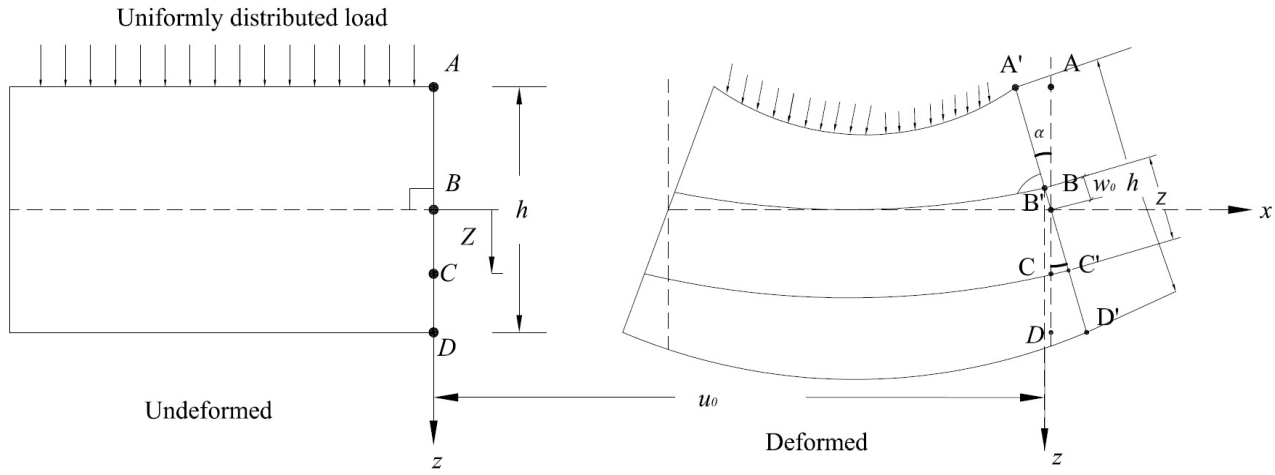

Fig. 4.3 Displacement of a point on any lamina

4.4. STRAIN-DISPLACEMENT RELATIONS

The strain components at a distance z from mid surface are $\varepsilon_x, \varepsilon_y, \gamma_{xy}, \gamma_{xz}$, and γ_{yz} which may be expressed as:

$$\{\varepsilon_x \quad \varepsilon_y \quad \gamma_{xy} \quad \gamma_{xz} \quad \gamma_{yz}\}^T = \{\varepsilon_x^0 \quad \varepsilon_y^0 \quad \gamma_{xy}^0 \quad \gamma_{xz}^0 \quad \gamma_{yz}^0\}^T + z\{\kappa_x \quad \kappa_y \quad \kappa_{xy} \quad \kappa_{xz} \quad \kappa_{yz}\}^T \tag{4.5}$$

Here, the mid-surface strains may be written considering von Kármán nonlinearity and first order shear deformation effect as:

$$\varepsilon_x^0 = \frac{\partial u_0}{\partial x} + \frac{1}{2}\left(\frac{\partial w_0}{\partial x}\right)^2; \varepsilon_y^0 = \frac{\partial v_0}{\partial y} + \frac{1}{2}\left(\frac{\partial w_0}{\partial y}\right)^2; \gamma_{xy}^0 = \frac{\partial u_0}{\partial y} + \frac{\partial v_0}{\partial x} - \frac{2w_0}{R_{xy}} + \left(\frac{\partial w_0}{\partial x}\right)\left(\frac{\partial w_0}{\partial y}\right)$$

$$\gamma_{xz}^0 = \left(\frac{\partial w_0}{\partial x}\right) + \alpha - \left(\frac{v_0}{R_{xy}}\right);\ \gamma_{yz}^0 = \left(\frac{\partial w_0}{\partial y}\right) + \beta - \left(\frac{u_0}{R_{xy}}\right)$$

In the above expressions, the component $R_{xy} = \infty$ for skew plates. The same logic applies to other places also throughout the thesis.

The mid-surface curvatures are described as:

$$\kappa_x = \frac{\partial \alpha}{\partial x};\ \kappa_y = \frac{\partial \beta}{\partial y}; \kappa_{xy} = \frac{\partial \alpha}{\partial y} + \frac{\partial \beta}{\partial x};\ \kappa_{xz} = \kappa_{yz} = 0$$

The strain components in consolidated generalized form is expressed as:

$$\{\varepsilon\} = \{\varepsilon_x{}^0 \quad \varepsilon_y{}^0 \quad \gamma_{xy}^0 \quad \kappa_x \quad \kappa_y \quad \kappa_{xy} \quad \gamma_{xz}^0 \quad \gamma_{yz}^0\}^T = \{\varepsilon_{inplane} \quad \varepsilon_{bending} \quad \varepsilon_{shear}\}^T + \{\varepsilon'_{inplane} \quad 0 \quad 0\}^T = \{\varepsilon_{linear}\} + \{\varepsilon_{nonlinear}\} \tag{4.6}$$

Here, the in-plane, bending and shear strain components are expressed as:

$$\{\varepsilon_{inplane}\} = \left\{\frac{\partial u_0}{\partial x} \quad \frac{\partial v_0}{\partial y} \quad \left(\frac{\partial u_0}{\partial y} + \frac{\partial v_0}{\partial x} - \frac{2w_0}{R_{xy}}\right)\right\}^T;$$

$$\{\varepsilon_{bending}\} = \left\{\frac{\partial \alpha}{\partial x} \quad \frac{\partial \beta}{\partial y} \quad \left(\frac{\partial \alpha}{\partial y} + \frac{\partial \beta}{\partial x}\right)\right\}^T; \tag{4.7}$$

$$\{\varepsilon_{shear}\} = \left\{\left(\frac{\partial w_0}{\partial x} + \alpha - \frac{v_0}{R_{xy}}\right) \quad \left(\frac{\partial w_0}{\partial y} + \beta - \frac{u_0}{R_{xy}}\right)\right\}^T;$$

The nonlinear inplane strains $\{\varepsilon'_{inplane}\}$ are described as:

$$\{\varepsilon'_{inplane}\} = \left\{\frac{1}{2}\left(\frac{\partial w_0}{\partial x}\right)^2 \quad \frac{1}{2}\left(\frac{\partial w_0}{\partial y}\right)^2 \quad \left(\frac{\partial w_0}{\partial x}\right)\left(\frac{\partial w_0}{\partial y}\right)\right\}^T$$

4.5. FINITE ELEMENT MODELLING AND SOLUTION

4.5.1. Selection of Finite Element and Structural Discretization

The accuracy of the results obtained through finite element analysis depends on the size of the finite elements. In the present work, the author chooses the eight-noded quadratic isoparametric plate element to model the skew plate and eight noded curved quadratic isoparametric shell element to model the skewed hypar shell. There are five degrees of freedom at each node [Chatterjee et al. (2021)] depicted in the Fig. 4.4. The plate and shell models are typically discretized in to 8×8 divisions in Fig. 4.5.

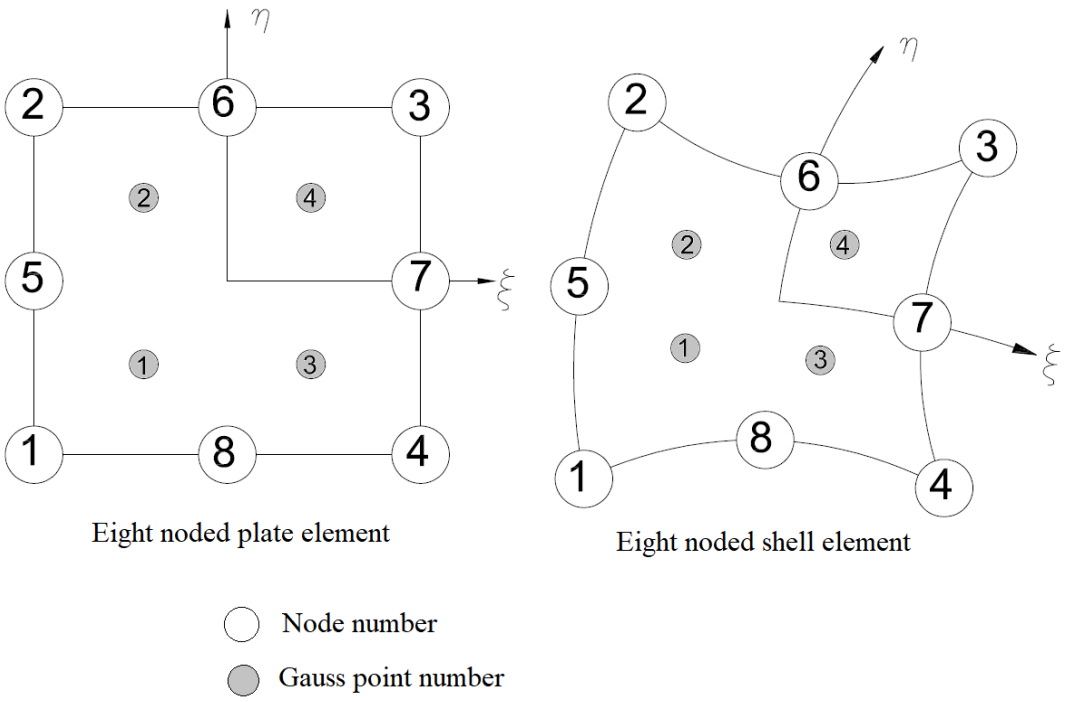

Fig. 4.4 The isoparametric plate and shell elements with natural coordinates

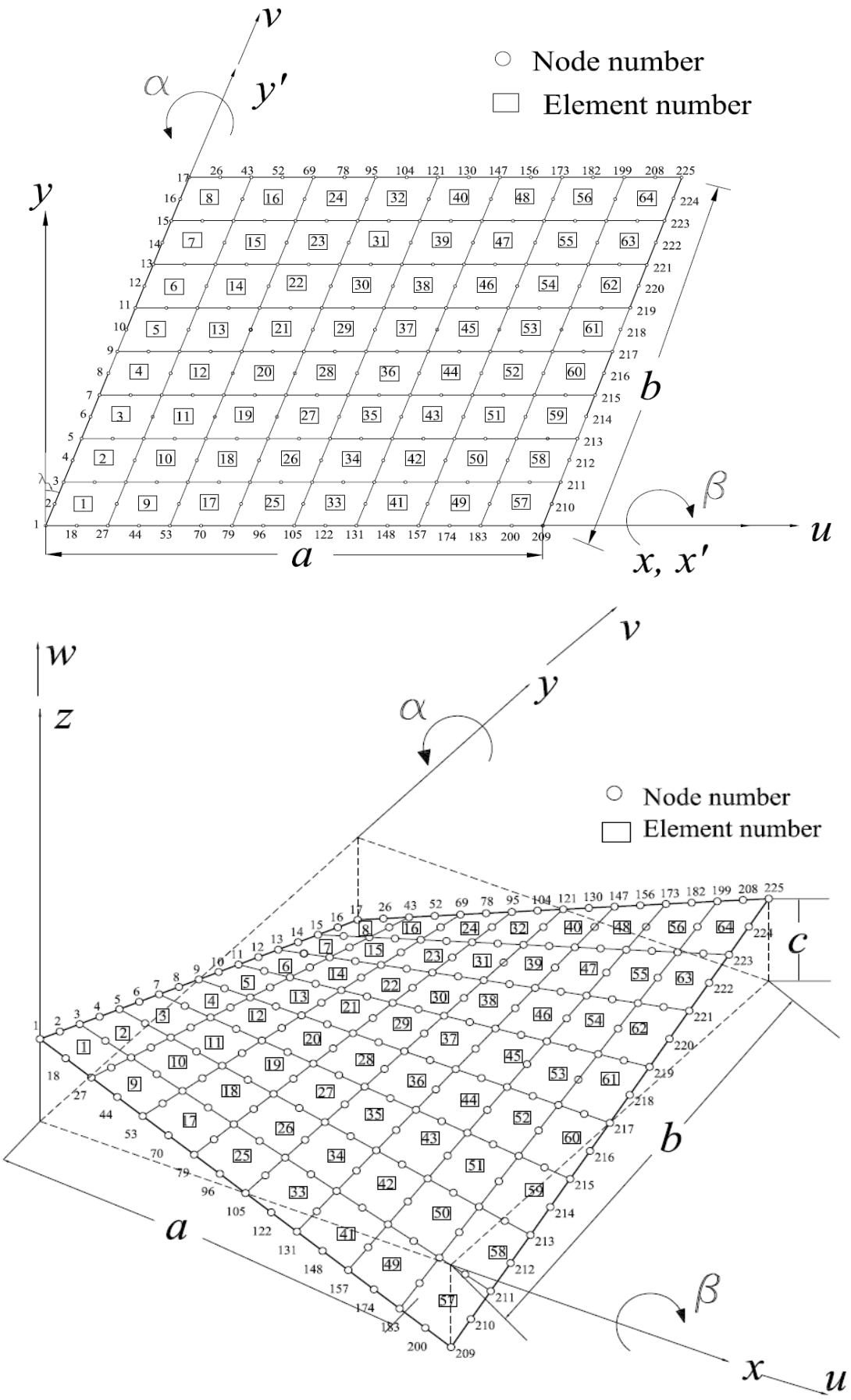

Fig. 4.5 An 8×8 discretization with element and node numbering

4.5.2. Selection of the Shape Function

The two dimensional shape functions are derived from the interpolation polynomial which describes the variation of displacement over the surface of the structural element and are expressed in natural coordinate system (ξ, η).

$$N_i = \frac{(1+\xi\xi_i)(1+\eta\eta_i)(\xi\xi_i+\eta\eta_i-1)}{4} \; for\; i = 1,2,3,4$$

$$N_i = \frac{(1+\xi\xi_i)(1-\eta^2)}{2} \; for\; i = 5,7 \tag{4.8}$$

$$N_i = \frac{(1+\eta\eta_i)(1-\xi^2)}{2} \; for\; i = 6,8$$

The displacement of any point within the element is expressed in terms of its nodal displacements as:

$$u_0 = \sum_{i=1}^{8} N_i u_i \; ; v_0 = \sum_{i=1}^{8} N_i v_i \; ; w_0 = \sum_{i=1}^{8} N_i w_i \; ; \alpha = \sum_{i=1}^{8} N_i \alpha_i \; ; \beta = \sum_{i=1}^{8} N_i \beta_i \tag{4.9}$$

Thus the generalized displacement $\{\delta_e\}$of any point within an element may be expressed in terms of nodal displacement $\{\delta\}$by

$$\{\delta_e\} = \sum_{i=1}^{8} [N_i]\{\delta\}_i \tag{4.10}$$

$$\begin{Bmatrix} u_0 \\ v_0 \\ w_0 \\ \alpha \\ \beta \end{Bmatrix} = \begin{bmatrix} N_i & 0 & 0 & 0 & 0 \\ 0 & N_i & 0 & 0 & 0 \\ 0 & 0 & N_i & 0 & 0 \\ 0 & 0 & 0 & N_i & 0 \\ 0 & 0 & 0 & 0 & N_i \end{bmatrix}_{i=1,2,3\ldots,8} \begin{Bmatrix} u_i \\ v_i \\ w_i \\ \alpha_i \\ \beta_i \end{Bmatrix}_{i=1,2,3\ldots,8}$$

The following relation expresses the derivatives of the shape functions N_i with respect to x and y in terms of their derivatives with respect to $\xi$and η through the Jacobian matrix [J].

$$\begin{Bmatrix} \frac{\partial N_i}{\partial x} \\ \frac{\partial N_i}{\partial y} \end{Bmatrix} = \begin{bmatrix} \frac{\partial \xi}{\partial x} & \frac{\partial \eta}{\partial x} \\ \frac{\partial \xi}{\partial y} & \frac{\partial \eta}{\partial y} \end{bmatrix} \begin{Bmatrix} \frac{\partial N_i}{\partial \xi} \\ \frac{\partial N_i}{\partial \eta} \end{Bmatrix} = [J]^{-1} \begin{Bmatrix} \frac{\partial N_i}{\partial \xi} \\ \frac{\partial N_i}{\partial \eta} \end{Bmatrix} \tag{4.11}$$

Here $[J]$ is expressed mathematically as: $\begin{bmatrix} \frac{\partial x}{\partial \xi} & \frac{\partial y}{\partial \xi} \\ \frac{\partial x}{\partial \eta} & \frac{\partial y}{\partial \eta} \end{bmatrix}$.

4.5.3. Strain-Displacement Matrices

The linear strains may be expressed in terms of shape functions and nodal displacement vector as:

$$\{\varepsilon_{linear}\} = \begin{Bmatrix} \frac{\partial u_0}{\partial x} \\ \frac{\partial v_0}{\partial y} \\ \frac{\partial u_0}{\partial y} + \frac{\partial v_0}{\partial x} - \frac{2w_0}{R_{xy}} \\ \frac{\partial \alpha}{\partial x} \\ \frac{\partial \beta}{\partial y} \\ \frac{\partial \alpha}{\partial y} + \frac{\partial \beta}{\partial x} \\ \frac{\partial w_0}{\partial x} + \alpha - \frac{v_0}{R_{xy}} \\ \frac{\partial w_0}{\partial y} + \beta - \frac{u_0}{R_{xy}} \end{Bmatrix} = \begin{Bmatrix} \frac{\partial \sum N_i u_i}{\partial x} \\ \frac{\partial \sum N_i v_i}{\partial y} \\ \frac{\partial \sum N_i u_i}{\partial y} + \frac{\partial \sum N_i v_i}{\partial x} - \frac{2 \sum N_i w_i}{R_{xy}} \\ \frac{\partial \sum N_i \alpha_i}{\partial x} \\ \frac{\partial \sum N_i \beta_i}{\partial y} \\ \frac{\partial \sum N_i \alpha_i}{\partial y} + \frac{\partial \sum N_i \beta_i}{\partial x} \\ \frac{\partial \sum N_i w_i}{\partial x} + \sum N_i \alpha_i - \frac{\sum N_i v_i}{R_{xy}} \\ \frac{\partial \sum N_i w_i}{\partial y} + \sum N_i \beta_i - \frac{\sum N_i u_i}{R_{xy}} \end{Bmatrix}_{i=1,2,\ldots\ldots,8} \tag{4.12}$$

$$= \begin{Bmatrix} \sum \frac{\partial N_i}{\partial x} u_i \\ \sum \frac{\partial N_i}{\partial y} v_i \\ \sum \frac{\partial N_i}{\partial y} u_i + \sum \frac{\partial N_i}{\partial x} v_i - \frac{2\sum N_i}{R_{xy}} w_i \\ \sum \frac{\partial N_i}{\partial x} \alpha_i \\ \sum \frac{\partial N_i}{\partial y} \beta_i \\ \sum \frac{\partial N_i}{\partial y} \alpha_i + \sum \frac{\partial N_i}{\partial x} \beta_i \\ \sum \frac{\partial N_i}{\partial x} w_i + \sum N_i \alpha_i - \frac{\sum N_i}{R_{xy}} v_i \\ \sum \frac{\partial N_i}{\partial y} w_i + \sum N_i \beta_i - \frac{\sum N_i}{R_{xy}} u_i \end{Bmatrix}_{i=1,2,\ldots\ldots,8}$$

$$= \sum \begin{bmatrix} \frac{\partial N_i}{\partial x} & 0 & 0 & 0 & 0 \\ 0 & \frac{\partial N_i}{\partial y} & 0 & 0 & 0 \\ \frac{\partial N_i}{\partial y} & \frac{\partial N_i}{\partial x} & \frac{-2N_i}{R_{xy}} & 0 & 0 \\ 0 & 0 & 0 & \frac{\partial N_i}{\partial x} & 0 \\ 0 & 0 & 0 & 0 & \frac{\partial N_i}{\partial y} \\ 0 & 0 & 0 & \frac{\partial N_i}{\partial y} & \frac{\partial N_i}{\partial x} \\ 0 & \frac{-N_i}{R_{xy}} & \frac{\partial N_i}{\partial x} & N_i & 0 \\ \frac{-N_i}{R_{xy}} & 0 & \frac{\partial N_i}{\partial y} & 0 & N_i \end{bmatrix} \begin{Bmatrix} u_i \\ v_i \\ w_i \\ \alpha_i \\ \beta_i \end{Bmatrix}_{i=1,2,\ldots,8}$$

which means

$$\{\varepsilon_{linear}\} = [B_l]\{\delta\} \quad (4.13)$$

Here $[B_l]$ is the linear part of the strain-displacement matrix$[B]$.The $[B_{nl}]$ is the nonlinear part of strain-displacement matrix $[B]$ and is a function of displacement.

$$[B] = [B_l] + [B_{nl}] \quad (4.14)$$

The nonlinear part of strain-displacement matrix $[B_{nl}]$may be given as:

$$[B_{nl}] = \begin{bmatrix} \partial w_0/\partial x & 0 & \partial w_0/\partial y \\ 0 & \partial w_0/\partial y & \partial w_0/\partial x \end{bmatrix}^T \sum_{i=1}^{8} \begin{bmatrix} 0 & 0 & \frac{\partial N_i}{\partial x} & 0 & 0 \\ 0 & 0 & \frac{\partial N_i}{\partial y} & 0 & 0 \end{bmatrix}$$

The generalised strain-displacement relations are now written as follows:

$$\{\varepsilon\} = \left(\left[[B_l] + 0.5[B_{nl}]\right]\right)\{\delta\} \tag{4.15}$$

4.6. LAMINATE CONSTITUTIVE RELATIONSHIP

4.6.1. Lamina Constitutive Relation in L, T, T' Axes System

The lamina constitutive relation for thin plate may be expressed in (L, T, T') coordinate system (refer Figs.4.1 and 4.2 and Section 4.2) as :

$$\begin{Bmatrix} \sigma_L \\ \sigma_T \\ \tau_{LT} \\ \tau_{TT'} \\ \tau_{LT'} \end{Bmatrix} = \begin{bmatrix} (E_L/(1-\nu_{LT}\nu_{TL}) & (\nu_{LT}\,E_L/1-\nu_{LT}\nu_{TL}) & 0 & 0 & 0 \\ (\nu_{LT}\,E_L/1-\nu_{LT}\nu_{TL}) & (E_T/1-\nu_{LT}\nu_{TL}) & 0 & 0 & 0 \\ 0 & 0 & G_{LT} & 0 & 0 \\ 0 & 0 & 0 & G_{TT'} & 0 \\ 0 & 0 & 0 & 0 & G_{LT'} \end{bmatrix} \begin{Bmatrix} \varepsilon_L \\ \varepsilon_T \\ \gamma_{LT} \\ \gamma_{TT'} \\ \gamma_{LT'} \end{Bmatrix} \tag{4.16}$$

$$\Rightarrow \{\sigma\}_{LT} = [Q]\{\varepsilon\}_{LT}$$

Here E_L, E_T are the longitudinal and transverse moduli of elasticities along L, T directions respectively. $G_{LT}, G_{TT'}, G_{LT'}$ are the respective shear moduli on LT, TT', LT' planes and ν_{LT} and ν_{TL} are the major and minor Poisson's ratios respectively. $[Q]$ is the lamina stiffness matrix and is the function of mechanical properties only.

4.6.2. Lamina Constitutive Relation in x, y, z Axes System

The stresses $\{\sigma\}_{xy}$in the x, y, z coordinate system may be written in terms of stresses $\{\sigma\}_{LT}$ as:

$$\begin{Bmatrix} \sigma_L \\ \sigma_T \\ \tau_{LT} \end{Bmatrix} = \begin{bmatrix} c^2 & s^2 & 2cs \\ s^2 & c^2 & -2cs \\ -cs & cs & c^2 - s^2 \end{bmatrix} \begin{Bmatrix} \sigma_x \\ \sigma_y \\ \tau_{xy} \end{Bmatrix} \Rightarrow \{\sigma\}_{LT} = [T]_1\{\sigma\}_{xy} \tag{4.17}$$

$$\begin{Bmatrix} \tau_{TT'} \\ \tau_{LT'} \end{Bmatrix} = \begin{bmatrix} c & s \\ -s & c \end{bmatrix} \begin{Bmatrix} \tau_{yz} \\ \tau_{xz} \end{Bmatrix} \Rightarrow \{\tau\}_{LT} = [TT]_1\{\tau\}_{xy}$$

Here $c = cos\phi$ and $s = sin\phi$

Similarly the strains $\{\varepsilon\}_{xy}$in the x, y, z coordinate system may be written in terms of stresses $\{\varepsilon\}_{LT}$ as:

$$\begin{Bmatrix}\varepsilon_L\\ \varepsilon_T\\ \gamma_{LT}\end{Bmatrix}=\begin{bmatrix}c^2 & s^2 & cs\\ s^2 & c^2 & -cs\\ -2cs & 2cs & c^2-s^2\end{bmatrix}\begin{Bmatrix}\varepsilon_x\\ \varepsilon_y\\ \gamma_{xy}\end{Bmatrix}\Rightarrow\{\varepsilon\}_{LT}=[T]_2\{\varepsilon\}_{xy} \tag{4.18}$$

and, $\begin{Bmatrix}\gamma_{TT'}\\ \gamma_{LT'}\end{Bmatrix}=\begin{bmatrix}c & s\\ -s & c\end{bmatrix}\begin{Bmatrix}\gamma_{yz}\\ \gamma_{xz}\end{Bmatrix}\Rightarrow\{\tau\}_{LT}=[TT]_1\{\gamma\}_{xy}$

Eq. (4.16) may be rewritten by combining Eqs. (4.17) and (4.18) as:

$$[T]_1\{\sigma\}_{xy}=[Q][T]_2\{\varepsilon\}_{xy}\Rightarrow\{\sigma\}_{xy}=[T]_1{}^{-1}[Q][T]_2\{\varepsilon\}_{xy}=[\bar{Q}]\{\varepsilon\}_{xy} \tag{4.19}$$

where $[\bar{Q}]=[T]_1{}^{-1}[Q][T]_2$

4.6.3. Laminate Constitutive Relation in x, y, z Axes System

The relation between force, moment and shear resultants (Refer Fig. 4.6) with mid-plane strains and curvatures may be represented as :

$$\{F\}=\{N_x\quad N_y\quad N_{xy}\ M_x\quad M_y\quad M_{xy}\ S_x\quad S_y\}^T=[D]\{\varepsilon\}=[D]\left(\{\varepsilon\}^0_{xy}+z\{\kappa\}_{xy}\right) \tag{4.20}$$

Here force resultants are: $\{N_x\quad N_y\quad N_{xy}\}^T=\int_{-h/2}^{h/2}\{\sigma_x\quad\sigma_y\quad\tau_{xy}\}^T dz$

$$\Rightarrow\sum_{k=1}^{n}\left[\bar{Q}_{ij}\right]_{k^{th}\ layer}\int_{z_{k-1}}^{z_k}\left(\{\varepsilon_x{}^0\quad\varepsilon_y{}^0\quad\gamma_{xy}{}^0\}^T+z\{\kappa_x\quad\kappa_y\quad\kappa_{xy}\}^T\right)dz$$

Moment resultants are: $\{M_x\quad M_y\quad M_{xy}\}^T=\int_{-h/2}^{h/2}\{\sigma_x\quad\sigma_y\quad\tau_{xy}\}^T.z.dz$

$$\Rightarrow\sum_{k=1}^{n}\left[\bar{Q}_{ij}\right]_{k^{th}\ layer}\int_{z_{k-1}}^{z_k}\left(z.\{\varepsilon_x{}^0\quad\varepsilon_y{}^0\quad\gamma_{xy}{}^0\}^T+z^2\{\kappa_x\quad\kappa_y\quad\kappa_{xy}\}^T\right)dz \tag{4.21}$$

Shear resultants are:$\{S_x\quad S_y\}^T=C.\int_{z_{k-1}}^{z_k}\{\tau_{xz}\quad\tau_{yz}\}^T dz$

$\Rightarrow C.\sum_{k=1}^{n}[\bar{Q}_{mn}]_{k^{th}\ layer}\int_{z_{k-1}}^{z_k}\{\gamma_{xz}\quad\gamma_{yz}\}^T.dz;$

here, shear correction factor $C=1$ for the class of thin plates and shells considered in the present study.

Combining Eqs.(4.20) and (4.21) we get the laminate stiffness matrix

$$[D] = \begin{vmatrix} [A]_{ij} & [B]_{ij} & 0 \\ [B]_{ij} & [D]_{ij} & 0 \\ 0 & 0 & [S]_{mn} \end{vmatrix}; i,j = 1,2,6;\ m,n = 4,5 \tag{4.22}$$

Mathematically the extensional stiffness matrix $[A]_{ij}$, coupling stiffness matrix$[B]_{ij}$, bending stiffness matrix $[D]_{ij}$and transverse shear stiffness matrix $[S]_{ij}$may be expressed as:

$$A_{ij} = \sum_{k=1}^{n} [\bar{Q}_{ij}]_k (z_k - z_{k-1})\,; B_{ij} = \frac{1}{2}\sum_{k=1}^{n} [\bar{Q}_{ij}]_k ({z_k}^2 - {z_{k-1}}^2);$$

$$D_{ij} = \frac{1}{3}\sum_{k=1}^{n} [\bar{Q}_{ij}]_k ({z_k}^3 - {z_{k-1}}^3)\,;\ i,j = 1,2,6$$

$$S_{mn} = f\sum_{k=1}^{n} [\bar{Q}_{mn}]_k (z_k - z_{k-1})\,;\ m,n = 4,5$$

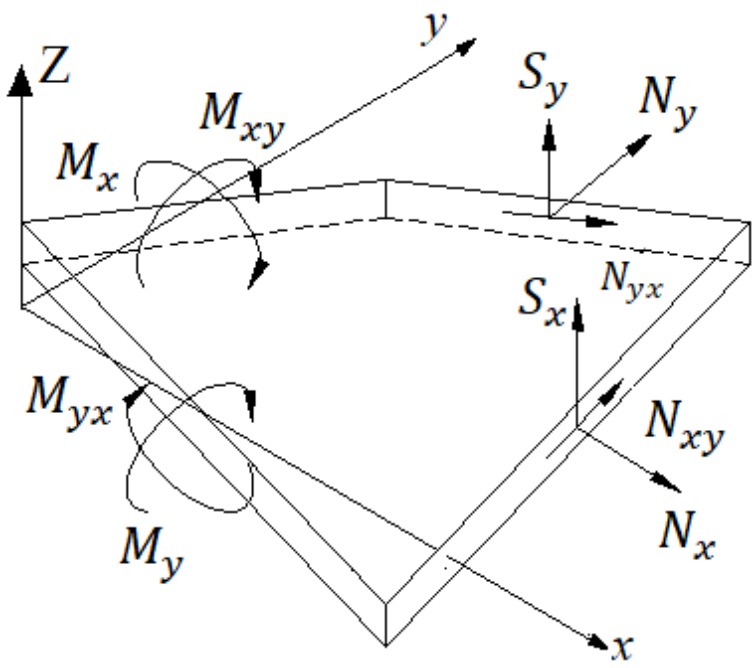

Fig. 4.6 Generalized force and moment resultant vector

4.7. PRINCIPLE OF VIRTUAL WORK AND GOVERNING NONLINEAR EQUILIBRIUM EQUATION

The principle of virtual work enables one to solve plate and shell problems when closed form solutions are not available or non-obvious. This mainly happens when the geometry of

the structure or the lamination sequence is highly complex and the assumed displacement function may not satisfy all the boundary conditions and governing partial differential equation. The assumed displacement function in such cases may be chosen so that this only satisfies the kinematic boundary conditions and not the force boundary conditions or the partial differential equation. This will result in mismatch of values between both the sides of the partial differential equation and will generate an error, $\{r\}^n$. The dimension of this error normally in case of transversely loaded plate or shell is same as that of the dimension of intensity of the applied pressure $\{P\}$. So, if this error is multiplied with the small differential area of the plate or shell element, it will give rise to a residual load in the z direction$\left(\text{equivalent to } \int_{\Omega}^{\square}(\{r\}^n\, dx\, dy\right)$. Next, the author considers some virtual displacement (any disturbance in plate or shell configuration consistent with its kinematic boundary conditions) in the z direction. Then the product of this virtual displacement (extremely small in magnitude) and this residual load would give rise to virtual work. The principle of virtual work states that the body is said to be in equilibrium if the integral of this virtual work over the domain of the system is zero$\left(\int_{\Omega}^{\square}\{r\}^n\, dx\, dy\, \delta w(x,y) = 0\right)$.

4.7.1. Equilibrium Equation

The above discussion may also be expressed in terms of internal and external load as:

$$\{r\} = \int_{\Omega}^{\square}[B]^T\{F\}dA - \{P\} = \{0\} \tag{4.23}$$

The external load generated due to applied force is

$$\{P\} = \sum_{i=1}^{8}\int_{A}^{\square}[N_i]^T\{f\}dA \tag{4.24}$$

Here, $\{f\} = \{f_x \quad f_y \quad f_z \quad m_x \quad m_y\}^T$ in which f_x, f_y, f_z are the intensities of uniformly distributed load per unit area along $x, y\, z$ directions respectively and m_x, m_y are the moments applied per unit area along x, y axes respectively. For the present work, the author only

considers the transversely downward pressure load. So, except f_z all other terms vanish. The area integral dA is evaluated using 2×2 Gauss quadrature rule.

With the help of Eqs.4.14, 4.19 and 4.20, Eq.4.23 may be rewritten as:

$$\int_A^{\square} ([B_l] + [B_{nl}])^T [D]\,([B_l] + 0.5[B_{nl}])dA\{\delta\} - \{P\} = \{0\} \tag{4.25}$$

$$[k]_S\{\delta\} = \{P\}$$

The secant stiffness matrix $[k]_S$ is given by

$$[k]_S = \int_A^{\square} [B_l]^T [D]\,[B_l]dA + 0.5\int_A^{\square} [B_l]^T\,[D][B_{nl}]dA + \int_A^{\square} [B_{nl}]^T\,[D][B_l]dA \tag{4.26}$$

$$+ 0.5\int_A^{\square} [B_{nl}]^T\,[D][B_{nl}]dA = [k]_L + [k]_{LS}$$

Here $[k]_L = \int_A^{\square} [B_l]^T [D]\,[B_l]dA$;

$$[k]_{LS} = 0.5\int_A^{\square} [B_l]^T\,[D][B_{nl}]dA + \int_A^{\square} [B_{nl}]^T\,[D][B_l]dA + \ 0.5\int_A^{\square} [B_{nl}]^T\,[D][B_{nl}]dA$$

4.7.2. Incremental Equilibrium Equation

The tangent stiffness matrix $[k]_T$ may be obtained by taking an appropriate variation of Eq.4.23 with respect to $\{\delta\}$ as:

$$d\{r\} = \int_{\mathrm{A}}^{\square} d[B]^T\{F\}dA\ + \int_A^{\square} [B]^T d\{F\}dA\ - d\{P\} = [k]_T d\{\delta\} - \ d\{P\} \tag{4.27}$$

Using Eqs.4.14 and 4.15 in Eq. 4.27 we get

$$\int_A^{\square} d([B_l]+[B_{nl}])^T\{F\}dA + \int_A^{\square} ([B_l]+[B_{nl}])^T[D]\,([B_l]+[B_{nl}])d\{\delta\}dA\text{-}d\{P\}=\{0\} \tag{4.28}$$

$$\Rightarrow [k]_F d\{\delta\} + ([k]_L + [k]_{LT})d\{\delta\} = d\{P\}$$

$$[k]_L = \int_A^{\square} ([B_l])^T[D][B_l]dA$$

$$\Rightarrow [k]_F d\{\delta\} = \int_A^{\square} d[B_{nl}]^T \{F\} dA \Rightarrow [k]_F =$$

$$\int_A^{\square} \begin{bmatrix} 0 & 0 & \frac{\partial N_i}{\partial x} & 0 & 0 \\ 0 & 0 & \frac{\partial N_i}{\partial y} & 0 & 0 \end{bmatrix}^T_{1,2,\ldots,8} \begin{bmatrix} N_x & N_{xy} \\ N_{xy} & N_y \end{bmatrix} \begin{bmatrix} 0 & 0 & \frac{\partial N_i}{\partial x} & 0 & 0 \\ 0 & 0 & \frac{\partial N_i}{\partial y} & 0 & 0 \end{bmatrix}_{1,2,\ldots,8} ;$$

$$[k]_{LT} = \int_A^{\square} [B_l]^T [D][B_{nl}] dA + \int_A^{\square} [B_{nl}]^T [D][B_l] dA + \int_A^{\square} [B_{nl}]^T [D][B_{nl}] dA$$

Thus, tangent stiffness matrix comprises of $[k]_T = [k]_L + [k]_{LT} + [k]_F$, where $[k]_F$ is the symmetric matrix which is function of stress level termed as initial stress matrix or geometric matrix [refer Mukhopadhyay et al. (2004)].

4.7.3. Solution of Equilibrium Equation Using Incremental Iterative Scheme

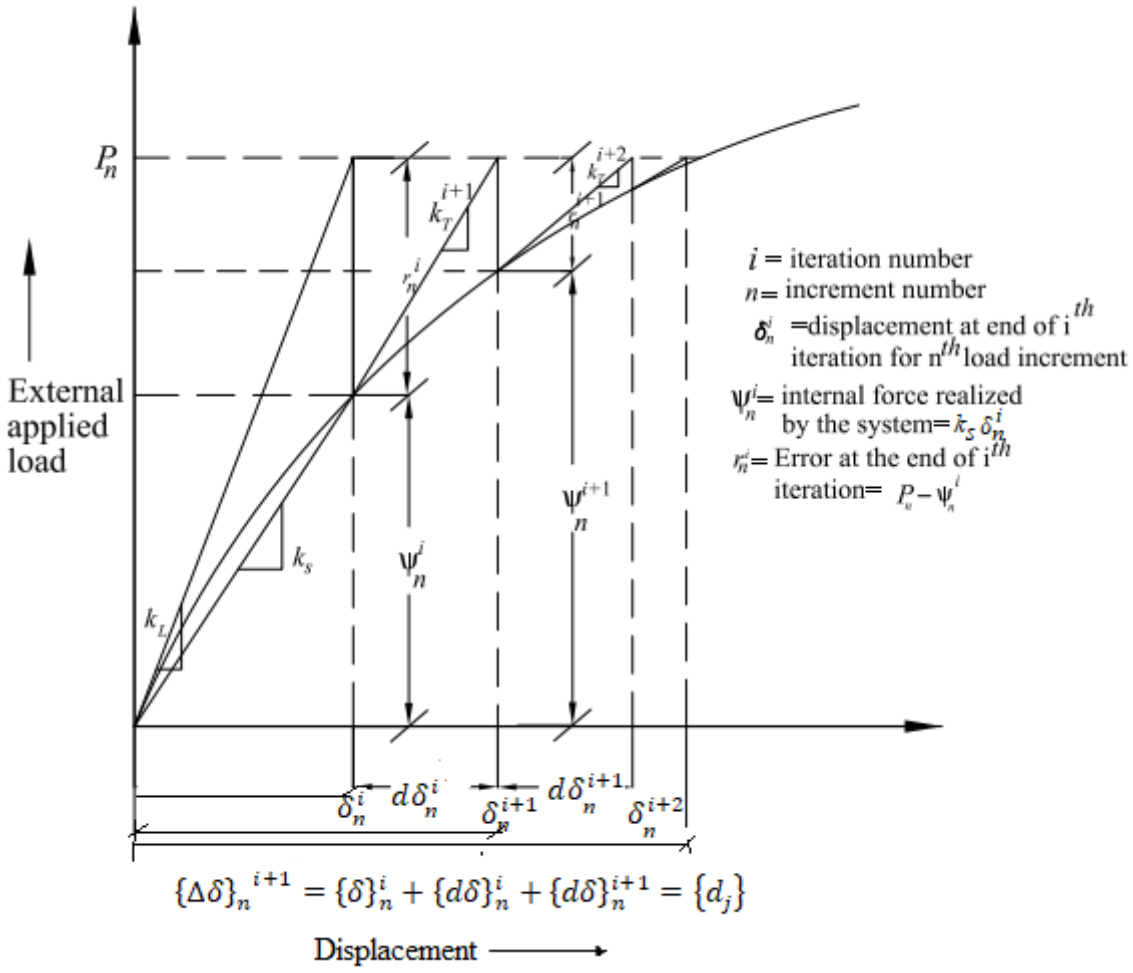

Fig. 4.7 Newton-Raphson iteration scheme

The governing nonlinear equilibrium equation as expressed in Eq. (4.23) is solved using Newton-Raphson (N-R) incremental iterative scheme as shown in Fig. 4.7. Since in geometric nonlinear problems, the stiffness matrix is a function of displacement, the total load is not applied at once but in steps. Initially some load is applied and the body is allowed to come to equilibrium at that load level. Thereafter the load is increased step by step till the full load is reached. For every small load step, the body is allowed to reach equilibrium and the displacement measure gets improved with respect to previous load step and become good enough to hold the external forces. Within each load increment, an iterative loop is run and displacement is measured so that equilibrium is attained and the internal force realized by the system is compared with the applied external load. The difference between the internal and external load values is termed as error. The relative error obtained at each $(i+1)^{th}$iteration is compared with that at i^{th}iteration. The stage when this relative error is within a tolerance (say 10^{-6}) , convergence is said to be achieved and next load increment is applied. This whole process is carried out till full load is applied. If starting displacement is δ^i then the better estimate of δ^{i+1} may be obtained by considering the first term of Taylor series as:

$$\{r\}_n{}^{i+1}\left(\{\delta\}_n{}^{i+1}\right) = \{r\}_n{}^{i}\left(\{\delta\}^i\right)_n + \left(\frac{d\{r\}^i}{d\{\delta\}^i}\right)_n \{d\delta\}^i = 0 \tag{4.29}$$

$$\text{where } \{\delta\}^{i+1} = \{\delta\}^i + \{d\delta\}^i \tag{4.30}$$

here $\left(\frac{d\{r\}^i}{d\{\delta\}^i}\right)_n = \left[k\left(\{\delta\}^i\right)\right]_T$ represents the tangent stiffness matrix.

Improved $\{\delta\}^{i+1}$ is obtained from Eq. (4.30) by calculating

$$\{d\delta\}^i = \left([k]_T{}^i\right)^{-1}\left(\{P\} - [k]_s{}^i\{\delta\}^i\right) \tag{4.31}$$

Thus improved displacement at the end of $(i+1)^{th}$ iteration at n^{th} increment is

$\{\Delta\delta\}_n{}^{i+1} = \{\delta\}_n^i + \{d\delta\}_n^i + \{d\delta\}_n^{i+1} = \{d_j\}$ (say, refer Fig.4.7).

4.8. LAMINA STRESS CALCULATION

Lamina strains are transformed from the global axes of the plate or shell to the local axes (L, $T$and T') of the lamina using transformation matrix (Eq. 4.18). Lamina stresses are obtained using the constitutive relations of the lamina (Eq. 4.16).

For the class of thin plates and shells considered here, the stress resultants are assessed at the Gauss points (2×2) using the shear correction factor of unity. Maximum stress, maximum strain, Tsai-Hill, Tsai-Wu, and Hoffman's failure criteria, as well as two other failure mode based criteria proposed by Hashin and Puck are utilized to evaluate the first ply failure loads of the composite plates and shells under investigation. If the determined failure index (FIN), [refer to Reddy and Reddy (1992)] reaches a value very close to unity, the lamina is declared as damaged. The first ply failure loads are computed using a schematic technique given in Fig. 4.8, which is briefly addressed in Section 4.10.

4.9. FAILURE THEORIES

4.9.1. Maximum Stress Failure Criterion

It states that failure starts off if at least one of the subsequent criteria is fulfilled,

Fibre breakage mode: $\left({\sigma_L}/{\sigma_{L_{Ten}}}^{u}\right) \geq 1$

Fibre buckling mode: $(-\sigma_L) \geq \sigma^{u}_{L_{Comp}}$

Matrix cracking mode: $\left({\sigma_T}/{\sigma_{T_{Ten}}}^{u}\right) \geq 1$

Matrix crushing mode: $(-\sigma_T) \geq \sigma^{u}_{T_{Comp}}$

Matrix shear failure mode: $\left({\tau_{LT}}/{\tau_{LT}}^{u}\right) \geq 1$ (4.32)

4.9.2. Maximum Strain Failure Criterion

It states that failure starts off if at least one of the subsequent criteria is fulfilled,

Fibre breakage mode: $\left({\varepsilon_L}/{\varepsilon_{L_{Ten}}{}^u}\right) \geq 1$

Fibre buckling mode: $(-\varepsilon_L) \geq \varepsilon_{L_{Comp}}^u$

Matrix cracking mode: $\left({\varepsilon_T}/{\varepsilon_{T_{Ten}}{}^u}\right) \geq 1$

Matrix crushing mode: $(-\varepsilon_T) \geq \varepsilon_{T_{Comp}}^u$

Matrix shear failure mode: $\left({\gamma_{LT}}/{\gamma_{LT}{}^u}\right) \geq 1$ (4.33)

4.9.3. Tsai-Hill Failure Criterion

It states that a lamina fails if at least one of the following conditions is satisfied,

$$\left({\sigma_L}/{\sigma_{L_{Ten}}{}^u}\right)^2 + \left({\sigma_T}/{\sigma_{T_{Ten}}{}^u}\right)^2 - \left(\left({1}/{\sigma_{L_{Ten}}{}^u}\right) + \left({1}/{\sigma_{T_{Ten}}{}^u}\right)\right)\sigma_L\sigma_T + \left({\tau_{LT}}/{\tau_{LT}{}^u}\right)^2 \geq 1; \sigma_L, \sigma_T > 0$$

$$\left({\sigma_L}/{\sigma_{L_{Comp}}{}^u}\right)^2 + \left({\sigma_T}/{\sigma_{T_{Comp}}{}^u}\right)^2 - \left(\left({1}/{\sigma_{L_{Comp}}{}^u}\right) + \left({1}/{\sigma_{T_{Comp}}{}^u}\right)\right)\sigma_L\sigma_T + \left({\tau_{LT}}/{\tau_{LT}{}^u}\right)^2 \geq 1; \sigma_L, \sigma_T < 0 \quad (4.34)$$

4.9.4. Tsai-Wu Failure Criterion

Tsai-Wu criteria can be expressed as,

$$\left(\left({1}/{\sigma_{L_{Ten}}{}^u}\right) - \left({1}/{\sigma_{L_{Comp}}{}^u}\right)\right)\sigma_L + \left(\left({1}/{\sigma_{T_{Ten}}{}^u}\right) - \left({1}/{\sigma_{T_{Comp}}{}^u}\right)\right)\sigma_T + \left({1}/{\sigma_{L_{Ten}}{}^u\sigma_{L_{Comp}}{}^u}\right)\sigma_L^2 + \left({1}/{\sigma_{T_{Ten}}{}^u\sigma_{T_{Comp}}{}^u}\right)\sigma_T^2 - \sqrt{\left(\sigma_{L_{Ten}}{}^u\sigma_{L_{Comp}}{}^u\sigma_{T_{Ten}}{}^u\sigma_{T_{Comp}}{}^u\right)}\sigma_L\sigma_T + \left({\tau_{LT}}/{\tau_{LT}^u}\right)^2 \geq 1 \quad (4.35)$$

4.9.5. Hoffman Failure Criterion

Hoffman criteria can be expressed as,

$$\left(1/2\right)\left(\left(1/{\sigma_{L_{Ten}}}^{u}{\sigma_{L_{Comp}}}^{u}\right)-\left(1/{\sigma_{T_{Ten}}}^{u}{\sigma_{T_{Comp}}}^{u}\right)\right)\sigma_L^2+\left(1/2\right)\left(\left(1/{\sigma_{L_{Ten}}}^{u}{\sigma_{L_{Comp}}}^{u}\right)+\left(1/{\sigma_{T_{Ten}}}^{u}{\sigma_{T_{Comp}}}^{u}\right)\right)(\sigma_L-\sigma_T)^2+\left(\left(1/{\sigma_{L_{Ten}}}^{u}\right)-\left(1/{\sigma_{L_{Comp}}}^{u}\right)\right)\sigma_L+\left(\left(1/{\sigma_{T_{Ten}}}^{u}\right)+\left(1/{\sigma_{T_{Comp}}}^{u}\right)\right)\sigma_T+\left(\tau_{LT}/\tau_{LT}^{u}\right)\geq 1 \quad (4.36)$$

4.9.6. Hashin Failure Criterion

Fibre breakage mode: $\left(\sigma_L/{\sigma_{L_{Ten}}}^{u}\right)^2+\left(\tau_{LT}/{\tau_{LT}}^{u}\right)^2\geq 1$

Fibre buckling mode: $-\sigma_L\geq {\sigma_{L_{Comp}}}^{u}$

Matrix cracking mode: $\left(\sigma_T/{\sigma_{T_{Ten}}}^{u}\right)^2+\left(\tau_{LT}/{\tau_{LT}}^{u}\right)^2\geq 1$

Matrix crushing mode:

$$\left[\left({\sigma_{T_{Comp}}}^{u}/2{\tau_{LT}}^{u}\right)^2-1\right]\left(\sigma_T/{\sigma_{T_{Comp}}}^{u}\right)+\left(\sigma_T/2{\tau_{TT,}}^{u}\right)^2+\left(\tau_{LT}/\tau_{LT}^{u}\right)\geq 1 \quad (4.37)$$

4.9.7. Puck Failure Criterion

Fibre breakage mode: $\left(1/2\right)\left(\left|\sigma_L/{\sigma_{L_{Ten}}}^{u}\right|+\left|\varepsilon_L/{\varepsilon_{L_{Ten}}}^{u}\right|\right)\geq 1$

Fibre buckling mode: $\left(1/2\right)\left(\left|\sigma_L/{\sigma_{L_{Comp}}}^{u}\right|+\left|\varepsilon_L/\varepsilon_{L_{Comp}}^{u}\right|\right)\geq 1$

Matrix cracking mode A: $(\sigma_T>0)$

$$\sqrt{\left(\tau_{LT}/{\tau_{LT}}^{u}\right)+\left[1-{p_{LT}}^{(+)}\left({\sigma_{T_{Ten}}}^{u}/\tau_{LT}^{u}\right)^2\right]\left(\sigma_T/{\sigma_{T_{Ten}}}^{u}\right)^2}+{p_{LT}}^{(+)}\left(\sigma_T/{\tau_{LT}}^{u}\right)\geq 1$$

Matrix crushing mode B: $\left((\sigma_T<0);0\leq\left|\sigma_T/\tau_{LT}\right|\leq {\tau_{TT,}}^{A}/\left|\tau_{LT}^{C}\right|\right)$

$$\left(1/\tau_{LT}^{u}\right)\left[\sqrt{(\tau_{LT})^2+({p_{LT}}^{(-)}\sigma_T)^2}+{p_{LT}}^{(+)}\sigma_T\right]\geq 1$$

Matrix crushing mode C: $\left((\sigma_T < 0); 0 \leq \left|{}^{\tau_{LT}}/_{\sigma_T}\right| \leq {}^{|\tau_{LT}^C|}/_{\tau_{TT}{}^A}\right)$

$$\left[\left({}^{\tau_{LT}}/_{2(1+p_{LT}{}^{(-)}\tau_{TT}{}^A)}\right)^2 + \left({}^{\sigma_T}/_{\sigma_{T\,Comp}{}^u}\right)^2\right]\left({}^{\sigma_{T\,Comp}{}^u}/_{(-\sigma_T)}\right) \geq 1 \tag{4.38}$$

$$p_{LT}{}^{(+)} = 0.3, p_{LT}{}^{(-)} = 0.3, \tau_{TT}{}^A = \left({}^{\tau_{LT}^u}/_{2p_{LT}{}^{(-)}}\right)\left(\sqrt{1 + {}^{p_{LT}{}^{(-)}\sigma_{T\,Comp}{}^u}/_{\tau_{LT}^u}} - 1\right)$$

$$\text{where,} \quad \tau_{LT}^C = \tau_{LT}^u\left[\sqrt{1 + \left({}^{2p_{LT}{}^{(-)}\tau_{TT}{}^A}/_{\tau_{LT}^u}\right)}\right]$$

4.10. SOLUTION STEPS TO FIRST PLY AND PROGRESSIVE FAILURE ANALYSIS

The nonlinear equilibrium equation [Eq. (4.23)] is solved using Newton-Raphson (N-R) iteration scheme which is shown in Fig. 4.9. The detailed discussions regarding this N-R iteration process are already reported in the Section 4.7. In this section the progressive failure analysis procedure along with the first ply failure are explained in details with schematic representation of first ply and progressive failure algorithm depicted in Fig. 4.8.

1. For the given initial external nodal load $\{P\}^n$, the static displacements $\{\delta\}^n$(for n =1st iteration say) of the plate or shell are determined using tangent stiffness matrix (in this case $[k]_T{}^n = [k]_L$) as:

$$\{\delta\}^n = [k]_T{}^{-1}\{P\}^n \tag{4.39}$$

2. The displacements so obtained at each node are used to compute the nonlinear stiffness matrices (both tangent stiffness $[k]_T{}^n$ and secant stiffness $[k]_S{}^n$) and internal load generated by the system is computed as:

$$(\{\psi\}^n = [k]_S{}^n\{\delta\}^n) \tag{4.40}$$

3. In the next step the residual load($\{r\}^n$)is evaluated as the difference between external force applied and internal force generated i.e, ($\{r\}^n = \{P\}^n - \{\psi\}^n$) which is further used to compute the incremental nodal displacement $d\{\delta\}^n$ using equation $d\{\delta\}^n = \left([k]_T{}^n\right)^{-1}\{r\}^n$. The final total nodal displacement at the end of n^{th} iteration is then obtained as $\Delta\{\delta\}^n = \{\delta\}^n + d\{\delta\}^n$.

4. The residual load convergence is checked by considering a pre- assumed tolerance value *C* of 1% as follows:

$$C = \sqrt{\{r\}^T\{r\} \Big/ \{P\}^T\{P\}} \times 100 \tag{4.41}$$

If *C* comes lesser than 1% then the total displacement obtained in step 3 is the corrected nonlinear displacement for the first load iteration. Otherwise steps 2 to 4 are again repeated till *C* comes less or equal to pre-set tolerance.

5. Once pre-set tolerance is reached the final internal load$\{\psi\}$realized due to the external load $\{P\}$and the displacement $\Delta\{\delta\}$ are noted. The nonlinear mid-plane strain vectors at four Gauss points are computed using the converged nonlinear static nodal mid-plane displacement fields $\Delta\{\delta\}^n$ due to external applied load which is explained as:

$$\begin{Bmatrix} \varepsilon_x{}^0 \\ \varepsilon_y{}^0 \\ \gamma_{xy}{}^0 \\ \gamma_{xz}{}^0 \\ \gamma_{yz}{}^0 \end{Bmatrix} = \begin{Bmatrix} \frac{\partial u_0}{\partial x} + \frac{1}{2}\left(\frac{\partial w_0}{\partial x}\right)^2 \\ \frac{\partial v_0}{\partial y} + \frac{1}{2}\left(\frac{\partial w_0}{\partial y}\right)^2 \\ \frac{\partial u_0}{\partial y} + \frac{\partial v_0}{\partial x} - \frac{2w_0}{R_{xy}} + \left(\frac{\partial w_0}{\partial x}\right)\left(\frac{\partial w_0}{\partial y}\right) \\ \frac{\partial w_0}{\partial x} + \alpha_x - \frac{v_0}{R_{xy}} \\ \frac{\partial w_0}{\partial y} + \alpha_y - \frac{u_0}{R_{xy}} \end{Bmatrix} \text{and} \begin{Bmatrix} \kappa_x \\ \kappa_y \\ \kappa_{xy} \\ \kappa_{xz} \\ \kappa_{yz} \end{Bmatrix} = \begin{Bmatrix} \frac{\partial \alpha_x}{\partial x} \\ \frac{\partial \alpha_y}{\partial y} \\ \frac{\partial \alpha_x}{\partial y} + \frac{\partial \alpha_y}{\partial x} \\ 0 \\ 0 \end{Bmatrix}$$

6. The mid-plane strains are used to compute the strain at any point on the laminate in (x, y, z) axes system using Eq. 4.5. Now the stress vector is developed by the constitutive relationship matrix as explained in Eq. 4.20. The resultant in-plane stress, bending stress and

transverse shear resultants are presented respectively in Eq. 4.21. Finally, from Eq. (4.20) and (4.21), the laminate stiffness matrix can be obtained as expressed in Eq. 4.22. The stresses and strains in the x, y, z coordinate system are transformed to L, T, T' axes system by the relationships as expressed in Eqs. 4.17 and 4.18.

7. The laminae stresses and strains at each Gauss point are then applied in different well established failure theories like independent failure criteria (maximum stress and maximum strain criteria), interactive failure criteria (Hoffman, Tsai-Hill and Tsai-Wu criteria) and partially interactive failure mode based criteria (Hashin and Puck criteria) to calculate the failure index (FIN) which is then compared to unity.

8. If $FIN \cong 1$ then the externally applied load $\{P\}^n$ is declared as the first ply failure load. The minimum value of the failure loads coming out from different above-mentioned failure criteria is considered as the first ply failure load for a particular skew plate or shell option and the corresponding failure criterion is treated as the governing first ply failure criterion for that case. Along with the first ply failure load, failed ply, failed location and the failure mode or failure tendencies are also determined. The search for next failure load is started as explained in step 10 and onwards. For any non-unity value of FIN, the external load $\{P\}^n$ is decreased or increased appropriately by some predefined decremental or incremental amount of external load dp_i for $FIN > 1$ or $FIN < 1$ respectively. Now again the searching of first ply failure load begins and steps 1 to 9 are repeated afresh till the value of $FIN \cong 1$.

9. The final displacement $\Delta\{\delta\}$ obtained as explained previously (step 3) at first ply failure analysis (or previous ply failure analysis whichever is applicable) is declared as the displacement $\{d_{judm}\}^n$ of undamaged shell or plate as shown in Fig. 4.9 for first ply/consecutive ply failure analysis. Now the constitutive relation and the stiffness matrices are recomputed by degrading the material properties of failed Gauss point as explained in the flow diagram in Fig. 4.8. These stiffness matrices are called the damaged stiffness.

10. In the next step, the new updated damaged displacement$\{d_{jdm}\}^n$ is computed from the current tangent stiffness matrix and the first ply failure or previous ply failure load by N-R scheme as stated in steps 1 to 4. The total damaged displacement is then updated at the end of first/consecutive ply failure load as $\{dj\}^n = \{d_{judm}\}^{n-1} + \{d_{jdm}\}^n$. Now this $\{dj\}^n$ is used for the next ply failure analysis.

11. Now, considering the FPF (or previous ply failure) load the initial external load, steps 1 to 10 are to be repeated to obtain the second ply failure (or consecutive ply failure) load. In this present study, the governing first ply failure criterion is taken up for the second ply failure (or consecutive ply failure) analysis. The total failure load at the end of second or more consecutive ply failure load is considered as addition of previous ply failure load and the current ply failure load. The updated total damaged displacement at the end of each failure progress will be as $\{dj\}^n = \{d_{judm}\}^{n-1} + \{d_{jdm}\}^n$.

12. Along with the failure load values, failure locations, failed plies and failure modes or tendencies are also determined at each stage of progressive failure of skewed plate or hypar shells.

13. If $\{dj\}^{n+1} > \{dj\}^n$ then the analysis proceeds towards next stage of failure. Otherwise, if $\{dj\}^{n+1} < \{dj\}^n$, then the progressive failure analysis will be stopped and the failure at the just previous progressive failure stage of analysis is considered as the ultimate failure stage. The load corresponding to the n^{th} failure stage is taken as the ultimate failure load.

On the basis of the mathematical approach presented in this chapter, numerical experimentations are carried out in Chapters 5 to 9, the outcomes of which are systematically presented and interpreted in the respective chapter.

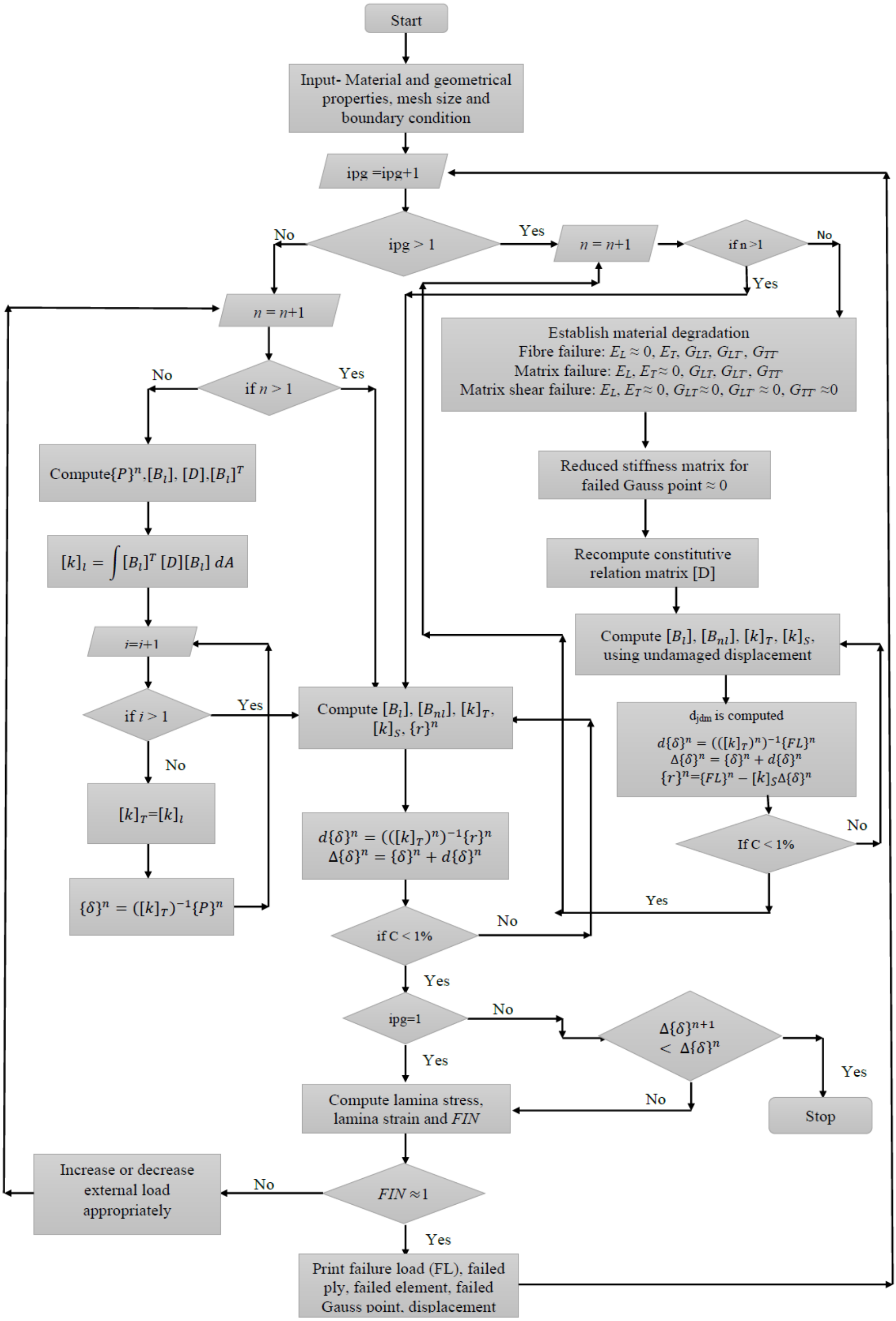

Fig.4.8 A flowchart showing the first ply and progressive failure analysis

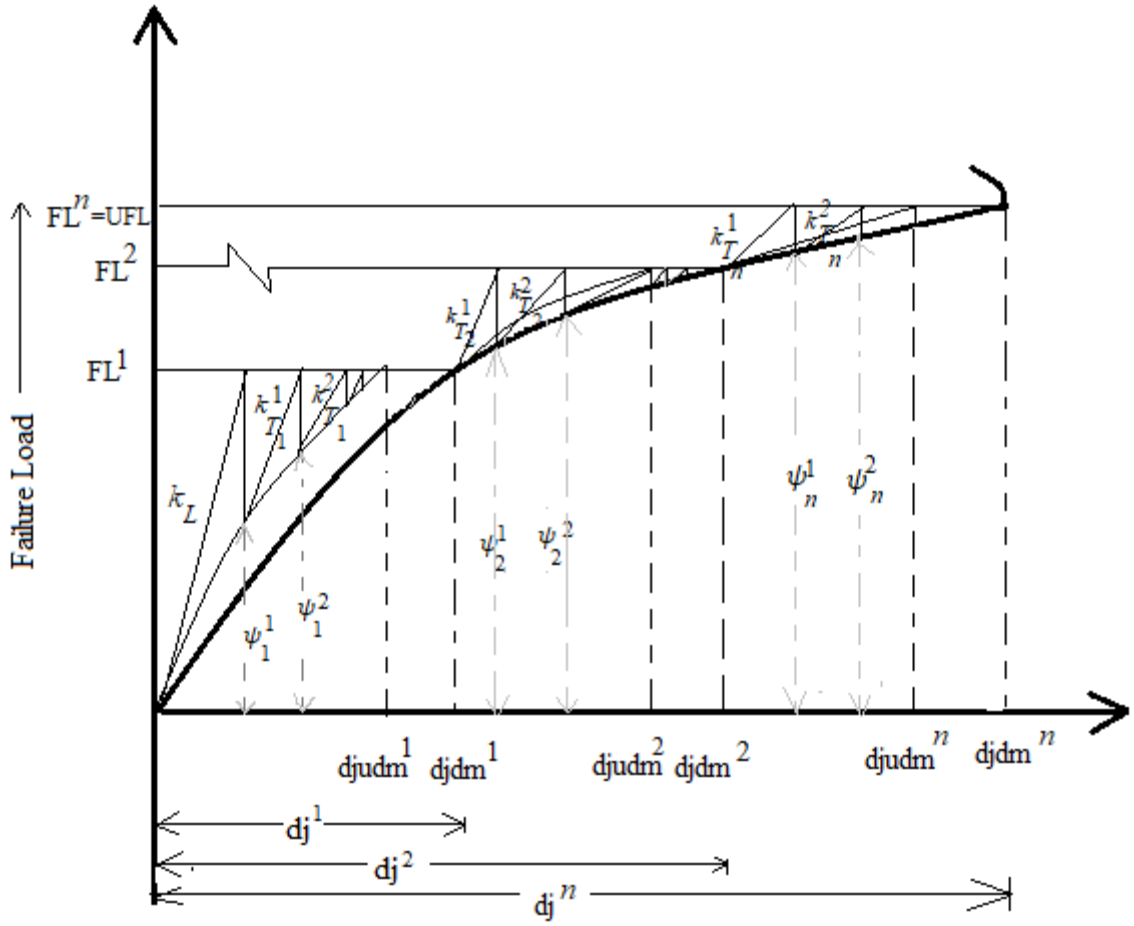

Fig.4.9 N-R iteration scheme for progressive failure analysis

Chapter 5

LINEAR FIRST PLY FAILURE OF LAMINATED COMPOSITE SKEW PLATES

5.1 GENERAL

The study of literature on failure of laminated composite structural elements reveals that composite skew plates have not been studied for failure in details. In this chapter, the author studies the first ply failure (FPF) and associated frequency reduction of composite skew plates considering practical parametric variations. Different well-established failure criteria including the recently introduced Puck's failure criterion are used to investigate the FPF response. The results are post processed to formulate specific recommendations regarding relative behaviour of different skew plate combinations in terms of FPF phenomenon and are presented in Section 5.2. All of the results reported in this chapter are arrived at through a thorough mesh convergence study. The element sizes are progressively reduced till further mesh refinement does not improve the results by more than 1%. The important findings from the present investigation are reported in Section 5.3 at the end of the chapter.

5.2 NUMERICAL STUDY AND DISCUSSIONS

In order to validate the present FPF formulation, the author compares the FPF load values of $[0^{\circ}_2/90^{\circ}]_s$ laminated plate reported by Kam et al. (1996) with the values obtained through present formulation. The comparison of these results is shown in Table 5.1. For appropriate modeling of this benchmark problem, the author assigns zero value to the skew angle to represent a rectangular plate configuration.

To validate the correct incorporation of laminated composite skew plate geometry in the present computer code, the non-dimensional fundamental frequencies of skew plates of two different skew angles are obtained by present approach and the results are compared with those reported by Singha and Daripa (2007) in Table 5.2.

Apart from solving the benchmark problems, the author carries out a number of numerical investigations of Q–1115 graphite epoxy laminated composite skew plates for different boundary conditions. Tables 5.3 and 5.4 furnish the material properties and the geometrical parameters of the skew plate configurations that are taken up for the present study.

The edges of the skew plates considered here are either clamped or simply supported and combining these two edge constraints four different boundary conditions are generated and designated as CCCC, SSSS, CSCS and CCSS combinations as shown in Fig. 5.1.

Four different stacking sequences combining antisymmetric (AS) and symmetric (SY) orders and cross-ply (CP) and angle-ply (AP) laminates are taken up here. In the present numerical investigation, the $\pm 45^{\circ}$ and 0°, 90° laminae are considered for angle and cross-ply combinations. Apart from the above mentioned parametric variations, the skew angle $(\lambda)$is varied discretely from 0° to 30° in steps of 5°.

Table 5.1 First ply failure loads in Newton for $[0^{\circ}_2/90^{\circ}]_s$ plate

Failure criteria	Side/ thickness ratio	Experimental values [Kam et al.(1996)]	Numerical values			
			[Kam et al.(1996)]	Present formulation with mesh on the full plate using mesh size		
			Using 3×3 mesh on quarter plate	4×4	6×6	8×8
Maximum stress	105.26	157.34	108.26	131.24	113.33	112.15
Maximum strain			122.86	154.83	130.11	127.56
Hoffman			106.45	122.61	104.58	103.36
Tsai-Hill			107.06	123.01	105.43	104.40
Tsai-Wu			112.77	130.52	111.56	110.46

Note: Each plan dimension = 100 mm, ply thickness = 0.155 mm, load details = central point load

Table 5.2 Non-dimensional frequencies $\left(\bar{\omega} = (\omega a^2/\pi^2 h)\sqrt{\rho/E_T}\right)$ of five layered [90˚/0˚/90˚/0˚/90˚] simply supported skew laminates

Skew angle		Mesh	Modes		
			1	2	3
0˚	Present study	8×8	1.9673	4.0223	6.6882
	Singha and Daripa (2007)		1.9137	3.9730	6.6448
30˚	Present study	8×8	2.9076	5.2589	8.4974
	Singha and Daripa (2007)		2.8380	5.1945	8.4640

Note: E_L/E_T = 40.0, G_{LT}/E_T = 0.6, $G_{TT'}/E_T$ = 0.5, ν_{LT} = 0.25, a/h =1000, ρ=1.0, $\left(a/b\right) = 1$

Table 5.3 Material properties of Q-1115 graphite-epoxy composite

Material constants		Strengths		Ultimate strains	
E_L	142.50 GPa	σ_L^t	2193.50 MPa	ε_L^t	0.01539
E_T	9.79 GPa	σ_L^c	2457.00 MPa	ε_L^c	0.01724
$E_{T'}$	9.79 GPa	$\sigma_T^t = \sigma_{T'}^t$,	41.30 MPa	$\varepsilon_T^t = \varepsilon_{T'}^t$,	0.00412
$G_{LT} = G_{LT'}$	4.72 GPa	$\sigma_T^c = \sigma_{T'}^c$,	206.80 MPa	$\varepsilon_T^c = \varepsilon_{T'}^c$,	0.02112
$G_{TT'}$	1.192 GPa	τ_{LT}^u	61.28 MPa	γ_{LT}^u	0.05141
$\nu_{LT} = \nu_{LT'}$	0.27	τ_{TT}^u,	78.78 MPa	γ_{TT}^u,	0.01669
$\nu_{TT'}$	0.25	τ_{LT}^u	78.78 MPa	γ_{LT}^u,	0.01669

Table 5.4 Geometrical dimensions of the skew plate

Skew plate dimensions	Values
Aspect ratio a/b	1
Width to thickness ratio b/h	100
Skew angles, λ	0°, 5°, 10°, 15°, 20°, 25°, 30°

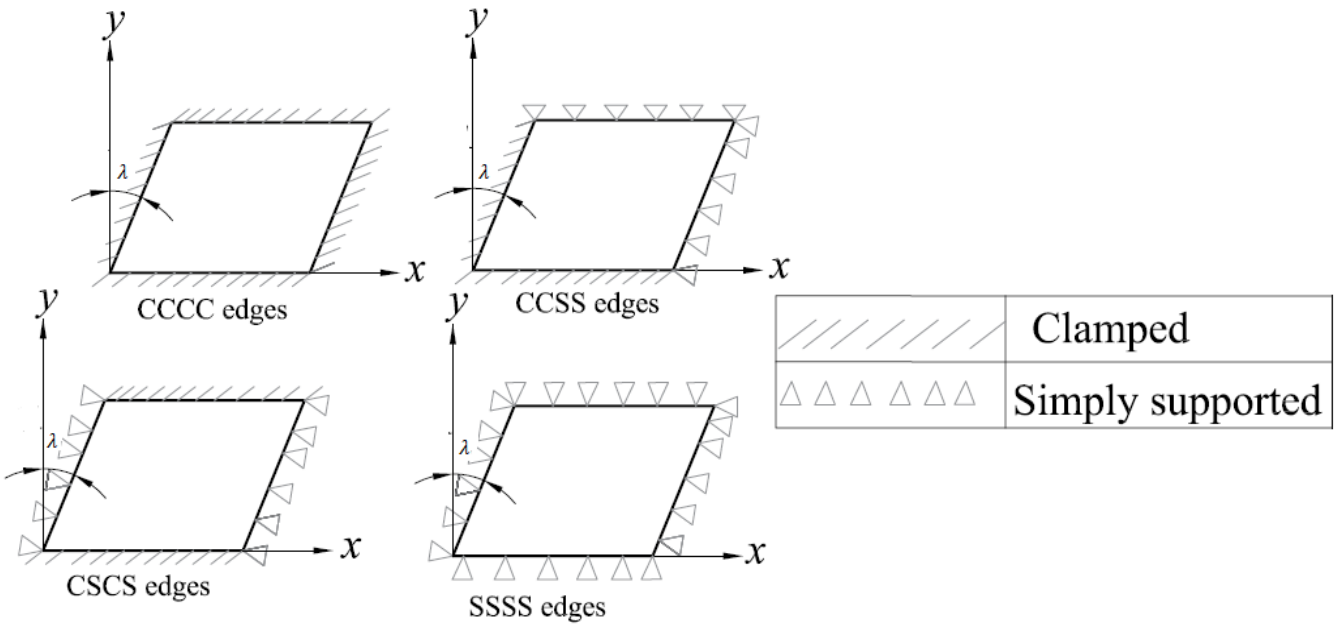

Fig. 5.1 Different types of boundary conditions

5.2.1. Benchmark Problems

In Table 5.1, the static FPF load values of a laminated composite plate obtained in the present approach are compared with those reported by Kam et al. (1996). A very good agreement between the results is seen which indicates the correct incorporation of the FPF formulation in the present finite element code.

The non-dimensional linear frequency values of five layered [90˚/0˚/90˚/0˚/90˚] simply supported skew plates obtained here are compared in Table 5.2 with those found in the paper of Singha and Daripa (2007). Again, the close agreement of results points to correct incorporation of the laminated skew plate geometry in the present formulation.

5.2.2. First Ply Failure Behaviour of Laminated Composite Skew Plates with Different Boundary Conditions

The FPF load values of symmetric and antisymmetric laminated composite skew plates with different skew angles and boundary conditions are calculated through the present finite element formulation. Different well-established failure criteria such as maximum stress, maximum strain and those proposed by Hoffman, Tsai-Hill, Tsai-Wu, Hashin and Puck are

used. The minimum non-dimensional failure load value obtained through different failure criteria is considered as the governing FPF load $\overline{\text{FPFL}}$ [$= \left({FL}/{E_T}\right)\left({a}/{h}\right)^4$] in each case and such results are only presented in Tables 5.5 - 5.8 for 8×8 mesh size to avoid multiplicity of results.

Table 5.9 summarize the outcomes observed from Table 5.5 to Table 5.8, with the governing failure criteria for different combinations of boundary conditions and laminations. For each of SYAP and SYCP laminates of clamped boundary condition and ASCP laminates with the CCSS boundary condition, an additional failure criterion is mentioned in parentheses. These criteria are not the governing ones, but they give values of FPF load very close (within 10%) to the governing values. It is evident from Table 5.10, that the maximum strain criterion for angle ply (both antisymmetric and symmetric) plates and the Puck criterion for symmetric cross ply plates are the only failure criteria that one may use to obtain the FPF loads.

For ASCP skew plate, though a single criterion cannot be identified but the failure theory to be adopted is either of Hoffman or that of Puck. This will also be useful because only two failure theories may be identified out of seven common theories that are normally adopted by the engineers.

Thus, it is concluded that only the maximum strain criterion and those of Hoffman or Puck are recommended for assessing the FPF load for the skew plate combinations considered here.

Table 5.5 Non-dimensional first ply failure loads ($\overline{\text{FPFL}}$)of skew plates for CCCC boundary condition

Lamination	Skew angle, λ (degree)	$\overline{\text{FPFL}}$	Failure theory	First failed ply	Failure mode/ failure tendency
ASAP (+45˚/-45˚)	0	492.339	Maximum strain	1	Transverse matrix cracking
	5	434.116	Maximum strain	1	Transverse matrix cracking
	10	388.151	Maximum strain	1	Transverse matrix cracking

Lamination	Skew angle, λ (degree)	$\overline{\text{FPFL}}$	Failure theory	First failed ply	Failure mode/ failure tendency
ASAP (+45˚/-45˚)	15	364.657	Maximum strain	1	Transverse matrix cracking
	20	360.572	Maximum strain	1	Transverse matrix cracking
	25	367.722	Maximum strain	1	Transverse matrix cracking
	30	374.872	Maximum strain	1	Transverse matrix cracking
ASCP (0˚/90˚)	0	1071.50	Hoffman	1	Fiber tensile
	5	1084.78	Hoffman	1	Fiber tensile
	10	1121.55	Hoffman	1	Fiber tensile
	15	1170.58	Hoffman	1	Fiber tensile
	20	1221.65	Hoffman	1	Fiber tensile
	25	1310.52	Hoffman	1	Transverse matrix cracking
	30	1459.65	Hoffman	1	Transverse matrix cracking
SYAP (+45˚/45˚/+45˚)	0	1039.83	Maximum strain	3	Transverse matrix cracking
	5	980.592	Maximum strain	3	Transverse matrix cracking
	10	801.839	Hoffman	1	Transverse matrix cracking
	15	680.286	Maximum strain	1	Transverse matrix cracking
	20	576.098	Maximum strain	1	Transverse matrix cracking
	25	522.983	Maximum strain	1	Transverse matrix cracking
	30	517.875	Maximum strain	1	Transverse matrix cracking
SYCP (0˚/90˚/0˚)	0	1692.54	Maximum strain	1	Transverse matrix cracking
	5	1689.47	Puck	1	Matrix crushing mode C
	10	1758.93	Maximum strain	1	Transverse matrix cracking
	15	1432.07	Puck	3	Matrix crushing mode C
	20	1067.41	Puck	3	Matrix crushing mode C
	25	938.713	Puck	3	Matrix crushing mode C
	30	945.863	Puck	3	Matrix crushing mode C

Note: a/b = 1, b/h = 100, mesh size =8×8

Table 5.6 Non-dimensional first ply failure loads ($\overline{\text{FPFL}}$)of skew plates for SSSS boundary condition

Lamination	Skew angle, λ (degree)	$\overline{\text{FPFL}}$	Failure theory	First failed ply	Failure mode/ failure tendency
ASAP (+45˚/-45˚)	0	427.988	Maximum strain	1	Transverse matrix cracking
	5	351.379	Maximum strain	1	Transverse matrix cracking
	10	317.671	Maximum strain	1	Transverse matrix cracking
	15	299.285	Maximum strain	1	Transverse matrix cracking
	20	292.135	Maximum strain	1	Transverse matrix cracking
	25	293.156	Maximum strain	1	Transverse matrix cracking
	30	302.349	Maximum strain	1	Transverse matrix cracking
ASCP (0˚/90˚/0˚)	0	536.261	Puck	1	Matrix crushing mode C
	5	404.494	Puck	1	Matrix crushing mode C
	10	596.527	Puck	1	Matrix crushing mode C
	15	586.312	Puck	1	Matrix crushing mode C
	20	642.492	Puck	1	Matrix crushing mode C

Lamination	Skew angle, λ (degree)	$\overline{\text{FPFL}}$	Failure theory	First failed ply	Failure mode/ failure tendency
ASCP (0˚/90˚/0˚)	25	989.785	Puck	1	Matrix crushing mode C
	30	1008.172	Puck	1	Matrix crushing mode C
SYAP (+45˚/45˚/45˚)	0	268.641	Maximum strain	3	Transverse matrix cracking
	5	281.920	Maximum strain	3	Transverse matrix cracking
	10	336.057	Maximum strain	3	Transverse matrix cracking
	15	307.456	Maximum strain	1	Transverse matrix cracking
	20	291.113	Maximum strain	1	Transverse matrix cracking
	25	289.070	Maximum strain	1	Transverse matrix cracking
	30	291.113	Maximum strain	1	Transverse matrix cracking
SYCP (0˚/90˚/0˚)	0	653.728	Puck	1	Matrix crushing mode C
	5	528.089	Puck	1	Matrix crushing mode C
	10	518.896	Puck	1	Matrix crushing mode C
	15	280.899	Puck	3	Matrix crushing mode C
	20	393.258	Puck	3	Matrix crushing mode C
	25	393.258	Puck	3	Matrix crushing mode C
	30	376.915	Puck	3	Matrix crushing mode C

Note: a/b = 1, b/h = 100, mesh size=8×8

Table 5.7 Non-dimensional first ply failure loads ($\overline{\text{FPFL}}$)of skew plates for CCSS boundary condition

Lamination	Skew angle, λ (degree)	$\overline{\text{FPFL}}$	Failure theory	First failed ply	Failure mode/ failure tendency
ASAP (+45˚/-45˚)	0	400.408	Maximum strain	1	Transverse matrix cracking
	5	347.293	Maximum strain	1	Transverse matrix cracking
	10	315.628	Maximum strain	1	Transverse matrix cracking
	15	306.435	Maximum strain	1	Transverse matrix cracking
	20	297.242	Maximum strain	1	Transverse matrix cracking
	25	302.349	Maximum strain	1	Transverse matrix cracking
	30	307.456	Maximum strain	1	Transverse matrix cracking
ASCP (0˚/90˚)	0	655.771	Puck	1	Matrix crushing mode C
	5	742.594	Puck	1	Matrix crushing mode C
	10	787.538	Hoffman	1	Fiber tensile
	15	843.718	Hoffman	1	Fiber tensile
	20	923.391	Hoffman	1	Fiber tensile
	25	995.914	Hoffman	1	Transverse matrix cracking
	30	1085.802	Hoffman	1	Transverse matrix cracking
SYAP (+45˚/45˚/+45˚)	0	350.357	Maximum strain	3	Transverse matrix cracking
	5	357.507	Maximum strain	3	Transverse matrix cracking
	10	407.559	Maximum strain	3	Transverse matrix cracking
	15	412.666	Maximum strain	1	Transverse matrix cracking
	20	384.065	Maximum strain	1	Transverse matrix cracking
	25	374.872	Maximum strain	1	Transverse matrix cracking

Lamination	Skew angle, λ	$\overline{\text{FPFL}}$	Failure theory	First failed ply	Failure mode/ failure tendency
SYAP (+45˚/45˚/+45˚)	30	382.022	Maximum strain	1	Transverse matrix cracking
SYCP (0˚/90˚/0˚)	0	637.385	Puck	1	Matrix crushing mode C
	5	820.225	Puck	1	Matrix crushing mode C
	10	875.383	Puck	1	Matrix crushing mode C
	15	536.261	Puck	3	Matrix crushing mode C
	20	448.417	Puck	3	Matrix crushing mode C
	25	550.562	Puck	3	Matrix crushing mode C
	30	556.690	Puck	3	Matrix crushing mode C

Note: a/b = 1, b/h = 100, mesh size=8×8

Table 5.8 Non-dimensional first ply failure loads ($\overline{\text{FPFL}}$) of skew plates for CSCS boundary condition

Lamination	Skew angle, λ (degree)	$\overline{\text{FPFL}}$	Failure theory	First failed ply	Failure mode/ failure tendency
ASAP (+45˚/-45˚)	0	366.70	Maximum strain	1	Transverse matrix cracking
	5	377.93	Maximum strain	1	Transverse matrix cracking
	10	401.43	Maximum strain	1	Transverse matrix cracking
	15	411.64	Maximum strain	1	Transverse matrix cracking
	20	399.38	Maximum strain	1	Transverse matrix cracking
	25	400.40	Maximum strain	1	Transverse matrix cracking
	30	415.73	Maximum strain	1	Transverse matrix cracking
ASCP (0˚/90˚)	0	990.80	Puck	2	Matrix crushing mode C
	5	1016.3	Puck	2	Matrix crushing mode C
	10	1205.3	Puck	2	Matrix crushing mode C
	15	1221.6	Puck	2	Matrix crushing mode C
	20	1343.2	Puck	1	Matrix crushing mode C
	25	1539.3	Puck	1	Matrix crushing mode C
	30	1599.5	Puck	1	Matrix crushing mode C
SYAP (+45˚/45˚/+45˚)	0	509.70	Maximum strain	3	Transverse matrix cracking
	5	645.55	Maximum strain	3	Transverse matrix cracking
	10	584.27	Maximum strain	1	Transverse matrix cracking
	15	517.87	Maximum strain	1	Transverse matrix cracking
	20	494.38	Maximum strain	1	Transverse matrix cracking
	25	497.44	Maximum strain	1	Transverse matrix cracking
	30	518.89	Maximum strain	1	Transverse matrix cracking
SYCP (0˚/90˚/0˚)	0	1607.7	Puck	1	Matrix crushing mode C
	5	1188.9	Puck	1	Matrix crushing mode C
	10	1499.4	Puck	1	Matrix crushing mode C
	15	1208.3	Puck	3	Matrix crushing mode C
	20	691.52	Puck	3	Matrix crushing mode C
	25	775.28	Puck	3	Matrix crushing mode C
	30	1035.7	Puck	3	Matrix crushing mode C

Note: a/b = 1, b/h = 100, mesh size =8×8

Table 5.9 List of governing failure criteria for different laminations and support conditions

Boundary conditions	Laminations			
	ASAP (+45˚/-45˚)	ASCP (0˚/90˚)	SYAP (+45˚/-45˚/45˚)	SYCP (0˚/90˚/0˚)
CCCC	Maximum strain	Hoffman	Hoffman (maximum strain)	Maximum strain (Puck)
CCSS	Maximum strain	Hoffman (Puck)	Maximum strain	Puck
CSCS	Maximum strain	Puck	Maximum strain	Puck
SSSS	Maximum strain	Puck	Maximum strain	Puck

5.2.3. Effect of Skew Angles on First Ply Failure Behaviour of Laminated Composite Skew Plates

Variations in the FPF load with skew angles λ for different laminations and boundary conditions are shown in Fig. 5.2 [(a) to (d)]. Since the FPF was studied is done for discrete values of skew angle, working equations correlating the FPF load values with λ are proposed. The minimum FPF load against the corresponding skew angle λ are determined, and the best-fit curve, with a Pearson's correlation coefficient close to 1 is depicted in Fig. 5.2. The equations of these curves may be used directly to predict the FPF load for any given skew angle in the range of 0^0 to 30^0. Although, in some cases, variations in FPF loads with skew angle show unified tendencies (for these cases, working equations connecting FPF load and skew angles are presented in Table 5.10), in many other cases, no direct correlation is observed between them. This research deals with practical evaluation of FPF loads, which may directly be used by practicing engineers. Naturally, the objective here is to assess the conservative values of the failure loads. Since, in laminated composite materials, unlike isotropic ones, the stacking sequences and fibre orientations interact with the geometry of skew plates in a complex way, the failure criterion does not remain in variant as the skew angle changes.

The above observations lead to the inference that a designer may use specific working equations for some skew plate combinations (as given in Table 5.10), but for other

combinations, values of the the FPF load corresponding to a particular skew angle shall be picked up from Fig. 5.2.

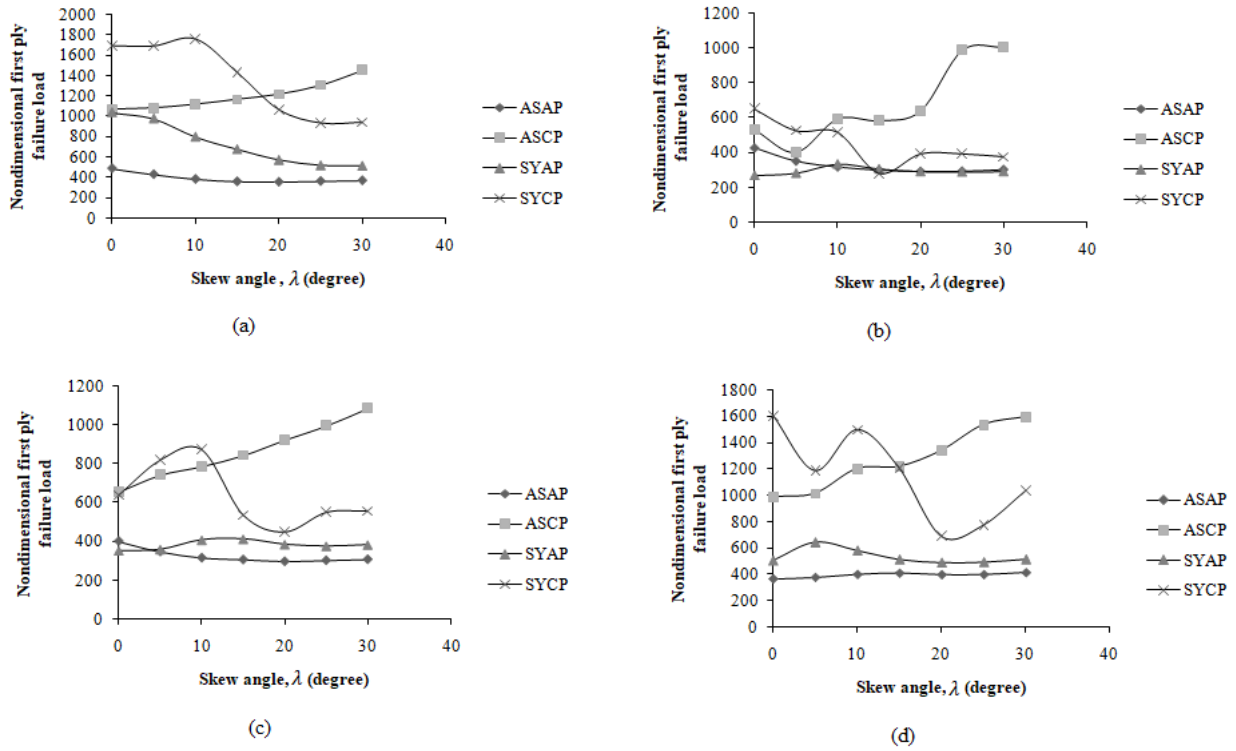

Fig. 5.2 Variation of first ply failure load with skew angle for (a) CCCC boundary condition, (b) SSSS boundary condition, (c) CCSS boundary condition and (d) CSCS boundary condition

Table 5.10 Equations connecting non-dimensional first ply failure load($\overline{\text{FPFL}}$) and skew angle ($\boldsymbol{\lambda}$)

Lamination	Equation	R^2
ASAP/CCCC	$\overline{FPFL} = 0.3\lambda^2 - 12.68\lambda + 490$	0.990
ASCP/CCCC	$\overline{FPFL} = 0.449\lambda^2 - 1.225\lambda + 1078$	0.992
SYAP/CCCC	$\overline{FPFL} = 0.444\lambda^2 - 32.67\lambda + 1076$	0.978
ASAP/SSSS	$\overline{FPFL} = 0.297\lambda^2 - 12.63\lambda + 419$	0.976
ASAP/CCSS	$\overline{FPFL} = 0.226\lambda^2 - 9.55\lambda + 395$	0.979
ASCP/CCSS	$\overline{FPFL} = 0.095\lambda^2 + 10.94\lambda + 666.9$	0.995
ASAP/CSCS	$\overline{FPFL} = 0.001\lambda^4 - 0.055\lambda^3 + 0.790\lambda^2 - 0.005\lambda + 366.2$	0.976
SYAP/CSCS	$\overline{FPFL} = -0.004\lambda^4 + 0.320\lambda^3 - 7.459\lambda^2 + 55.19\lambda + 511.5$	0.985

Note: R^2denotes the correlation between the non-dimensional FPF load $\overline{\text{FPFL}}$ and skew angle (λ)

5.2.4. Guidelines for Selecting a Particular Plate Combination from Several Options

It is quite natural that a skew plate becomes damaged after a FPF, and its frequency changes. Therefore, general free vibration of an undamaged plate (before FPF) and a damaged plate just after a FPF is worth investigating.

One of the most common approaches of evaluating damage in a structure by a non-destructive test is by measuring its fundamental frequency and comparing the value with the expected frequency of an undamaged structure. In fact, the ratio between the frequencies of damaged and undamaged plates indicates the degree of damage of the plate due to the FPF. Lower the ratio, higher is the degree of damage of the plate. It is observed that, in most of the cases, the fundamental frequency due to a FPF damage dropped drastically and decreases almost by 50%, with few exceptions.

One hundred twelve skew plate options that are considered here may be ranked in order of decreasing FPF load values and the first twenty are shown in Table 5.11 in order of their ranks and may be defined as "preferred options". The frequency reduction ratios of these preferred options are also collected in Table 5.11 to enable a design engineer to take a firm decision about his/her choice considering both strength and FPF vulnerability of the skew plates. The plate combination which emerge as preferred option are all of cross-ply category and the boundary condition is either fully clamped or two opposite edges clamped the other two being simply supported. This unified tendency clearly sends an engineering message that which boundary condition and stacking sequence should be preferred together with the corresponding skew angle.

The author in the present work eliminated the stiffness contribution of failed node post FPF and recomputed the updated global stiffness of the plate which has been used to get the damaged frequency ($[K] - \omega^2[M] = 0$). Further a frequency reduction ratio is evaluated as the

ratio of the damaged frequency evaluated post FPF and the natural frequency as given in Table 5.11.

In engineering, normally a 10 % variation is considered to be nominal and it is found from Table 5.11 that first five plate combinations show close values of FPF load – within 10 % with respect to that of the best option. Though failure is never preferred but the results indicate that the reduction of fundamental frequency with failure is minimum for ASCP/CSCS/30˚ combination when the first five best options are considered. The table also speaks the truth that both un-skewed and skewed configuration can show good and comparable results provided the laminations are properly tailored and the boundary conditions are adjusted accordingly. The above findings are expected to form a basis for practicing engineers to select a particular plate combination under a set of practical constraints (such as nature of loading, boundary conditions, stacking orders, skew angles etc.).

Table 5.11 Ranks of different skew plate combinations in terms of first ply failure load and frequency reduction ratio due to FPF

Ranks in term of first ply failure load	Plate combination	$\overline{\text{FPFL}}$	(First ply failure load/maximum first ply failure load)×100 %	Frequency reduction ratio due to first ply failure
1	SYCP/CCCC/10*	1758.938	100.00	0.50
2	SYCP/CCCC/0	1692.543	96.23	0.50
3	SYCP/CCCC/5	1689.479	96.05	0.50
4	SYCP/CSCS/0	1607.763	91.41	0.50
5	ASCP/CSCS/30	1599.591	90.94	0.84
6	ASCP/CSCS/25	1539.326	87.51	0.87
7	SYCP/CSCS/10	1499.489	85.25	0.50
8	ASCP/CCCC/30	1459.653	82.98	0.53
9	SYCP/CCCC/15	1432.073	81.42	0.49
10	ASCP/CSCS/20	1343.207	76.36	0.92
11	ASCP/CCCC/25	1310.521	74.51	0.56
12	ASCP/CCCC/20	1221.655	69.45	0.60
12	ASCP/CSCS/15	1221.655	69.45	0.93
13	SYCP/CSCS/15	1208.376	68.70	0.50
14	ASCP/CSCS/10	1205.312	68.52	0.93
15	SYCP/CSCS/5	1188.968	67.60	0.50
16	ASCP/CCCC/15	1170.582	66.55	0.65
17	ASCP/CCCC/10	1121.552	63.76	0.72

Ranks in term of first ply failure load	Plate combination	$\overline{\text{FPFL}}$	(First ply failure load/maximum first ply failure load)×100 %	Frequency reduction ratio due to first ply failure
18	ASCP/CCSS/30	1085.802	61.73	0.50
19	ASCP/CCCC/5	1084.780	61.67	0.81
20	ASCP/CCCC/0	1071.501	60.92	0.927

Note: SYCP/CCCC/10 means a symmetric cross-ply clamped plate with $\lambda = 10°$

5.3. CONCLUDING REMARKS

The following conclusions are evident from the present study.

- The finite element code used here is capable to study the FPF behaviour of a laminated composite skew plate. The results of the benchmark problems establish this fact positively.
- For angle-ply (both antisymmetric and symmetric) plates the maximum strain criterion and for symmetric cross-ply plates the Puck criterion may be suggested as governing failure theory that may be used to obtain the most conservative FPF loads.
- For antisymmetric cross-ply skew plate, though a single criterion cannot be identified, but the failure theory to be adopted is either of Hoffman or that of Puck.
- To get an initial idea about the most conservative failure load carrying capacity of a skew plate, working equations and figures are suggested in this present thesis for predicting failure load values with respect to different skew angles.
- To identify the good skew plate options among all the cases taken up here, a rank matrix is proposed here which may be used to get an idea about the relative performances of different plate combinations.
- The plate combinations which emerged as preferred option are all of cross-ply category and the boundary conditions are either fully clamped or two opposite edges clamped the other two being simply supported.

Chapter 6

NONLINEAR FIRST PLY FAILURE OF LAMINATED COMPOSITE CLAMPED SKEW PLATES

6.1. GENERAL

An eight-noded isoparametric curved quadratic plate element based on Sanders' and von Kármán nonlinearity is added in the the finite element code to generate results presented in this chapter. The first ply failure (FPF)loads are evaluated based on various well-acknowledged failure theories like maximum stress, maximum strain and those proposed by Hoffman, Tsai – Hill, Tsai – Wu, Hashin and Puck. Effect of variation of skew angles on FPF loads of laminated composite skew plates for various stacking pattern is reported and studied in depth. The failure criterion corresponding to which the failure load value is minimum, for each skew angle, is only reported in this chapter in Section 6.2. The effects of skew angle on the FPF load are summarised in the form of charts and working equations. The engineers and researchers may use the charts and equations directly to predict the FPF load provided the geometry of the plate is known. Besides FPF loads the failed plies as well as the failure modes are also reported.

6.2. NUMERICAL STUDY AND DISCUSSIONS

The author establishes the correctness of the present computer code in predicting nonlinear FPF load through solution of a benchmark problem. The nonlinear FPF load evaluated from the present code for partially clamped laminated composite plate under central point load is compared with the results as obtained by Kam et al. (1996) and furnished in Table 6.1.

The material properties and the geometrical properties of the graphite-epoxy skew plate options considered in the present study are furnished in Table 5.3 and Table 6.2 respectively. The skew plates are subjected to uniformly distributed static transverse load from clamped conditions along all four edges of the plate.

Table 6.1 FPF load in Newton for a $[0_2^\circ/90^\circ]_S$ laminated composite plate

Failure criteria	Length/plate thickness	Experimental failure load (Kam et al. (1996))	FPF loads (Kam et al.(1996))	FPF loads (present formulation)
Maximum stress			147.63	139.94
Maximum strain			185.32	194.58
Hoffman	105.26	157.34	143.16	137.12
Tsai-Wu			157.78	150.71
Tsai-Hill			144.42	151.22

Note: Each plan dimension= 100 mm, ply thickness = 0.155 mm; load applied = central concentrated load

Table 6.2 Geometrical properties

Parameters	Values
Aspect ratio (*a/b*)	1
Width to thickness ratio (*a/h*)	100
Skew angles, λ	0°, 5°, 10°, 15°, 20°, 25°, 30°
Laminations	Antisymmetric angle-ply (ASAP) $+45°/-45°$ Antisymmetric cross-ply (ASCP) $0°/90°$ Symmetric angle-ply (SYAP) $+45°/-45°/+45°$ Symmetric cross-ply (SYCP) $0°/90°/0°$

In this section, the results of numerical experiments with clamped (CCCC) skew plate options for varied skew angles and laminations are reported. The non-dimensional uniformly distributed FPF load in the form of superimposed pressure $\overline{FPFL} = \left({FL}/{E_T}\right)\left({a}/{h}\right)^4$ is obtained from the FPF load values (FL) for different skew plate options. These non-dimensional FPF load values along with the other FPF related information such as governing failure criteria failed plies and failed modes are reported in Table 6.3 to Table 6.4. The minimum FPF load value obtained from different failure criteria taken up here for a particular

plate option is considered as the FPF load value for that plate option and the corresponding failure criterion is treated as the governing failure criterion.

Table 6.3 Non-dimensional uniformly distributed FPF loads ($\overline{FPFL}$) for angle ply laminates

Lamination	Skew angle, λ (degree)	Governing Failure criteria	$\overline{FPFL}$	Failed ply	Failure mode/ failure tendency
(+45˚/-45˚)	0	Maximum strain	492.34^{L}	1	Matrix cracking
		Maximum strain	1070.48^{NL}	1	Matrix cracking
	5	Maximum strain	434.12^{L}	1	Matrix cracking
		Maximum strain	828.39^{NL}	1	Matrix cracking
	10	Maximum strain	388.15^{L}	1	Matrix cracking
		Maximum strain	688.46^{NL}	1	Matrix cracking
	15	Maximum strain	364.66^{L}	1	Matrix cracking
		Maximum strain	611.85^{NL}	1	Matrix cracking
	20	Maximum strain	360.57^{L}	1	Matrix cracking
		Maximum strain	557.71^{NL}	1	Matrix cracking
	25	Maximum strain	367.72^{L}	1	Matrix cracking
		Maximum strain	526.05^{NL}	1	Matrix cracking
	30	Maximum strain	374.87^{L}	1	Matrix cracking
		Maximum strain	516.85^{NL}	1	Matrix cracking
(+45˚/-45˚/+45˚)	0	Maximum strain	1039.84^{L}	3	Matrix cracking
		Hoffman	2552.60^{NL}	1	Matrix cracking
	5	Maximum strain	980.59^{L}	3	Matrix cracking
		Hoffman	1918.28^{NL}	1	Matrix cracking
	10	Hoffman	801.84^{L}	1	Matrix cracking
		Hoffman	1408.58^{NL}	1	Matrix cracking
	15	Maximum strain	680.29^{L}	1	Matrix cracking
		Maximum strain	1090.91^{NL}	1	Matrix cracking
	20	Maximum strain	576.10^{L}	1	Matrix cracking
		Maximum strain	851.89^{NL}	1	Matrix cracking
	25	Maximum strain	522.98^{L}	1	Matrix cracking
		Maximum strain	712.97^{NL}	1	Matrix cracking
	30	Maximum strain	517.87^{L}	1	Matrix cracking
		Maximum strain	646.58^{NL}	1	Matrix cracking

Note: *L* and *NL* represent the linear and nonlinear FPF load values respectively

Table 6.4 Non-dimensional uniformly distributed FPF loads ($\overline{FPFL}$)for cross ply laminates

Lamination	Skew angle, λ (degree)	Governing Failure criteria	$\overline{FPFL}$	Failed ply	Failure mode/ failure tendency
(0˚/90˚)	0	Hoffman	1071.50^{L}	1	Fibre breakage
		Hoffman	2923.39^{NL}	1	Fibre breakage
	5	Hoffman	1084.78^{L}	1	Fibre breakage
		Hoffman	2912.15^{NL}	1	Fibre breakage
	10	Hoffman	1121.55^{L}	1	Fibre breakage
		Hoffman	2943.82^{NL}	1	Fibre breakage
	15	Hoffman	1170.58^{L}	1	Fibre breakage

Lamination	Skew angle, λ (degree)	Governing Failure criteria	$\overline{\text{FPFL}}$	Failed ply	Failure mode/ failure tendency
	15	Hoffman	3023.49^{NL}	1	Matrix cracking
	20	Hoffman	1221.65^{L}	1	Fibre breakage
		Hoffman	3107.25^{NL}	1	Matrix cracking
	25	Hoffman	1310.52^{L}	1	Matrix cracking
		Hoffman	3201.23^{NL}	1	Matrix cracking
	30	Hoffman	1459.65^{L}	1	Matrix cracking
		Hoffman	3431.05^{NL}	1	Matrix cracking
(0˚/90˚/0˚)	0	Maximum strain	1692.54^{L}	1	Matrix cracking
		Maximum strain	2951.99^{NL}	1	Matrix cracking
	5	Puck	1689.48^{L}	1	Matrix crushing, mode C
		Maximum strain	2984.68^{NL}	1	Matrix cracking
	10	Maximum strain	1758.94^{L}	1	Matrix cracking
		Maximum strain	3008.17^{NL}	1	Matrix cracking
	15	Puck	1432.07^{L}	3	Matrix crushing, mode C
		Maximum strain	3024.51^{NL}	1	Matrix cracking
	20	Puck	1067.42^{L}	3	Matrix crushing, mode C
		Puck	2574.05^{NL}	3	Matrix crushing, mode C
	25	Puck	938.71^{L}	3	Matrix crushing, mode C
		Puck	1683.35^{NL}	3	Matrix crushing, mode C
	30	Puck	945.86^{L}	3	Matrix crushing, mode C
		Puck	1440.25^{NL}	3	Matrix crushing, mode C

Note: *L* and *NL* represent the linear and nonlinear FPF load values respectively

Table 6.1 establishes the correct incorporation of geometric linear and nonlinear strains in the present finite element formulation for the computation of FPF load values. The results obtained by the present computer code show close agreement with those obtained by Kam et al. (1996). The author compute the non-dimensional frequency of laminated composite skew plates using a lumped mass matrix scheme and an initial un-degraded stiffness matrix for the solution of the Eigenvalue problem. Table 5.2 reports the non-dimensional frequencies obtained in the first three modes by the present approach and those computed by Singha et al. (2007). The compliance of results confirms the appropriate inclusion of skew plate geometry in the present computer code.

It is established from the present numerical experiments that the maximum strain criterion and Hoffman or Puck failure criteria dominate the FPF of angle ply and cross ply laminates respectively. So for clamped supported skew plate, one can directly use maximum

strain failure criteria for angle ply laminates and Hoffman or Puck failure criteria for cross ply plate to evaluate the minimum failure load at which FPF occurs.

Three-layered symmetric angle ply laminates +45˚/-45˚/+45˚ show nearly about 2.3 times higher FPF strength compared to two-layered antisymmetric angle ply +45˚/-45˚ laminates. But in the case of cross ply laminates, two-layered antisymmetric 0˚/90˚ skew plates with skew angle 30˚ shows 1.15 times higher FPF load compared to the highest FPF load among three-layered symmetric cross ply skew plate options. The cross ply laminate 0˚/90˚ (λ = 30˚) shows 1.34 times higher failure load compared to angle ply laminates (+45˚/-45˚/+45˚ and skew angle, λ=5˚) among all the cases considered here. So it is stated that antisymmetric cross ply 0˚/90˚ may be considered as the best plate options.

In maximum cases for clamped boundary conditions for both symmetric and antisymmetric angle and cross ply laminates, FPF is identified at the topmost ply under uniformly distributed transverse load. This can be explained as due to the development of tension near the support top resulting in fiber breakage or matrix cracking. In few cases in three layered symmetric cross ply and angle ply, FPF is observed at the bottom-most ply (ply number =3). Thus topmost ply is the most vulnerable ply for two-layered skew plate options and sometimes the bottom-most one is the vulnerable one for three-layered skew plate laminates.

Fig. 6.1 represents the variation of non-dimensional FPF load ($\overline{\text{FPFL}}$) with skew angle (λ) for different combinations of skew plate options. The author obtained working equations correlating the non-dimensional uniformly distributed FPF load values ($\overline{\text{FPFL}}$) with skew angles. Thus if the geometry of the skew plate is measured by some instrument then the FPF load carrying capacity may be predicted using the working equations and charts which is shown in Fig. 6.1. One can easily compute the FPF load values for any other intermediate values of skew angle (between 0˚ and 30˚) from Fig. 6.1.

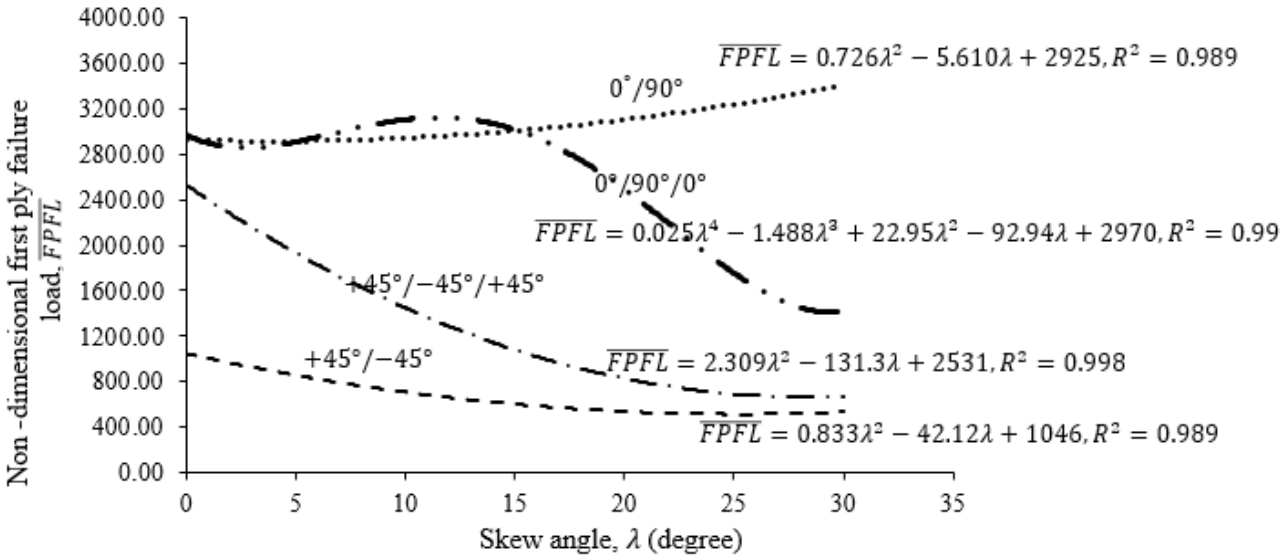

Fig. 6.1 Variation of first ply failure load with skew angle for different lamination

6.3. CONCLUDING REMARKS

The following conclusions are evident from the present study.

- The results of benchmark problems confirm that the present finite element program may be directly applied as a tool to correctly predict the FPF load value of laminated composite skew plates.
- The FPF load carrying capacity of cross ply skew plate options is found to be more compared to angle ply one.
- In most of the cases for two-layered skew plate options, the topmost ply fails first for clamped boundary conditions under static transverse load. In a few cases among three-layered laminated bottommost ply fails before the rest of the two plies.
- Working equations and charts connecting the non-dimensional FPF load ($\overline{\text{FPFL}}$) and skew angle may be used directly to predict the FPF load. If the geometry of the plate is measured by some device then FPF capacity may be predicted for a skew plate with skew angle lying in the range of 0˚ to 30˚.

Chapter 7

NONLINEAR PROGRESSIVE FAILURE PREDICTION OF CLAMPED COMPOSITE THIN SKEW PLATES UNDER TRANSVERSE LOADING

7.1. GENERAL

A review of literature about industrially important composite skew plates, which are used as roofing and flooring units to cover non-rectangular parallelogram shaped plan areas, shows that the aspect of progressive failure has not received any attention from researchers which is essential to comprehensively understand failure behaviour from initiation to the ultimate stage. In the present approach stiffness degradation of a damaged plate is considered only at the point of damage in the corresponding lamina at all stages of first and progressive failure and the present outputs match excellently with published experimental results. This realistic modelling of failure behaviour is the novelty of this chapter. Apart from reporting the failure load values, the failure zones and nature of damage progress on the skew plate surfaces are also presented which are expected to be valuable inputs for non-destructive health monitoring.

7.2. NUMERICAL STUDY AND DISCUSSIONS

The capability of the present formulation in accurate prediction of nonlinear first ply failure (FPF) load values is concluded in Chapter 6 and progressive failure behaviour of laminated composite partially clamped square plates may be understood by studying Fig. 7.1. In Fig. 7.1, load – deflection curve of a plate undergoing progressive damage as obtained from present study is compared with those obtained by Kam et al. (1996) both analytically and experimentally.

Apart from the above benchmark problems, a number of other cases of thin clamped skew plates with a/h = 100 subjected to uniformly distributed static transverse pressure are solved here and the findings are interpreted from practical engineering perspectives. The Q-1115 graphite-epoxy composite material is considered and the mechanical properties are the same as those reported by Kam et al. (1996) as furnished in Table 5.3. The first ply failure (FL) and ultimate ply failure(UFL)pressure values are non-dimensionalized as $\overline{FPFL} = \frac{FL}{E_T}\left(a/h\right)^4$ and $\overline{UPFL} = \frac{UFL}{E_T}\left(a/h\right)^4$ respectively. In the present study the $(0°/90°)$, $(0°/90°/0°), (+45°/-45°)$ and$(+45°/-45°/+45°)$ laminations are denoted as ASCP, SYCP, ASAP and SYAP respectively. Here, the ratio of the shorter plan dimension to the thickness of the plate is considered as 100 and the ratio of the plan dimensions is fixed as unity. The author carries out numerical experimentation with her own problems, generating and interpreting different failure related results which are reported in the following subsections using a number of tables and figures for presenting the data lucidly. For both benchmark and other problems, only converged results obtained through appropriate choice of finite element mesh are presented.

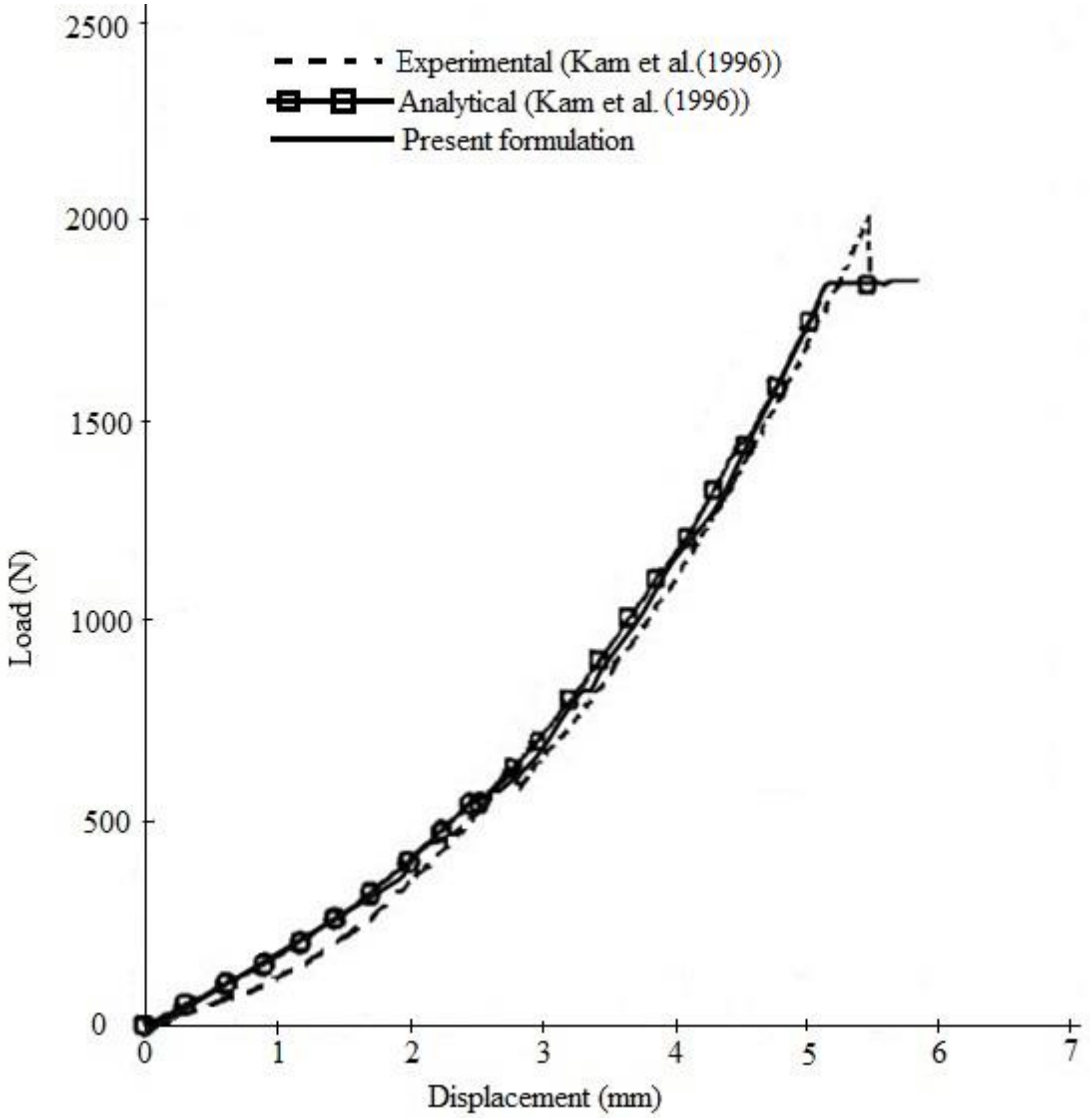

Fig. 7.1 Load-displacement curves of a $[0°/90°/0°/90°]_s$ partially clamped square plate with proper stiffness reduction for progressive failure behaviour

7.2.1. Benchmark Problems

Close agreement of the current result with the published one as evident from Fig.7.1 establishes the correctness of the present approach.

7.2.2. Behaviour of Laminated Composite Skew Plates at Ultimate Failure

The nonlinear FPF pressure values for different stacking arrangements of composite skew plates of clamped boundary condition are presented in previous Chapter 6. For proper understanding of the progressive failure behaviour of laminated composite skew plates, some of the nonlinear FPF pressure values are furnished again in Table 7.1 in this chapter. In addition

to the governing FPF pressure values, failed plies, failure locations, failure modes as well as the ultimate ply failure pressure values are also furnished in this table. The results are also presented systematically in Figs. 7.2 – 7.4 for lucid understanding.

The variations of non-dimensionalized nonlinear ultimate ply failure pressure values with skew angles are presented in Fig. 7.2 which unfolds a number of interesting findings. This figure may be used to graphically interpolate the tentative nonlinear ultimate ply failure pressure values for any value of skew angle ranging between 0° to 30° which are expected to be helpful to practicing design engineers.

It is observed that the cross ply plates show consistently higher results of ultimate failure pressure values compared to the angle ply ones. This finding clearly indicates that an engineer shall pick up cross ply options if skew plates are to be used in place of rectangular ones in a practical situation. The antisymmetric cross ply skew plates (ASCP) prove to be better choices up to skew angle of 20° but symmetric cross ply (SYCP) yields better results beyond this skew angle in terms of ultimate ply failure pressures. In contrast to cross ply skew plates, the symmetric stacking sequence (SYAP) proves to be a better choice than the antisymmetric one (ASAP) consistently for all combinations of angle ply plates in terms of ultimate failure. The above observations indicate a complex interaction between stacking sequence and skew angle and so an elaborate study is required to identify the best combination of these two parameters to achieve the highest ultimate load carrying capacity in a given practical situation.

Table 7.1. Non-dimensionalized first and ultimate ply failure pressures for laminated composite skew plates for different skew angles

Stacking sequence	Skew angle	First ply failure					Ultimate failure
		Governing failure criteria	$(\overline{\mathrm{FPFL}})$	First failed ply	First ply failure location $(x/a, y/b)$	Failure mode	$(\overline{\mathrm{UPFL}})$
ASCP (0°/90°)	0°	Hoffman	2923.39	1	(0.35, 0.47)	Fibre breakage	4497.44
	5°	Hoffman	2912.15	1	(0.69, 0.52)	Fibre breakage	4538.30
	10°	Hoffman	2943.82	1	(0.74, 0.52)	Fibre breakage	4706.84
	15°	Hoffman	3023.49	1	(0.79, 0.51)	Matrix cracking	4707.86
	20°	Hoffman	3107.25	1	(1.14, 0.45)	Matrix cracking	5294.58
	25°	Hoffman	3201.23	1	(1.18, 0.43)	Matrix cracking	5191.01
	30°	Hoffman	3431.05	1	(1.11, 0.24)	Matrix cracking	4879.47
SYCP (0°/90°/0°)	0°	Maximum strain	2951.99	1	(0.47, 0.97)	Matrix cracking	4366.70
	5°	Maximum strain	2984.68	1	(0.56, 0.97)	Matrix cracking	4376.91
	10°	Maximum strain	3008.17	1	(0.45, 0.959)	Matrix cracking	4337.08
	15°	Maximum strain	3024.51	1	(0.53, 0.942)	Matrix cracking	4260.47
	20°	Puck	2574.05	3	(0.685, 0.917)	Matrix crushing, mode C	4005.51
	25°	Puck	1683.35	3	(0.383, 0.772)	Matrix crushing, mode C	5236.57
	30°	Puck	1440.25	3	(1.05, 0.13)	Matrix crushing, mode C	5066.49
ASAP (+45°/-45°)	0°	Maximum strain	1070.48	1	(0.28, 0.97)	Matrix cracking	3043.92
	5°	Maximum strain	828.39	1	(0.99, 0.27)	Matrix cracking	2187.95
	10°	Maximum strain	688.46	1	(0.15, 0.71)	Matrix cracking	2336.06
	15°	Maximum strain	611.85	1	(0.21, 0.70)	Matrix cracking	2274.77
	20°	Maximum strain	557.71	1	(0.27, 0.68)	Matrix cracking	2208.38

Stacking sequence	Skew angle	First ply failure					Ultimate failure
		Governing failure criteria	($\overline{FPFL}$)	Stacking sequence	Skew angle	Governing failure criteria	($\overline{FPFL}$)
	25°	Maximum strain	526.05	1	(0.33, 0.66)	Matrix cracking	2201.23
	30°	Maximum strain	516.85	1	(1.11, 0.23)	Matrix cracking	2455.57
SYAP (+45°/-45°/+45°)	0°	Hoffman	2552.60	1	(0.03,0.53)	Matrix cracking	4011.23
	5°	Hoffman	1918.28	1	(1.01, 0.47)	Matrix cracking	3797.75
	10°	Hoffman	1408.58	1	(1.06, 0.47)	Matrix cracking	2398.88
	15°	Maximum strain	1090.91	1	(0.22, 0.70)	Matrix cracking	2748.72
	20°	Maximum strain	851.89	1	(1.07,0.26)	Matrix cracking	2785.49
	25°	Maximum strain	712.97	1	(1.09, 0.25)	Matrix cracking	2417.77
	30°	Maximum strain	646.58	1	(0.38, 0.63)	Matrix cracking	2485.19

Note: $a/b = 1$, $a/h = 100$

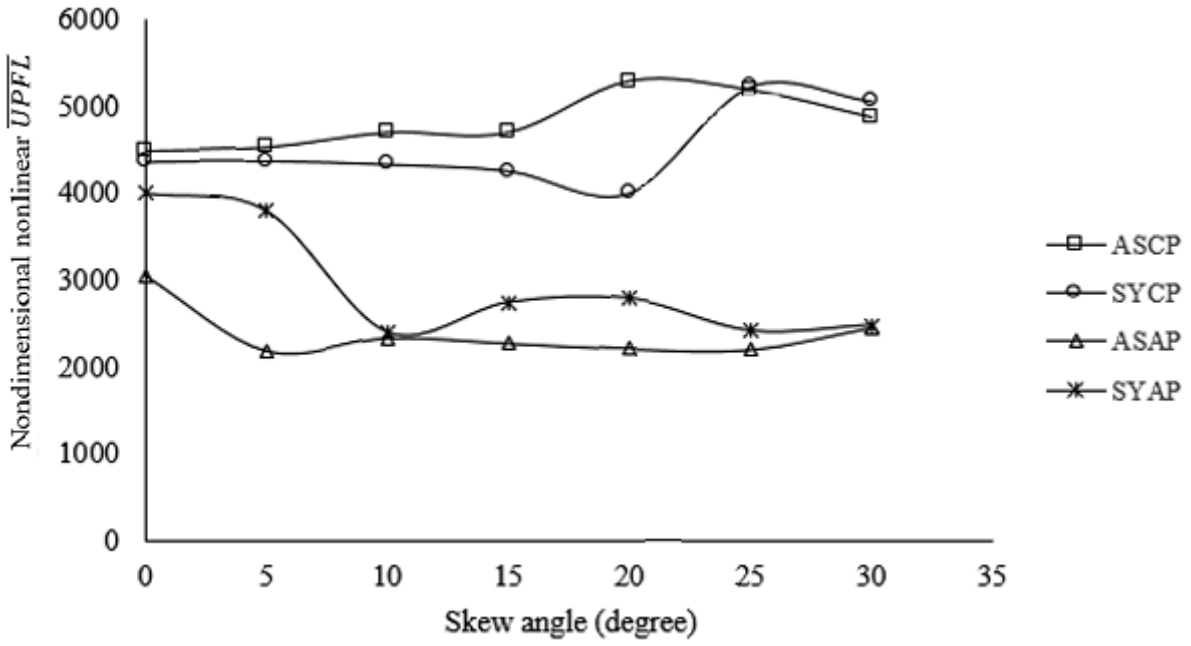

Fig. 7.2 Variation of nonlinear ultimate ply failure pressure with skew angles

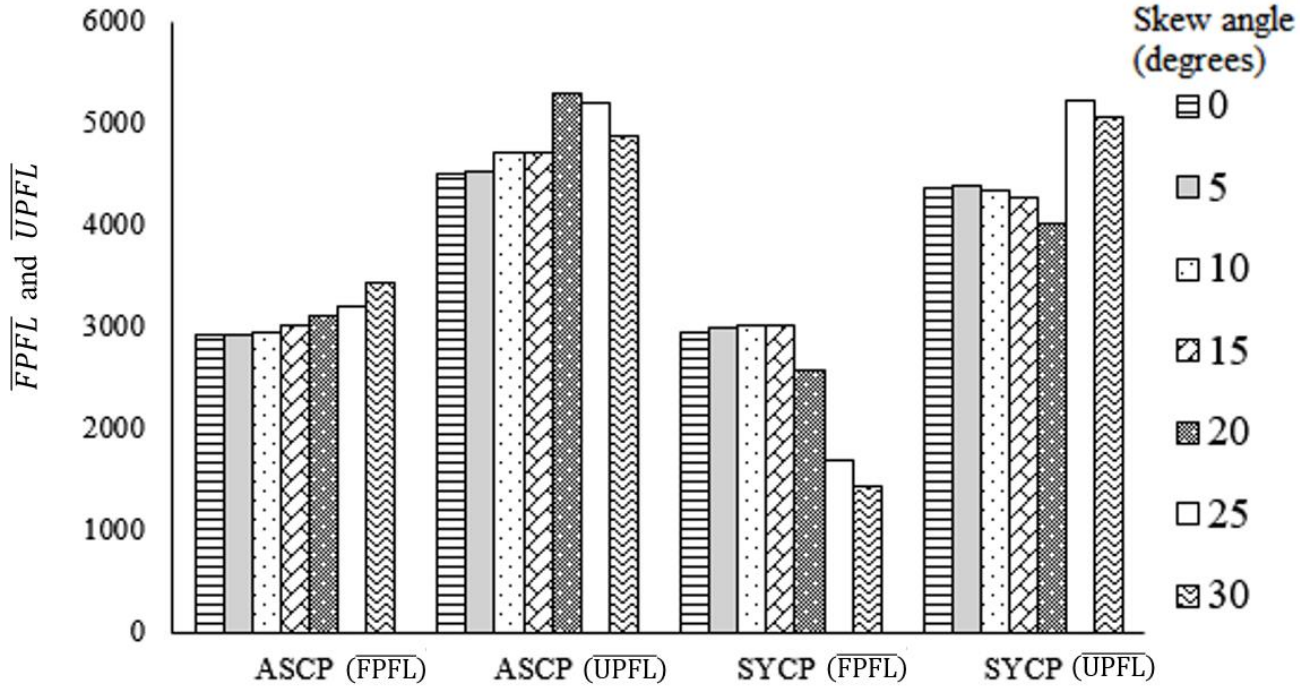

Fig. 7.3 Non-dimensional nonlinear first and ultimate ply failure pressures for different cross ply skew plates

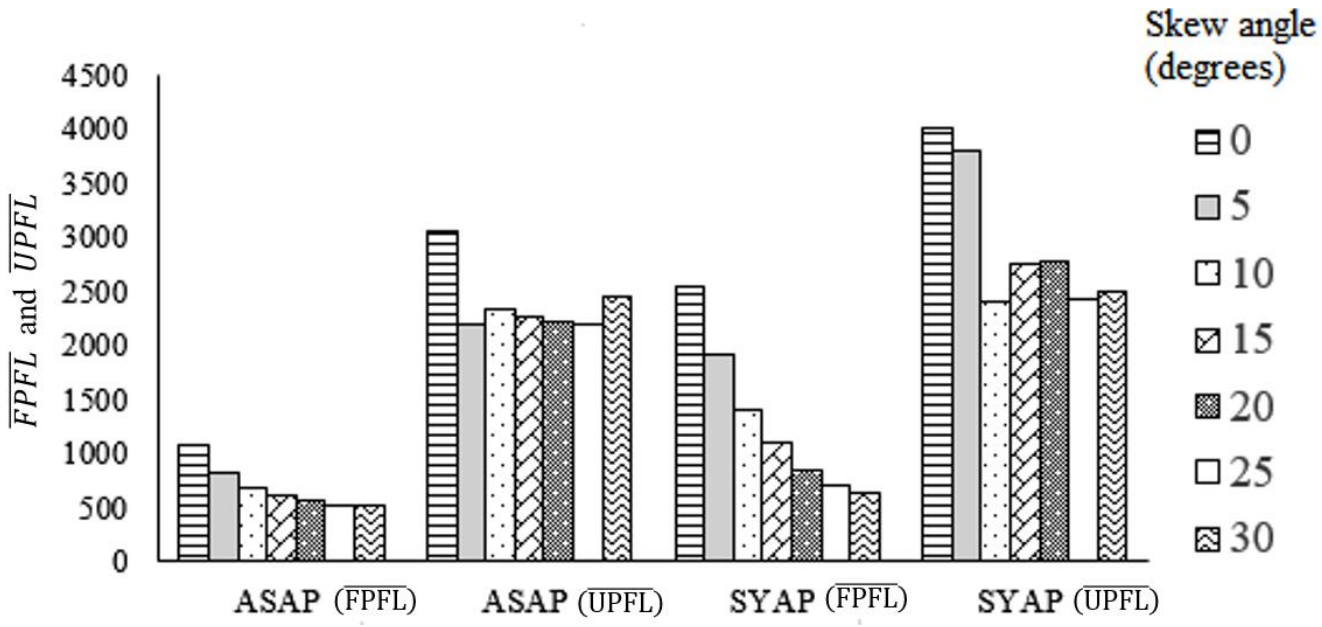

Fig. 7.4 Non-dimensional nonlinear first and ultimate ply failure pressures for different angle ply skew plates

7.2.3. Evaluation of Working Failure Pressures and Values of Load factors

In practical civil engineering design, serviceability is a very important consideration. In tune with the different design codes, the permissible deflection is assumed to be 0.004 times the shorter plan dimension of the skew plates in the present study. The pressure values corresponding to this permissible deflection are considered as the serviceability failure pressures and these values are furnished in Table 7.2.

The results presented in Tables 7.1 and 7.2 clearly indicate that the pressure values corresponding to serviceability criterion are far less than the actual FPF pressure values obtained through accurate nonlinear analysis. This brings out the fact that the composite skew plates do have high post serviceability reserve strength before failure.

Working failure pressure may be defined as the lesser of the pressure corresponding to serviceability failure and the FPF pressure divided by a practical partial factor of safety (say 3 considering all uncertainties in fabrication of the laminates). From this angle, it is found that the working load obtained from the criterion of serviceability shall be adopted. It is evident

from Table 7.2 that the working pressure value monotonically increases with increase of skew angle for all laminates except the SYAP one. For SYAP stacking sequence as well, the same tendency is observed beyond 10° onwards while between 0° and 10° the behaviour shows an opposite trend. Hence, for this lamination, skew angle in the range of 0° to 10° must be used cautiously and the working load values for the rectangular plates cannot be assumed to be conservatively valid for simplicity.

The load factor values are calculated as the ratio between the ultimate failure pressures to the working failure pressure values and these are reported in Table 7.2 together with the working failure pressure values which happen to be identical with the serviceability pressure values here. The load factor values are quite high in all the cases of laminates taken up here and those for anti-symmetric cross ply laminates are conspicuously highest among all stacking sequences. Hence it is inferred that the laminated composite skew plates in general have high reserve strength beyond serviceability failure and the user of these plates will get sufficient warning for replacing the plate units before ultimate failure in case damage initiates in service condition.

Table 7.2 Non-dimensionalized serviceability failure pressures with load factors

Stacking sequence		Skew angles, λ						
		0°	5°	10°	15°	20°	25°	30°
ASCP (0°/90°)	Non-dimensionalized serviceability failure pressure	88.87	89.89	93.97	99.08	108.27	122.57	143
	Load factors	50.61	50.49	50.10	47.52	48.90	42.35	34.12
SYCP (0°/90°/ 0°)	Non-dimensionalized serviceability failure pressure	189	192.03	201.23	217.57	243.11	282.94	340.14
	Load factors	23.10	22.79	21.55	19.58	16.48	18.51	14.90
ASAP (+45°/- 45°)	Non-dimensionalized serviceability failure pressure	83.76	84.78	88.87	96.02	106.23	121.55	143
	Load factors	36.34	25.81	26.29	23.69	20.79	18.11	17.17

Stacking sequence		Skew angles, λ						
		0°	5°	10°	15°	20°	25°	30°
SYAP (+45°/-45°/+45°)	Non-dimensionalized serviceability failure pressure	137.9	129.72	126.66	128.7	134.83	147.09	167.52
	Load factors	29.09	29.28	18.94	21.36	20.66	16.44	14.84

Note: $a/b = 1$, $a/h = 100$

7.2.4. Flaw Detection at Failure Initiation and Damage Spread at Ultimate Failure

Although the ultimate failure pressure values of the composite skew plates are much greater in magnitude compared to the FPF ones, still it is important for the user to know when FPF sets in. Non-destructive flaw detection techniques must be adopted to detect possible failure initiation and a prior knowledge of the areas which are to be acoustically tested for this purpose will be helpful for an engineer to plan out the testing scheme. In order to facilitate such planning, the areas of failure initiation are indicated in Table 7.3 by mentioning such areas as 'A', 'B', 'C' and 'D' as explained in Fig. 7.5.

Damaged areas at ultimate failure situation are studied meticulously for different skew angles and laminations. The nature of damage progress till ultimate failure is represented in Figs. 7.7 to 7.13 for various skew plate options and zones of failure mentioned in Table 7.3 are used to describe the failure areas- damage restricted mostly to zones A and B are peripheral, that mostly within Zones C and D are central while a scattered failure pattern involves all the failure zones.

The typical pictorial representation of damaged areas for skew angles 0° to 30° are furnished in Figs. 7.6 to 7.12 ((a)-(d)). Different colour shades are used to indicate the lamina which fails within a particular element. In cases where different laminae of the same element fail at ultimate failure stage, a particular element is filled with different colours to indicate the failed laminae. The numbers written within the triangles represent the element numbers.

In case of cross ply plates, area of damage at ultimate failure stage is relatively less than that of angle ply plates. In fact, in cross ply plates the progressive damage remains restricted

somewhat within a few localised pockets while the majority of the plate area remains undamaged till ultimate failure and the plate areas adjacent to the supports also do not undergo progressive damage. On the other hand, in case of angle ply plates, greater areas including those near the supports are affected by progressing failure and this is why the angle ply plates undergo ultimate failure at relatively lower values of surface pressure compared to the cross ply ones.

Table 7.3 Failure zones with nature of damaged area at ultimate failure

			At ultimate ply failure	
Stacking sequence	Skew angle	Zone of failure initiation	Percentage of the damaged area	Nature of damaged area
ASCP	0°	C	3.125	Central
(0°/90°)	5°	C	3.125	Central
	10°	C	3.125	Central
	15°	C	3.125	Central
	20°	A	26.563	Scattered
	25°	A	3.125	Scattered
	30°	A	3.125	Scattered
SYCP	0°	A	3.125	Scattered
(0°/90°/0°)	5°	A	3.125	Scattered
	10°	A	26.563	Scattered
	15°	A	25	Scattered
	20°	A	29.687	Scattered
	25°	A	75	Scattered
	30°	A	76.563	Scattered
ASAP	0°	A	79.687	Scattered
(+45°/-45°)	5°	A	50	Scattered
	10°	A	53.125	Peripheral
	15°	A	50	Peripheral
	20°	A	50	Peripheral
	25°	A	45.312	Peripheral
	30°	A	48.437	Peripheral
SYAP	0°	A	48.437	Scattered
(+45°/-45°/+45°)	5°	A	70.312	Scattered
	10°	A	32.812	Central
	15°	A	71.875	Scattered
	20°	A	71.875	Scattered
	25°	A	54.687	Scattered
	30°	A	59.375	Scattered

Note: $a/b = 1$, $a/h = 100$

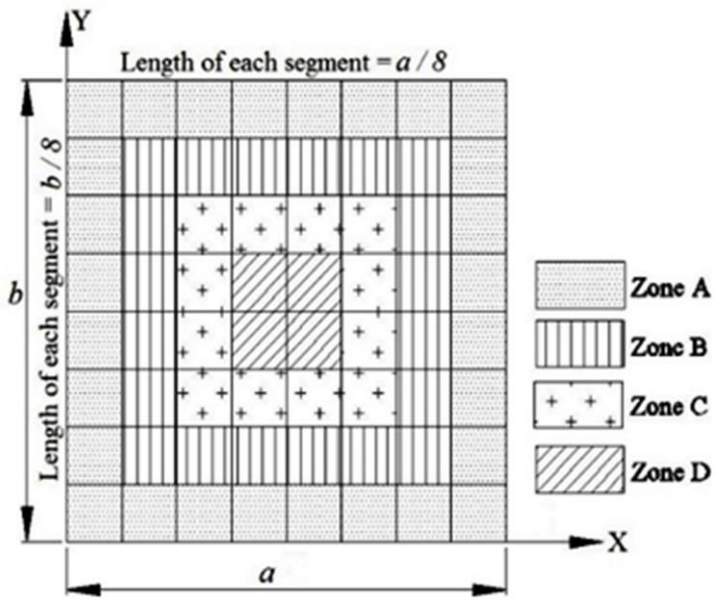

Fig. 7.5 Schematic representation of failure zones at first ply failure

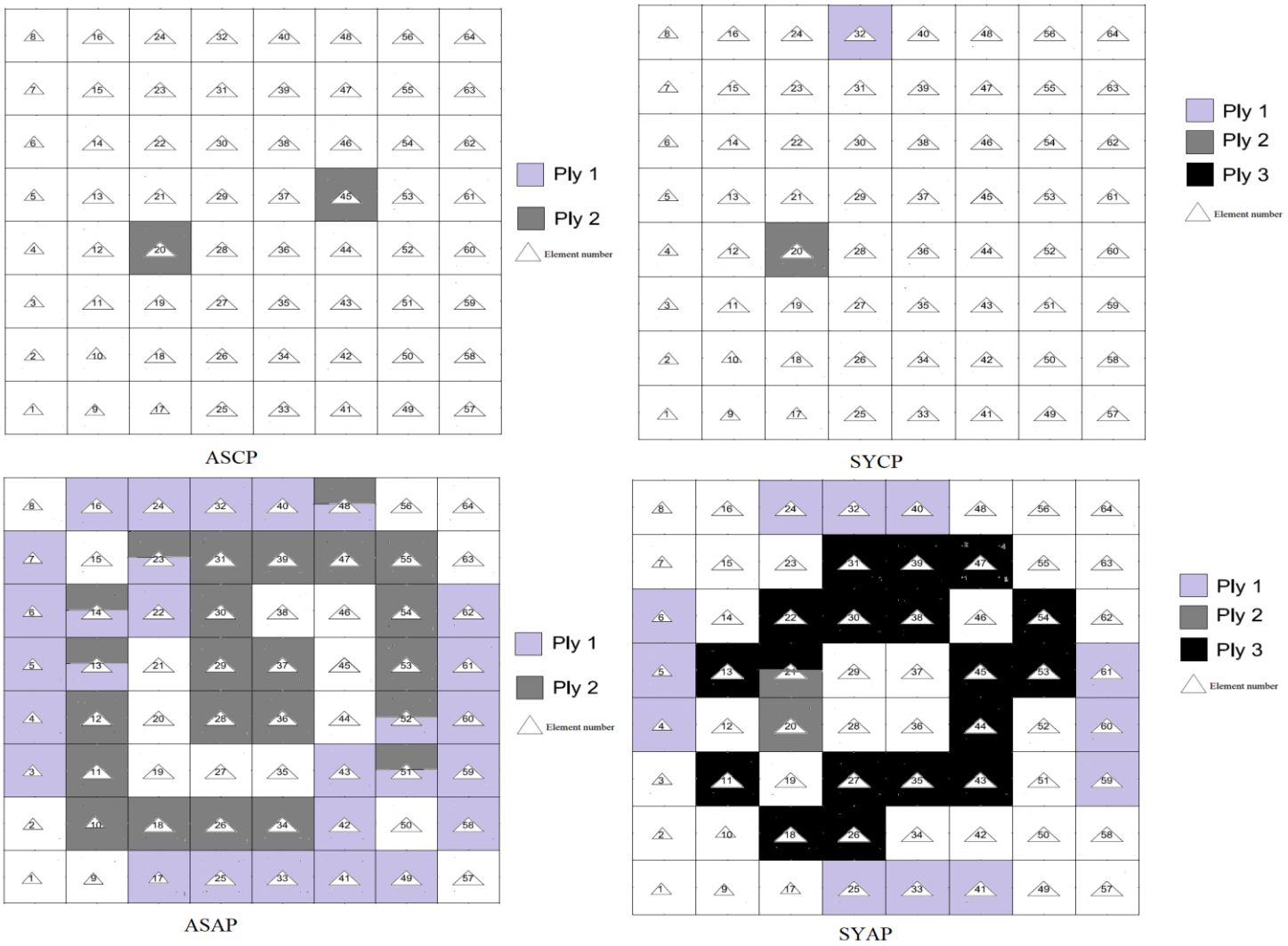

Fig.7.6 Damaged locations at ultimate failure situation of clamped skew plate with skew angle = 0° for different laminations

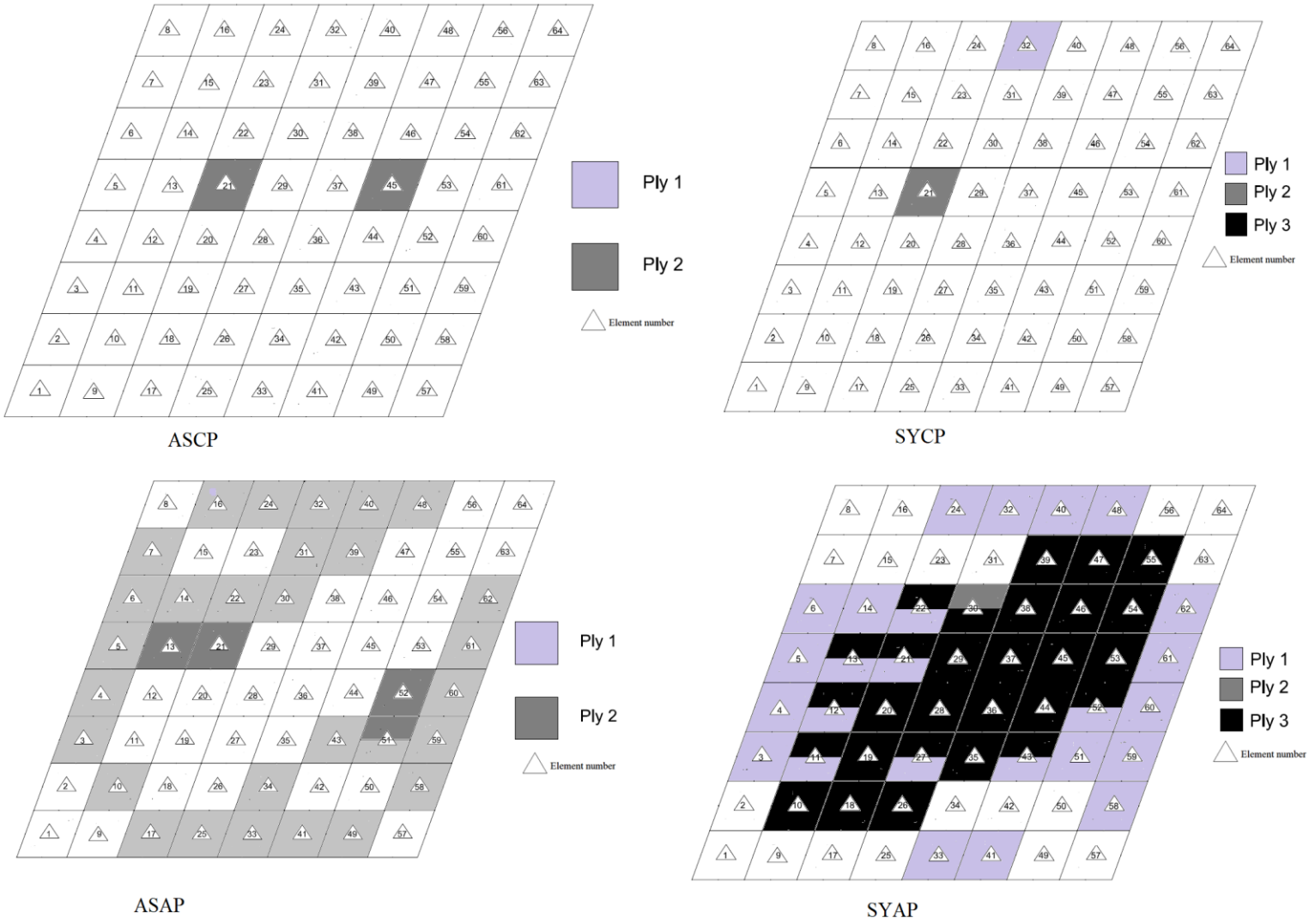

Fig. 7.7 Damaged locations at ultimate failure situation of clamped skew plate with skew angle = 5° for different laminations

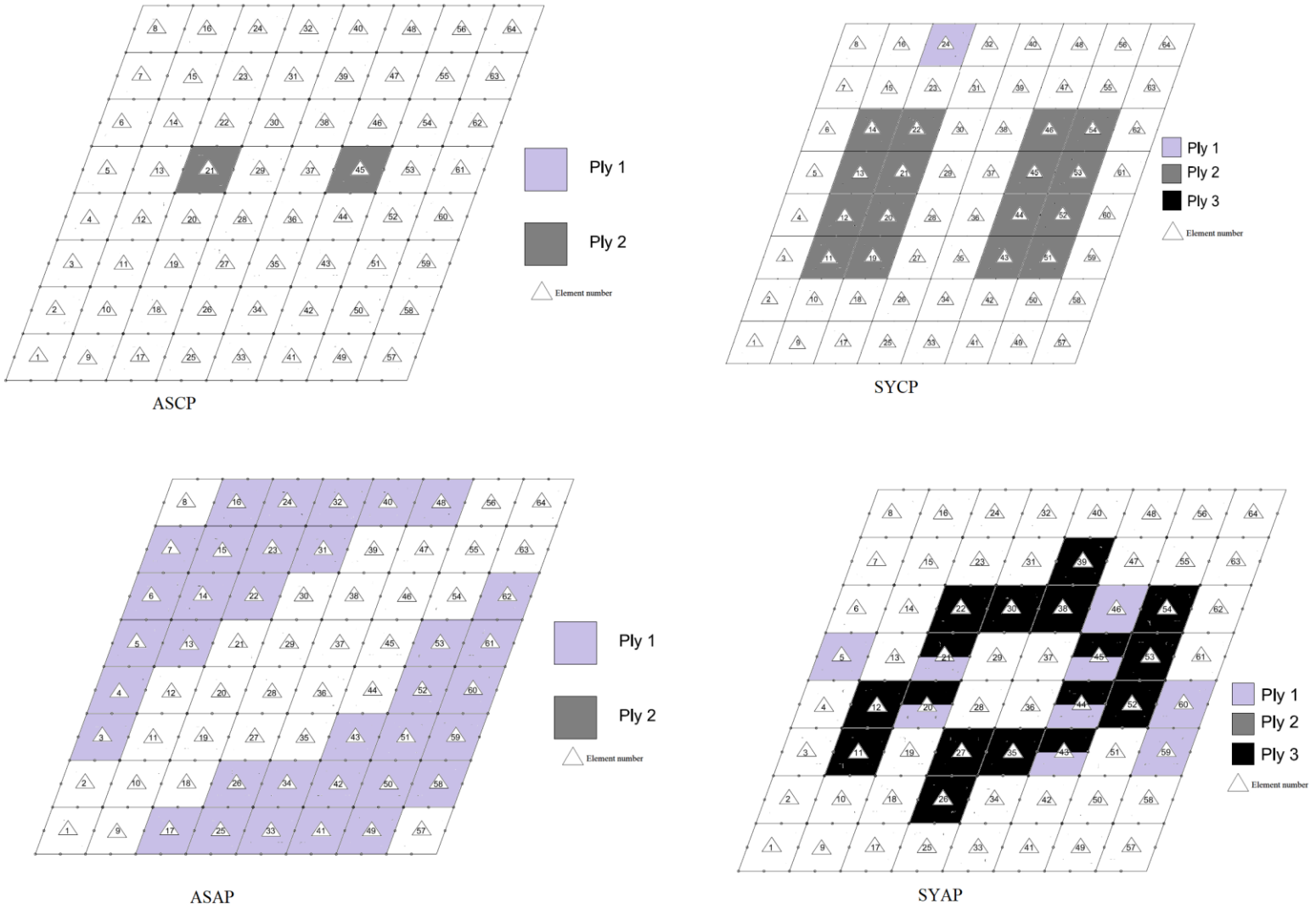

Fig. 7.8 Damaged locations at ultimate failure situation of clamped skew plate with skew angle = 10° for different laminations

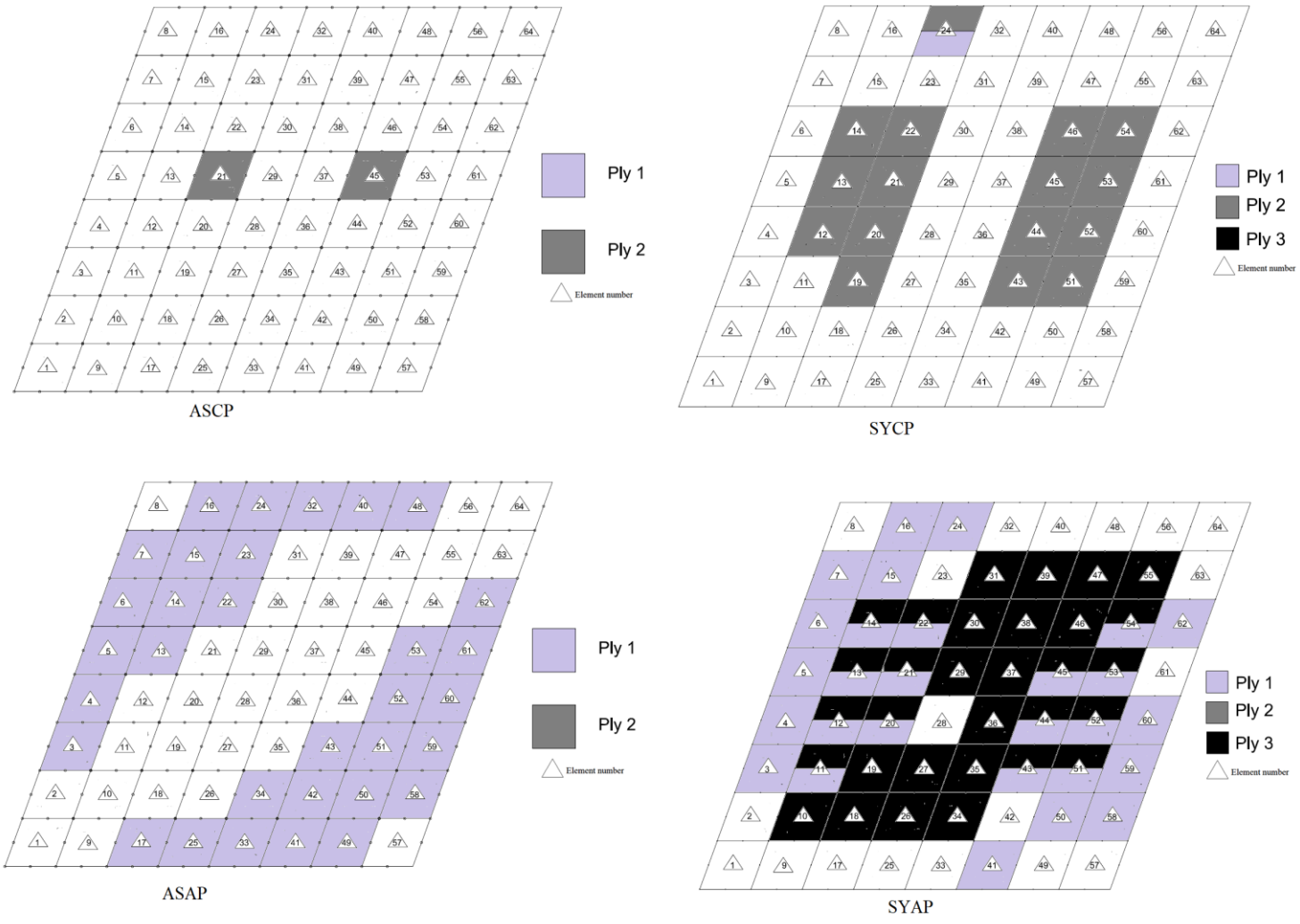

Fig. 7.9 Damaged locations at ultimate failure situation of clamped skew plate with skew angle = 15° for different laminations

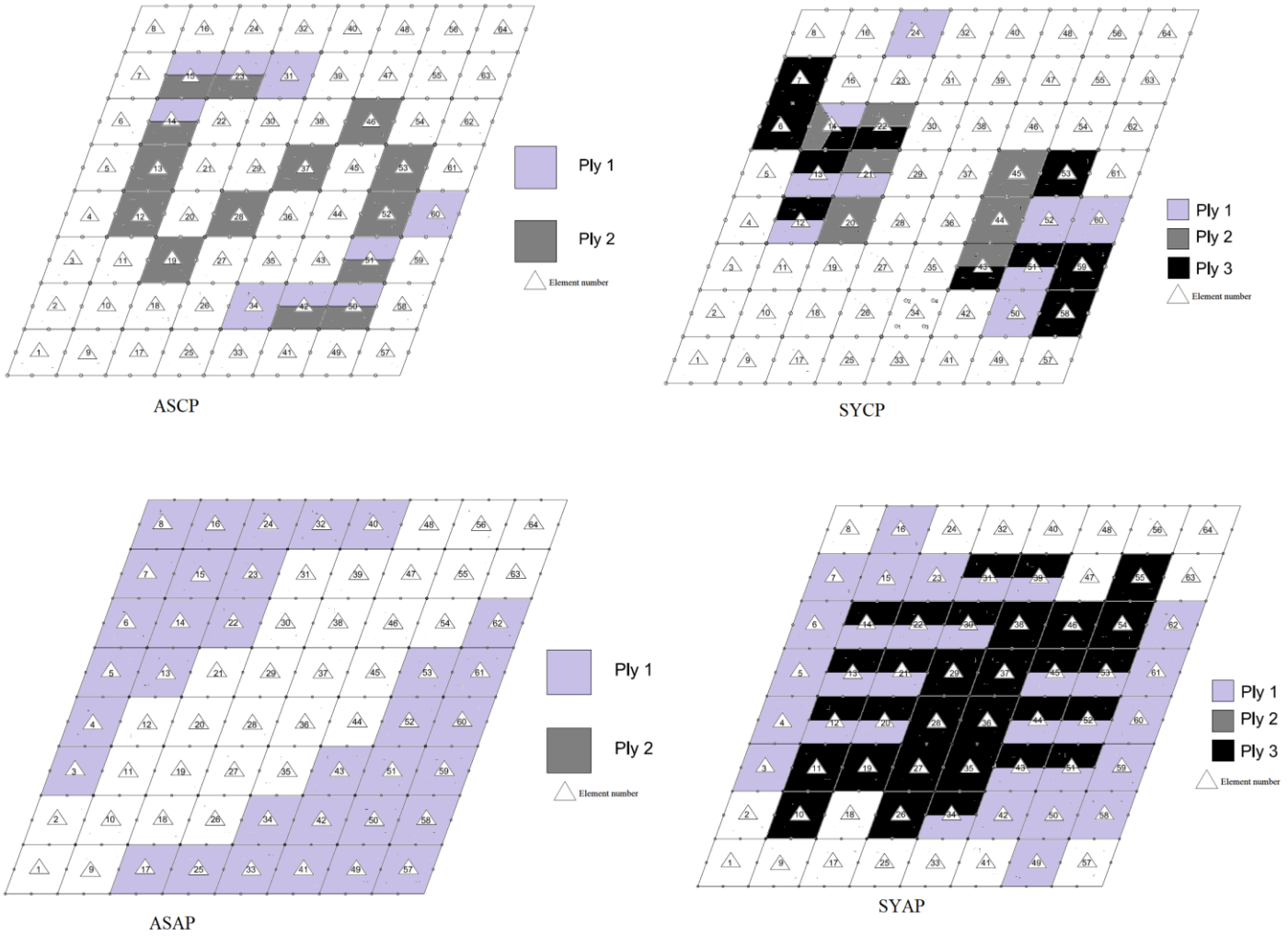

Fig. 7.10 Damaged locations at ultimate failure situation of clamped skew plate with skew angle = 20° for different laminations

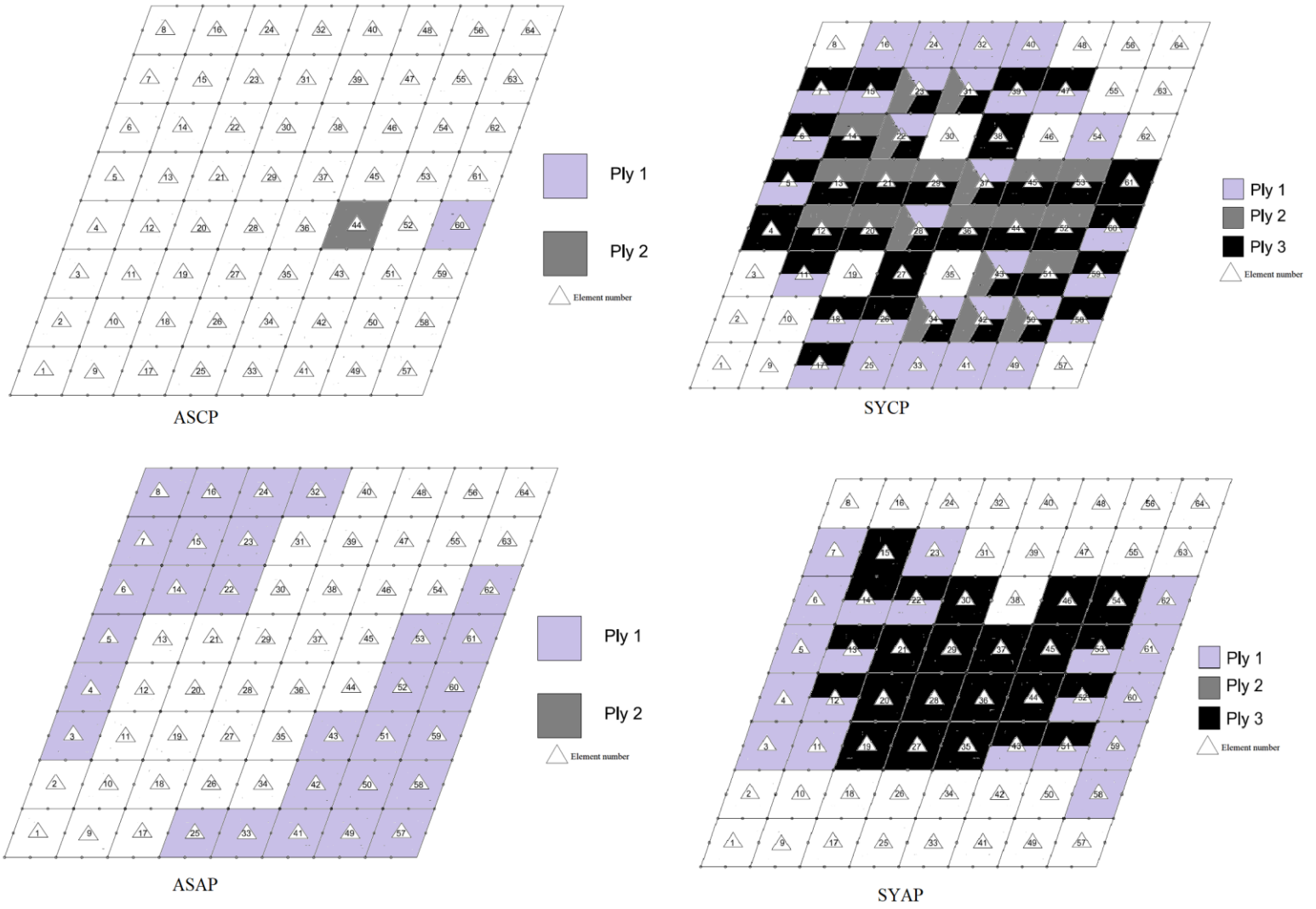

Fig. 7.11 Damaged locations at ultimate failure situation of clamped skew plate with skew angle = 25° for different laminations

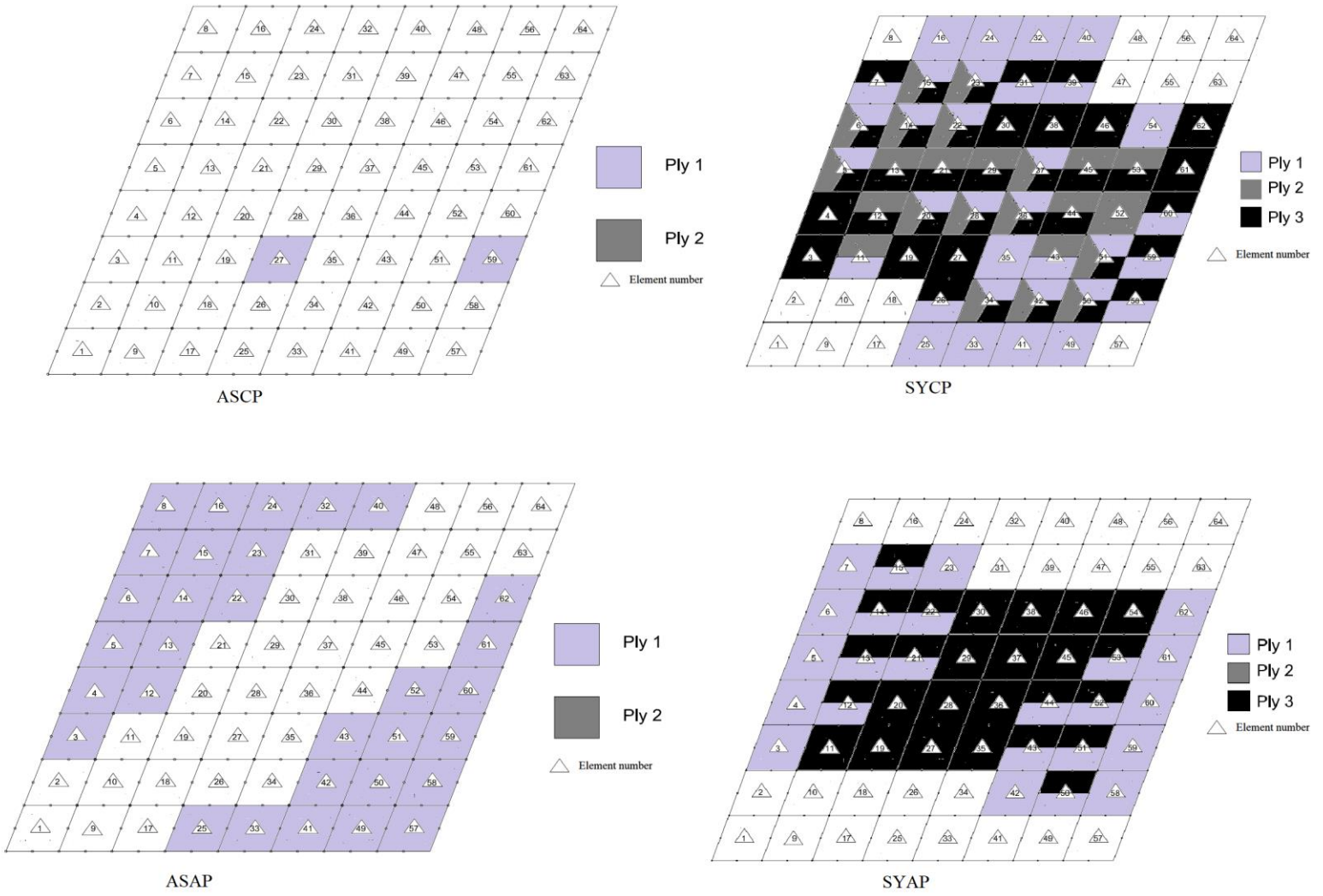

Fig. 7.12 Damaged locations at ultimate failure situation of clamped skew plate with skew angle = 30° for different laminations

7.3. CONCLUDING REMARKS

The current investigation yields the following key findings.

- The correctness of the present finite element code to analyse the failure characteristics of composite skew plates is established through solution of benchmark problems.
- Among the stacking orders considered in this study the cross ply ones prove to be better than the angle ply counterparts consistently and the former can withstand higher magnitudes of first and ultimate ply failure pressures than the later.
- Among two cross ply thin skew plates, the one which is better in terms of FPF pressure may not be the preferred choice in terms of ultimate ply failure pressure.
- The introduction of skew angle in a rectangular plate always tends to soften it for angle ply laminates and the FPF pressure values consistently decrease with increase of skew angles.
- It is found that the laminated composite skew plates in general have high reserve strength beyond serviceability failure and the user will get sufficient warning for replacing the plate units before ultimate failure.
- In case of cross ply plates, area of damage at ultimate failure stage is relatively less than that for angle ply plates.
- The results given in this thesis will help in outlining non-destructive flaw detection testing sequence which is to be adopted to identify possible failure initiation and its progress.

Chapter 8

NONLINEAR PROGRESSIVE FAILURE OF COMPOSITE SKEW PLATES WITH PRACTICAL NON-UNIFORM EDGE CONDITIONS

8.1. GENERAL

Composite skew plates are aesthetically appealing light weight structural units finding wide applications in floors and roofs of commercial buildings. To meet the requirements of different practical situations, these plates often have different boundary restraints along different edges and hence the aspect of failure behaviour considering non-uniform boundary condition is an important area of study. With this objective, the present thesis uses an eight noded isoparametric finite element together with von Kármán's approach of nonlinear strains to study first ply and progressive failure up to ultimate damage of skew plates being subjected to uniform surface pressure. Parameters like skew angles, laminations and boundary conditions are varied and the results are practically analyzed. Interpretation of results from practical angles and proposing the relative performances of the different plate combinations in terms of ranks will be of much help to practicing engineers in selecting the best suited plate option among many combinations.

8.2. NUMERICAL STUDY AND DISCUSSIONS

A number of problems considering various edge conditions, stacking sequences and skew angles are also solved and the results are interpreted from practical engineering standpoints. The material properties used are of graphite epoxy and are same as those reported in the paper of Kam et al. (1996). The non-dimensional form of nonlinear first ply failure load ($\overline{\text{FPFL}}$) and ultimate ply failure load ($\overline{\text{UPFL}}$) are obtained from first ply failure load (FL) and

ultimate ply failure load (UFL) as $\overline{FPFL} = \frac{FL}{E_T}\left(a/h\right)^4$ and $\overline{UPFL} = \frac{UFL}{E_T}\left(a/h\right)^4$ respectively, where E_T is the transverse Young's Modulus of elasticity of the material graphite epoxy. Only converged results obtained through appropriate choice of finite element mesh are presented for all problems.

In this section, the results of numerical experimentations carried out by the author are furnished. Four different laminations combining symmetric (SY) and antisymmetric (AS), cross (CP) and angle ply (AP) laminae are taken up here. The SYCP, ASCP, SYAP and ASAP denote the (0°/90°/0°), (0°/90°), (+45°/-45°/+45°) and (+45°/-45°) respectively. Apart from these, seven different skew angles between 0° to 30° varying in steps of 5° and two irregular edge conditions CCSS and CSCS (as explained in Fig. 8.1) are considered. The plies are numbered sequentially from top to bottom in the increasing order.

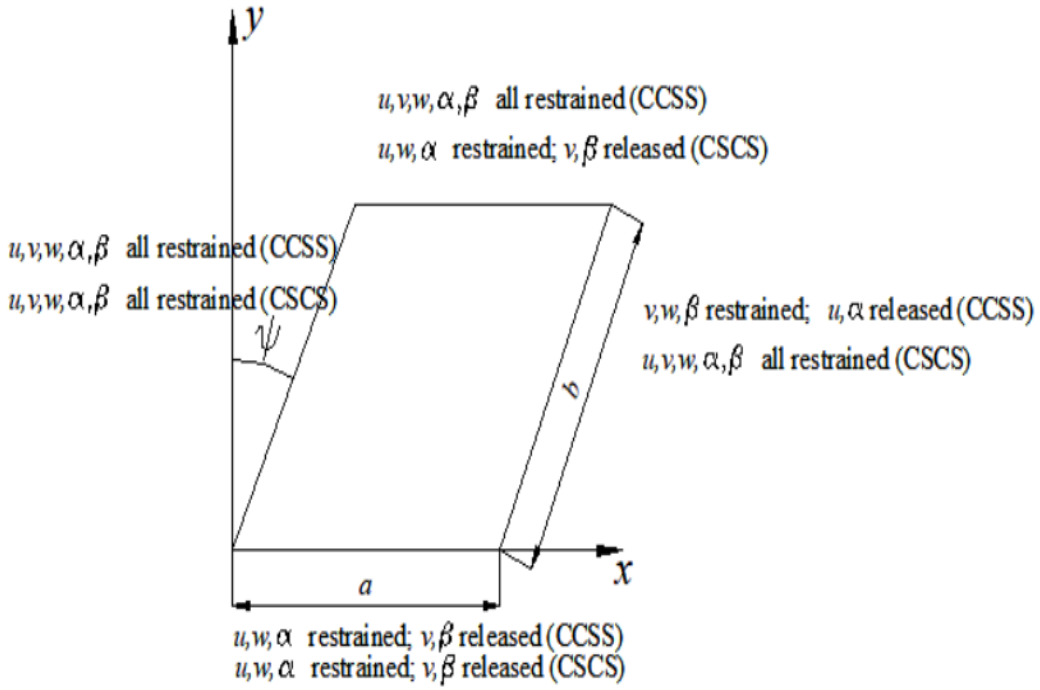

Fig. 8.1 Schematic representation of the boundary conditions

8.2.1. Behaviour of CCSS Skew Plates

The failure characteristics of CCSS skew plates are evident from the contents of Tables 8.1, 8.2, 8.3, 8.4 and 8.9 and Figs. 8.2(a) and 8.3(a).

It is observed from Table 8.1 that all ASCP skew plates have the Hoffman's criterion as the governing one while the first ply failure (FPF) of ASAP plate is governed by the maximum strain criterion whatever may be the skew angle. This leads to infer that for any intermediate value of skew angle, the failure loads of antisymmetric skew plates may be calculated by employing one criterion each for cross and angle ply laminates and considerable computational time may be saved.

Unlike antisymmetric plates, the symmetric ones do not show any particular failure criterion as the governing one and a detailed analysis using all of the well-established failure criteria is recommended to arrive at the conservative value of failure load acceptable from practical engineering standpoint.

It is evident from Table 8.1 and Fig. 8.2(a) that for CCSS boundary condition cross ply laminations show higher $\overline{\text{FPFL}}$ values and must be preferred with respect to angle ply stacking sequences and for both cross and angle ply laminates the antisymmetric stacking orders show better performances. Naturally, ASCP is the best choice for engineers in terms of FPF for all skew angles.

The $\overline{\text{FPFL}}$ value of ASCP plates exhibit a marginal increasing trend with increase of skew angle while for other three laminations (SYCP, ASAP, SYAP), such loads decrease with increase of skew angle either marginally or substantially.

The variation of ultimate ply failure loads ($\overline{\text{UPFL}}$) with increase of skew angle is a bit complicated for symmetric laminates as depicted in Fig. 8.3(a), while for antisymmetric laminates the $\overline{\text{UPFL}}$ value is somewhat non-responsive to any change of skew angle.

Keeping the FPF behaviour in mind, the antisymmetric cross ply shall be an engineer's choice but from ultimate failure point of view symmetric cross ply laminates show better performances than antisymmetric ones for some of the skew angles. Although, the $\overline{\text{FPFL}}$ is most important to an engineer but the ultimate failure load is also important in cases of severe overloading. Keeping this non unified relative behaviour of different laminations in mind, rank matrices presented in Tables 8.2, 8.3, 8.4 and 8.9 are prepared to help an engineer in decision making. While assigning ranks to plate combinations, more than one option may have the same rank if they yield identical values of the first ply or ultimate failure load or percentage area of damage at ultimate failure that form the basis of such ranking. The overall rank matrix presented in Table 8.9 considers the performances of skew plate combinations in terms of first and ultimate ply failures together with extent of damage at ultimate failure as all of these three considerations are to be taken in account in practical engineering decision making process.

Table 8.1 Failure data of CCSS skew plates

Type of lamina	Skew angle, λ	Governing failure criteria	$\overline{\text{FPFL}}$	First failed ply	First ply failure location (x/a, y/b)	$\overline{\text{UPFL}}$	Percentage of damaged area at ultimate failure
ASCP (0°/90°)	0°	Hoffman	2925.43	1	(0.401,0.525)	4515.83	3.125
	5°	Hoffman	2933.61	1	(0.442,0.472)	4544.43	3.125
	10°	Hoffman	2967.31	1	(0.690,0.518)	4701.74	3.125
	15°	Hoffman	3034.73	1	(0.453,0.386)	4723.19	21.875
	20°	Hoffman	3105.21	1	(0.203,0.492)	4925.43	3.125
	25°	Hoffman	3211.44	1	(0.243,0.474)	5199.18	3.125
	30°	Hoffman	3444.33	1	(0.987,0.808)	6174.67	28.125
	0°	Maximum strain	2949.95	1	(0.598,0.026)	6919.31	78.125
	5°	Maximum strain	2980.59	1	(0.653,0.026)	7000.00	64.063
	10°	Maximum strain	3003.06	3	(1.013,0.221)	3003.06	1.56
SYCP (0°/90°/0°)	15°	Puck	2664.96	3	(1.033,0.217)	2819.20	23.4375
	20°	Puck	1732.38	3	(1.053,0.212)	6105.21	67.187
	25°	Puck	1406.54	3	(1.073,0.206)	6288.05	65.625
	30°	Puck	1238.00	3	(1.098,0.206)	6619.00	67.187

Type of lamina	Skew angle, λ	Governing failure criteria	$\overline{\text{FPFL}}$	First failed ply	First ply failure location (x/a, y/b)	$\overline{\text{UPFL}}$	Percentage of damaged area at ultimate failure
	0°	Maximum strain	954.03	1	(0.973,0.473)	2557.71	39.0625
	5°	Maximum strain	824.31	1	(0.083,0.649)	2576.10	51.5625
	10°	Maximum strain	682.33	1	(0.139,0.641)	2292.13	42.188
ASAP (+45°/-45°)	15°	Maximum strain	603.68	1	(0.193,0.628)	2208.38	39.06
	20°	Maximum strain	548.52	1	(0.272,0.682)	2281.92	45.312
	25°	Maximum strain	513.79	1	(0.330,0.659)	2185.90	40.625
	30°	Maximum strain	502.55	1	(0.399,0.656)	2312.56	40.625
SYAP	0°	Hoffman	1278.86	1	(0.401,0.026)	1278.86	1.56
(+45°/-45°/+45°)	5°	Tsai-Wu/ Hashin/ Puck	1210.42	3	(0.776,0.496)	1210.42	1.56
	10°	Maximum strain	1083.76	1	(1.056,0.467)	2591.42	54.687
	15°	Maximum strain	959.14	1	(1.097,0.459)	1456.59	23.437
	20°	Maximum strain	828.40	1	(0.246,0.609)	2191.01	48.437
	25°	Maximum strain	693.56	1	(0.296,0.587)	2173.65	48.437
	30°	Maximum strain	627.17	1	(0.357,0.583)	2449.44	67.187

Note: a/b = 1, a/h = 100

Table 8.2 Rank matrix for CCSS skew plates in terms of $\overline{\text{FPFL}}$

Lamination	Skew angle , λ						
	0°	5°	10°	15°	20°	25°	30°
ASCP	2	2	2	1	1	1	1
SYCP	1	1	1	2	2	2	2
ASAP	4	4	4	4	4	4	4
SYAP	3	3	3	3	3	3	3

Table 8.3 Rank matrix for CCSS skew plates in terms of $\overline{\text{UPFL}}$

Lamination	Skew angle, λ						
	0°	5°	10°	15°	20°	25°	30°
ASCP	2	2	1	1	2	2	2
SYCP	1	1	2	2	1	1	1
ASAP	3	3	4	3	3	3	4
SYAP	4	4	3	4	4	4	3

Table 8.4 Rank matrix for CCSS skew plates in terms of damage extent at ultimate failure

Lamination	Skew angle, λ						
	0°	5°	10°	15°	20°	25°	30°
ASCP	2	2	2	1	1	1	1
SYCP	4	4	1	2	4	4	3
ASAP	3	3	3	3	2	2	2
SYAP	1	1	4	2	3	3	3

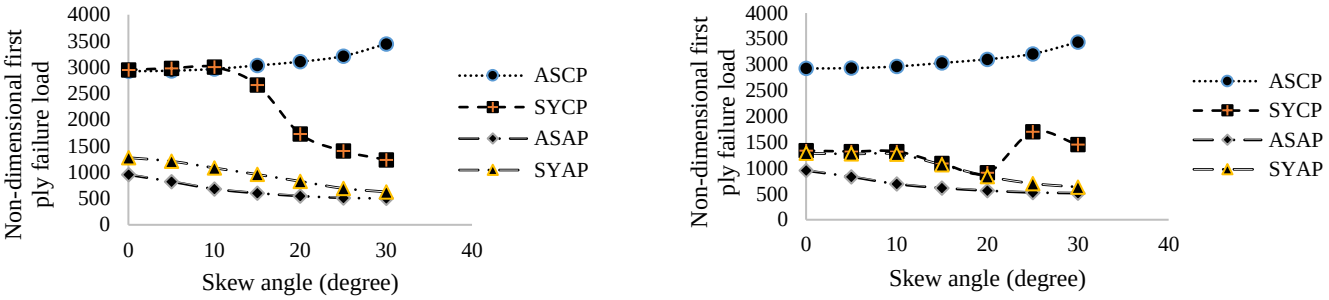

(a) CCSS boundary condition (b) CSCS boundary condition

Fig. 8.2 Variation of first ply failure load with skew angle for CCSS and CSCS boundary conditions

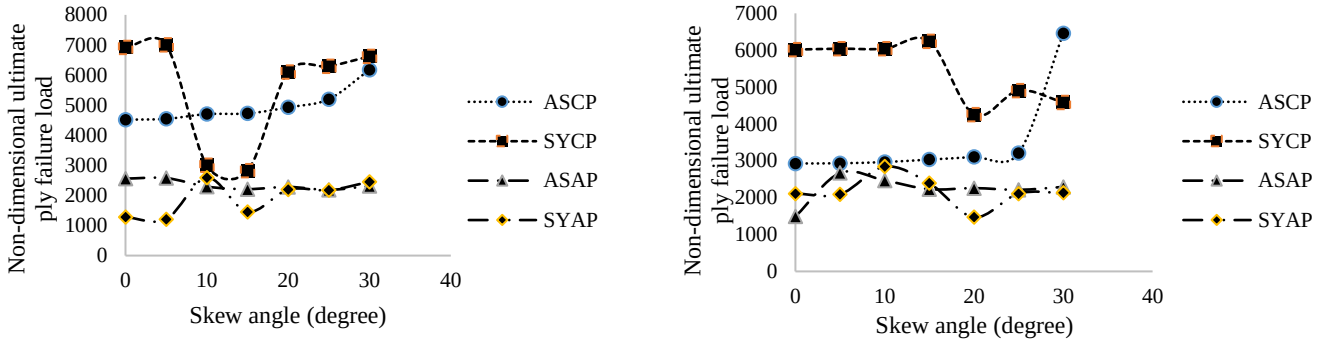

(a) CCSS boundary condition (b) CSCS boundary condition

Fig. 8.3 Variation of ultimate ply failure load with skew angle for CCSS and CSCS boundary conditions

8.2.2. Behaviour of CSCS Skew Plates

The failure behaviour of CSCS skew plates may be understood by examining Tables 8.5, 8.6, 8.7, 8.8 and 8.9 and Figs. 8.2(b) and 8.3(b). Interestingly, like CCSS plates, for CSCS

plates also the antisymmetric combinations show the Hoffman's and maximum strain criteria as the governing ones for cross ply and angle ply stacking sequences respectively for all skew angles considered here. So, a general inference may be drawn that in order to assess the failure loads of antisymmetric skew plates case specific failure criteria may be used to cut short the computational effort. But for symmetrically laminated skew plates, such unified trend is not observed and detailed study using all failure criteria is required.

It is evident from Fig. 8.3(b) that the antisymmetric cross ply skew plate option is convincingly better than the other three laminations considered in the present study in terms of FPF behaviour which is of prime importance to a design engineer. Moreover, with increase of skewness, the FPF resisting capacity of ASCP plates shows an improving tendency. The $\overline{\text{FPFL}}$ of angle ply laminates decreases for higher values of skew angles and the effect of change of skew angle on the $\overline{\text{FPFL}}$ of symmetric cross ply plates is rather complicated. Keeping the above facts in mind, for CSCS boundary condition the ASCP plate options may be recommended to be used preferentially.

Another interesting observation for CSCS skew plates, like CCSS ones, is that the highest ultimate ply failure load is achieved for symmetric cross ply skew plate combinations. The fact that among any two given laminations the one which is better in terms of FPF may not be so in terms of $\overline{\text{UPFL}}$ values, necessitates detailed failure analysis to understand the relative behaviour of different combinations at ultimate failure without making any conjecture from the results of $\overline{\text{FPFL}}$ values.

Table 8.5 Failure data of CSCS skew plates

Type of lamina	Skew angle, λ	Governing failure criteria	$\overline{\text{FPFL}}$	First failed ply	FPF location (x/a, y/b)	$\overline{\text{UPFL}}$	Percentage of damaged area at ultimate failure
ASCP (0°/90°)	0°	Hoffman	2928.50	1	(0.598,0.526)	2928.50	1.56
	5°	Hoffman	2933.61	1	(0.644,0.524)	2933.61	1.56
	10°	Hoffman	2966.29	1	(0.483,0.467)	2966.29	1.56
	15°	Hoffman	3034.73	1	(0.161,0.507)	3034.73	1.56

Type of lamina	Skew angle, λ	Governing failure criteria	$\overline{\text{FPFL}}$	First failed ply	FPF location (x/a, y/b)	$\overline{\text{UPFL}}$	Percentage of damaged area at ultimate failure
	20°	Hoffman	3105.21	1	(1.138,0.447)	3105.21	1.56
	25°	Hoffman	3209.40	1	(0.835,0.134)	3209.40	1.56
	30°	Hoffman	3438.20	1	(0.357,0.583)	6455.57	29.687
	0°	Maximum stress	1338.10	1	(0.276,0.974)	6017.36	43.75
	5°	Maximum stress	1321.76	1	(0.683,0.970)	6040.86	42.1875
	10°	Maximum stress	1321.76	1	(0.479,0.025)	6040.86	37.5
SYCP (0°/90°/0°)	15°	Maximum stress	1089.89	1	(0.606,0.024)	6238.00	50
	20°	Maximum stress	908.07	1	(0.809,0.917)	4252.30	20.312
	25°	Puck	1700.72	3	(1.073,0.206)	4905.01	32.813
	30°	Puck	1453.52	3	(1.098,0.206)	4585.29	25
	0°	Maximum strain	950.97	1	(0.526,0.026)	1490.30	25
	5°	Maximum strain	831.46	1	(1.004,0.347)	2670.07	59.375
	10°	Maximum strain	691.52	1	(0.139,0.641)	2466.80	54.688
ASAP (+45°/-45°)	15°	Maximum strain	613.89	1	(1.065,0.338)	2229.83	53.13
	20°	Maximum strain	562.82	1	(0.437,0.447)	2259.45	54.687
	25°	Maximum strain	527.07	1	(1.092,0.247)	2213.48	43.75
	30°	Maximum strain	514.81	1	(0.399,0.656)	2292.13	43.75
SYAP	0°	Hoffman	1286.01	1	(0.401,0.026)	2112.36	21.875
(+45°/-	5°	Hoffman	1272.73	1	(0.403,0.026)	2092.95	20.312
45°/+45°)	10°	Hoffman	1271.71	1	(0.117,0.518)	2843	79.687
	15°	Maximum strain	1062.31	1	(1.065,0.338)	2392.24	65.625
	20°	Maximum strain	838.61	1	(0.246,0.609)	1470.89	34.375
	25°	Maximum strain	700.72	1	(0.296,0.587)	2110.32	46.875
	30°	Maximum strain	633.30	1	(1.163,0.318)	2134.83	50

Note: $a/b = 1$, $a/h = 100$

Table 8.6 Rank matrix for CSCS skew plates in terms of $\overline{\text{FPFL}}$

Lamination	Skew angle, λ						
	0°	5°	10°	15°	20°	25°	30°
ASCP	1	1	1	1	1	1	1
SYCP	2	2	2	2	2	2	2
ASAP	4	4	4	4	4	4	4
SYAP	3	3	3	3	3	3	3

Table 8.7 Rank matrix for CSCS skew plates in terms of $\overline{\text{UPFL}}$

Lamination	Skew angle, λ						
	0°	5°	10°	15°	20°	25°	30°
ASCP	2	2	2	2	2	2	1
SYCP	1	1	1	1	1	1	2
ASAP	4	3	4	4	3	3	3
SYAP	3	4	3	3	4	4	4

Table 8.8 Rank matrix for CSCS skew plates in terms of damage extent at ultimate failure

Lamination	Skew angle, λ						
	0°	5°	10°	15°	20°	25°	30°
ASCP	1	1	1	1	1	1	2
SYCP	4	3	2	2	2	2	1
ASAP	3	4	3	3	4	3	3
SYAP	2	2	4	4	3	4	4

8.2.3. Overall Performances of Different Skew Plate Options

The relative performances of different skew plate options are discussed in the preceding sections. Such performances depend on the criterion that is chosen as the basis of such comparison. So, in order to reach the final decision regarding the selection of a particular option in a given practical situation, due regards should be given on the performance of particular choice in terms of first ply and ultimate failure load values together with the area of damage at ultimate failure. To facilitate such selection, Table 8.9 is prepared where sum of the ranks of different skew plates are calculated which are again sorted to arrive at the overall ranks of the different options.

It is clearly evident from Table 8.9 that cross ply skew plates consistently show better performances than the angle ply ones and it is very interesting to note that all of the cross ply combinations taken up in the present study are better choices than all of the angle ply ones.

Furthermore, it is observed that the top ranking options (up to rank 10) have the laminae anti-symmetrically stacked and this leads to directly infer that ASCP plates shall be preferred by practicing engineers for skew plates even having high values of skew angles. This is true for both the boundary conditions considered in the present study.

When a particular value of skew angle is to be adopted in a given practical situation, the choice of lamination shall be done very carefully as evident from the results furnished in Table 8.9. The plate combinations with lowest and highest ranks in terms of FPF load both correspond to the same skew angle (30°) and boundary condition (CCSS) but with different stacking orders. Similarly, in terms of ultimate ply failure load too, the best and worst options are both 5°/CCSS plates but with laminations SYCP and SYAP respectively.

Table 8.9 Overall rank matrix of skew plate combinations

Skew plate option (lamination/skew angle in degree/boundary condition) (Column 1)	Ranks in terms of $\overline{\text{FPFL}}$ (Column 2)	Ranks in terms of $\overline{\text{UPFL}}$ (Column 3)	Ranks in terms of % damaged area at ultimate failure (Column 4)	Sum of ranks furnished in columns (2) , (3) and (4) (Column 5)	Ranks in terms of values given in Column 5 (Column 6)
ASCP/30/CSCS	2	4	8	14	1
ASCP/30/CCSS	1	7	7	15	2
ASCP/25/CCSS	3	11	2	16	3
ASCP/20/CCSS	5	12	2	19	4
ASCP/15/CCSS	6	14	4	24	5
ASCP/25/CSCS	4	20	1	25	6
ASCP/10/CCSS	9	15	2	26	7
ASCP/20/CSCS	5	21	1	27	8
ASCP/15/CSCS	6	22	1	29	9
ASCP/5/CCSS	12	17	2	31	10
SYCP/10/CCSS	7	23	1	31	10
SYCP/5/CCSS	8	1	24	33	11
ASCP/0/CCSS	14	18	2	34	12
ASCP/10/CSCS	10	24	1	35	13
ASCP/5/CSCS	12	25	1	38	14
SYCP/25/CSCS	17	13	9	39	15
SYCP/0/CCSS	11	2	27	40	16
ASCP/0/CSCS	13	26	1	40	16
SYCP/30/CSCS	18	16	6	40	16
SYCP/10/CSCS	21	9	11	41	17
SYCP/5/CSCS	21	9	14	44	18
SYCP/0/CSCS	20	10	15	45	19
SYCP/15/CCSS	15	28	5	48	20

Skew plate option (lamination/skew angle in degree/boundary condition) (Column 1)	Ranks in terms of $\overline{FPFL}$ (Column 2)	Ranks in terms of $\overline{UPFL}$ (Column 3)	Ranks in terms of % damaged area at ultimate failure (Column 4)	Sum of ranks furnished in columns (2) , (3) and (4) (Column 5)	Ranks in terms of values given in Column 5 (Column 6)
SYCP/25/CCSS	19	5	25	49	21
SYCP/20/CCSS	16	8	26	50	22
SYCP/15/CSCS	28	6	19	53	23
SYCP/30/CCSS	26	3	26	55	24
SYCP/20/CSCS	34	19	3	56	25
SYAP/0/CSCS	22	47	4	73	26
ASAP/0/CCSS	32	32	12	76	27
SYAP/5/CSCS	24	49	3	76	27
SYAP/0/CCSS	23	53	1	77	28
SYAP/10/CSCS	25	27	28	80	29
SYAP/10/CCSS	29	30	22	81	30
SYAP/5/CCSS	27	54	1	82	31
SYAP/15/CCSS	31	52	5	88	32
ASAP/5/CSCS	36	29	23	88	32
ASAP/5/CCSS	38	31	20	89	33
ASAP/0/CSCS	33	50	6	89	33
SYAP/15/CSCS	30	35	25	90	34
ASAP/10/CCSS	42	37	14	93	35
ASAP/10/CSCS	41	33	22	96	36
SYAP/20/CSCS	35	51	10	96	36
SYAP/20/CCSS	37	43	18	98	37
ASAP/15/CCSS	46	42	12	100	38
ASAP/30/CCSS	52	36	13	101	39
ASAP/20/CCSS	48	38	16	102	40
ASAP/30/CSCS	50	37	15	102	40
SYAP/25/CCSS	40	45	18	103	41
SYAP/30/CCSS	44	34	26	104	42
SYAP/25/CSCS	39	48	17	104	42
ASAP/25/CSCS	49	41	15	105	43
ASAP/15/CSCS	45	40	21	106	44
ASAP/25/CCSS	51	44	13	108	45
ASAP/20/CSCS	47	39	22	108	45

8.3. CONCLUDING REMARKS

Following points may be concluded from the present numerical study.

- It is concluded that for skew angle up to 30°, the FPF loads of antisymmetric skew plates may be calculated by employing one criterion each for cross and angle ply laminates which

are those of Hoffman and the maximum strain criterion respectively and considerable computational time may be saved.

- On the other hand, for the symmetric laminates no such unified trend is noticed and a detailed analysis using all well-established failure criteria is required to arrive at the acceptable values of FPF loads.
- It may be inferred from the present study that the antisymmetric cross ply laminate is the best choice for engineers in terms of FPF for skew angles up to 30°.
- It is established that stacking sequence plays an extremely vital role in final selection of a skew plate combination with given skew angle and boundary condition and a combination with a wrong choice of lamination may show drastically reduced value of first ply and ultimate ply failure loads.
- Moreover, it is concluded that among any two given laminations the one which is better in terms of FPF may not be so in terms of ultimate failure load.

Chapter 9

NONLINEAR FIRST PLY FAILURE OF COMPOSITE THIN SKEWED HYPAR SHELL ROOFS

9.1 GENERAL

Application of thin-walled shell structures in civil, naval, aeronautical and boiler engineering has evolved as efficient shapes enabling the bending and membrane stiffnesses to combine to resist the loads. Aesthetically appealing shell roofs, like the skewed hypar ones, are widely used in civil engineering construction of roofs in hangers, sports auditoriums, exhibition halls, railway stations and in other places demanding large column-free areas. To meet this practical requirement, the edges of shell units have to be kept free at places. The application of skewed hypar shell as civil engineering roofing unit is an established fact. Such use has gained a greater momentum when this shell is fabricated with advanced materials like the laminated composites. The use of laminated composite materials for the construction of shell roofs has gained popularity due to a number of well-established reasons. Laminated composite materials though having several advantages are weak in transverse shear and show failure under static transverse loading which may remain undetected at an initial stage and can cause catastrophic collapse at a later stage. The application of aesthetically expressive laminated composite skewed hypar shell roof as a canopy for car parking, warehouse shed, grandstands, etc. (Bandyopadhyay, (2000)) inspired the author to study the failure aspects of this shell configuration in details.

In the present work, the author attempts to address the effect of free edges on first ply failure (FPF) strength of laminated composite thin skewed hypar shell roofs considering

geometric nonlinearity. For accurate modelling of the failure behaviour of this thin shell, nonlinear strains are considered together with eight noded isoparametric serendipity finite element. Different well-established failure criteria including the failure criterion of Puck are used to extract the FPF pressure values, failure locations and failure modes as well. The finite element code developed is used for numerical experimentation with parametric variations and the results are post processed and interpreted to extract meaningful engineering conclusions. Further this investigation is aimed towards proposing design guidelines regarding failure characteristics of skewed hypar laminated composite shells with partially free boundaries considering both the aspects of collapse and serviceability using well-established failure criteria.

9.2 NUMERICAL STUDY AND DISCUSSIONS

A number of benchmark problems as elaborated here are taken from the published literature and solved to examine the efficiency of the present finite element code.

- Geometrically nonlinear static central displacements of the isotropic clamped cylindrical shell under uniformly distributed surface pressures, as reported by Palazotto and Dennis (1992) earlier, are solved and same as presented in Fig. 9.1.
- Non-dimensional fundamental frequencies of laminated composite twisted plates, reported earlier by Qatu and Leissa (1991 b), are solved and presented in Table 9.2.

In order to validate the correct incorporation of geometrically nonlinear static bending formulation in the present code, the author solves the first benchmark problem. Fig.9.1 shows the central displacement values obtained from the present code and those reported earlier by Palazotto and Dennis (1992) for an isotropic clamped cylindrical shell surface.

In order to ensure the correct incorporation of the skewed hypar shell geometry in the present computer code, the second benchmark problem is solved and the results are furnished in Table 9.1. The author uses a simple lumped mass matrix scheme here along with the

undamaged stiffness matrix to solve the non-dimensional fundamental frequency values of composite twisted plates. These frequency values obtained from the present computer code are compared with the frequency values reported by Qatu and Leissa (1991 b) in Table 9.1.

Apart from the benchmark problems, several additional examples of graphite-epoxy skewed hypar shells combining different laminations and boundary conditions combining clamped (with all degrees of freedom restrained and being represented by the letter C) and free (with all degrees of freedom free and being represented by the letter F) edges are solved employing the linear and nonlinear approaches to arrive at the uniform pressures corresponding to FPF. The material properties of Q–1115 graphite-epoxy composite are used here as reported in Table 5.3. The plies are numbered from top to bottom of the laminate. For each boundary condition, two and three-layered anti-symmetric (AS) and symmetric (SY), cross (CP) and angle ply (AP) laminations are considered for developing ASCP (0°/90°), SYCP (0°/90°/0°), ASAP (45°/-45°) and SYAP (45°/-45°/45°) laminates. The FPF pressure values (FL) which are non-dimensionalized as $(\overline{FPFL} = (FL/E_T)(a/h)^4)$ and the other related failure information are furnished in Table 9.2 and Table 9.3 for each shell options using different well-established failure criteria like maximum stress, maximum strain and those proposed by Hoffman, Tsai-Hill, Tsai-Wu, Hashin and Puck.

The minimum failure pressure values obtained from the above-mentioned criteria are considered as the first ply collapse failure pressure (marked by italics in Tables 9.2 and 9.3) on which engineering factor of safety may be imposed. The failure pressures corresponding to the permissible deflection of skewed hypar shell (considered as 0.004 times of shorter plan dimension) are taken here as the FPF pressures from serviceability point of view. These working failure pressures are also reported in Tables 9.2 and 9.3. For brevity, the shell combinations are represented by short designations. For example, an anti-symmetric angle ply shell clamped along $x = 0$ and $x = a$ and having free edges along $y = 0$ and $y = b$ is

designated by the symbol CFCF/ASAP. Again CFFC/SYCP represents the symmetric cross ply shell option which is clamped along $x = 0$ and $y = 0$ and have free edges along $x = a$ and $y = b$ respectively.

The author critically discusses the results of the present numerical experiments in this section for both benchmark problems and other additional examples taken up here. As the geometrically nonlinear analysis gives more accurate results than the results obtained from the geometrically linear analysis, the discussions presented in Subsections 9.4 to 9.7 are based on results obtained from nonlinear FPF analysis. But only to suggest practical design approaches to the engineers, the last Subsection 9.8 is discussed considering both linear and nonlinear analysis of FPF of composite skewed hypar shells, keeping in mind the fact that the linear approach is easier to implement.

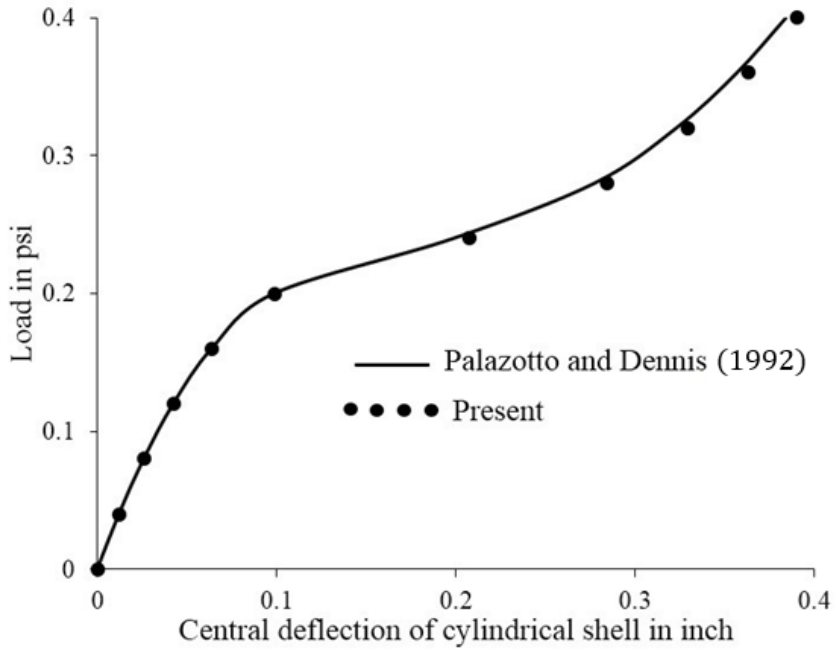

Note: a = 508 mm, h = 3.175 mm, rise to width ratio = 0.0496, radius of curvature = 2540 mm
Note: semi-sector angle = 0.1 radian, $E_T = 3.1$ GPa , ν = 0.3

Fig. 9.1 Nonlinear deflection of isotropic cylindrical shell

Table 9.1 Non-dimensional natural frequencies for $(\varphi/-\varphi/\varphi)$ graphite-epoxy twisted plates

Angle of twist	φ (degree)	0	15	30	45	60	75	90
$\theta = 0°$	Qatu and Leissa (1991 b)	1.0035	0.9296	0.7465	0.5286	0.3545	0.2723	0.2555
	Present formulation	0.9985	0.9250	0.7444	0.5280	0.3542	0.2720	0.2552
$\theta = 30°$	Qatu and Leissa (1991 b)	0.9566	0.8914	0.7205	0.5149	0.3443	0.2606	0.2436
	Present formulation	0.9501	0.8841	0.7180	0.5143	0.3446	0.2611	0.2446

Note: E_L= 138 GPa, E_T=8.96 GPa, G_{LT}= 7.1GPa, ν_{LT}= 0.3, *a/b* = 1, *a/h* = 100

9.2.1 Benchmark Problems

The non-dimensional static geometrically nonlinear central displacement values of isotropic cylindrical shells obtained from the present formulation are compared with the displacement values published by Palazotto and Dennis (1992) in Fig. 9.1. The close agreement of these results establishes the correct incorporation of geometrically nonlinear bending formulation in the present finite element code.

For checking proper incorporation of skewed hypar shell geometry in the present formulation, which is structurally similar to a twisted plate, the present author reports the non-dimensional fundamental frequency values of composite twisted plates in Table 9.1 and these frequency values are compared with the frequency values reported by Qatu and Leissa (1991 b) in the same table. The close agreement of these results proves the proper incorporation of the hypar shell geometry in the present formulation.

9.2.2 Nonlinear First Ply Failure Behaviour of Cross and Angle Ply Skewed Hypar Shells for Different Boundary Conditions

The uniformly distributed non-dimensional FPF pressure values of skewed hypar shells with various boundary conditions are reported in Tables 9.2 and 9.3 considering both geometrically linear and nonlinear strains. The failure modes and failed plies along with the corresponding failure criteria are also mentioned in these tables. The least failure pressure value

obtained through different collapse failure criteria for each case is considered as the collapse failure pressure for that shell option and the failure criterion which governs the minimum FPF pressure is identified. The Puck and maximum strain failure criteria yield the minimum values of the FPF pressures for most of the shell combinations of CFCF and CFFC boundary conditions. For two exceptional cases, (i.e. CFCF/ASAP and CFFC/ASCP), the maximum strain and Tsai-Wu failure criteria give the lowest values of failure pressures respectively but these values are very close (within 5.1% and 2.2% respectively) to the values obtained through the Puck and maximum strain failure criteria respectively. So, the author suggests the Puck and maximum strain failure criteria as the governing failure criteria of all the cases of CFCF and CFFC edge conditions respectively.

It is interestingly noticed from the results furnished in Tables 9.2 and 9.3 that the cross ply shells perform better than the angle ply shell options in terms of FPF pressures for CFCF and CFFC edge conditions. The failure pressure values of cross ply shells may be up to 1.3 and 3.3 times the pressure values obtained from angle ply shells for these two edge conditions respectively. The close look at the results reported in these tables also reflects the fact that the anti-symmetric cross ply skewed hypar shells give the maximum FPF pressure values among all the cases taken up here for each boundary condition.

Apart from the failure pressure values, the failed plies and the failure modes/tendencies are also indicated in Tables 9.2 and 9.3 for different stacking sequences and boundary conditions. This information may help the practicing engineers in fabricating new laminates by appropriately tailoring the failed plies and also to determine location and direction of stiffeners to arrest such failure.

Table 9.2 Non-dimensional first ply failure pressures ($\overline{FPFL}$) for CFCF hypar shells

Lamination	Failure theory	$\overline{FPFL}$	Failure zone	Failed ply	Failure mode/ failure tendency
ASCP	Maximum stress	3782.43^{L}	A	2	Matrix cracking
		3773.24^{NL}	A	2	Matrix cracking
	Maximum strain	3712.97^{L}	A	2	Matrix cracking
		3656.79^{NL}	A	2	Matrix cracking
	Hoffman	3411.64^{L}	A	2	Matrix cracking
		3368.74^{NL}	A	1	Fiber breakage
	Tsai-Hill	3544.43^{L}	A	2	Matrix cracking
		3518.90^{NL}	A	2	Matrix cracking
	Tsai-Wu	3414.71^{L}	A	2	Matrix cracking
		3384.07^{NL}	A	2	Matrix cracking
	Hashin	3540.35^{L}	A	2	Matrix cracking
		3516.85^{NL}	A	2	Matrix cracking
	Puck	*1813.07*^{L}	*A*	*2*	*Matrix crushing mode C*
		1676.20^{NL}	*A*	*2*	*Matrix crushing mode C*
	Serviceability	931.56^{L}	A		
		933.61^{NL}	A		
SYCP	Maximum stress	2855.98^{L}	A	2	Matrix cracking
		2861.08^{NL}	A	2	Matrix cracking
	Maximum strain	2802.86^{L}	A	2	Matrix cracking
		2804.90^{NL}	A	2	Matrix cracking
	Hoffman	2705.82^{L}	A	2	Matrix cracking
		2700.72^{NL}	A	2	Matrix cracking
	Tsai-Hill	2766.09^{L}	A	2	Matrix cracking
		2767.11^{NL}	A	2	Matrix cracking
	Tsai-Wu	2707.87^{L}	A	2	Matrix cracking
		2702.76^{NL}	A	2	Matrix cracking
	Hashin	2760.98^{L}	A	2	Matrix cracking
		2764.04^{NL}	A	2	Matrix cracking
	Puck	*1493.36*^{L}	*A*	*2*	*Matrix crushing mode C*
		1407.56^{NL}	*A*	*2*	*Matrix crushing mode C*
	Serviceability	1019.41^{L}	A		
		1032.69^{NL}	A		
ASAP	Maximum stress	1331.97^{L}	A	1	Matrix cracking
		1340.14^{NL}	A	1	Matrix cracking
	Maximum strain	*1255.36*^{L}	*A*	*1*	*Matrix cracking*
		1261.49^{NL}	*A*	*1*	*Matrix cracking*
	Hoffman	1317.67^{L}	A	1	Matrix cracking
		1324.82^{NL}	A	1	Matrix cracking
	Tsai-Hill	1345.25^{L}	A	1	Matrix cracking

Lamination	Failure theory	$\overline{\text{FPFL}}$	Failure zone	Failed ply	Failure mode/ failure tendency
		1352.40 ^{NL}	A	1	Matrix cracking
	Tsai-Wu	1301.33 ^{L}	A	1	Matrix cracking
		1307.46 ^{NL}	A	1	Matrix cracking
	Hashin	1321.76 ^{L}	A	1	Matrix cracking
		1328.91 ^{NL}	A	1	Matrix cracking
	Puck	1319.71 ^{L}	A	1	Matrix cracking mode A
		1326.86 ^{NL}	A	1	Matrix cracking mode A
	Serviceability	623.08 ^{L}	A		
		625.13 ^{NL}	A		
SYAP	Maximum stress	1591.42 ^{L}	A	1	Matrix cracking
		1589.38 ^{NL}	A	1	Matrix cracking
	Maximum strain	1494.38 ^{L}	A	1	Matrix cracking
		1502.55 ^{NL}	A	1	Matrix cracking
	Hoffman	1575.08 ^{L}	A	1	Matrix cracking
		1572.01 ^{NL}	A	1	Matrix cracking
	Tsai-Hill	1609.81 ^{L}	A	1	Matrix cracking
		1601.63 ^{NL}	A	1	Matrix cracking
	Tsai-Wu	1553.63 ^{L}	A	1	Matrix cracking
		1553.63 ^{NL}	A	1	Matrix cracking
	Hashin	1579.16 ^{L}	A	1	Matrix cracking
		1577.12 ^{NL}	A	1	Matrix cracking
	Puck	*1324.82* ^{L}	*A*	*2*	*Matrix crushing mode C*
		1330.95 ^{NL}	*A*	*2*	*Matrix crushing mode C*
	Serviceability	767.11 ^{L}	A		
		764.04 ^{NL}	A		

Note: "*L*" and "*NL*" indicate the linear and nonlinear failure pressures respectively
Note: $a/b = 1$, $a/h = 100$, $c/a = 0.2$

Table 9.3 Non-dimensional first ply failure pressures ($\overline{\text{FPFL}}$) for CFFC hypar shells

Lamination	Failure theory	$\overline{\text{FPFL}}$	Failure zone	Failed ply	Failure mode / failure tendency
ASCP	Maximum stress	2058.22 ^{L}	A	1	Matrix cracking
		2088.87 ^{NL}	A	1	Matrix cracking
	Maximum strain	2023.49 ^{L}	A	2	Matrix cracking
		2078.65 ^{NL}	A	1	Matrix cracking
	Hoffman	1922.37 ^{L}	A	2	Matrix cracking
		2042.90 ^{NL}	A	2	Matrix cracking
	Tsai-Hill	2008.17 ^{L}	A	2	Matrix cracking
		2088.87 ^{NL}	A	2	Matrix cracking
	Tsai-Wu	*1910.11* ^{L}	*A*	*2*	*Matrix cracking*
		2033.71 ^{NL}	*A*	*2*	*Matrix cracking*

Lamination	Failure theory	$\overline{\text{FPFL}}$	Failure zone	Failed ply	Failure mode / failure tendency
	Hashin	1987.74 ^{L}	A	2	Matrix cracking
		2085.80 ^{NL}	A	2	Matrix cracking
	Puck	1968.34 ^{L}	A	2	Matrix cracking mode A
		2072.52 ^{NL}	A	2	Matrix cracking mode A
	Serviceability	254.34 ^{L}	A		
		250.26 ^{NL}	A		
SYCP	Maximum stress	1782.43 ^{L}	A	1	Matrix cracking
		1788.56 ^{NL}	A	1	Matrix cracking
	Maximum strain	*1753.83* ^{L}	*A*	*1*	*Matrix cracking*
		1759.96 ^{NL}	*A*	*1*	*Matrix cracking*
	Hoffman	1780.39 ^{L}	A	1	Matrix cracking
		1786.52 ^{NL}	A	1	Matrix cracking
	Tsai-Hill	1786.52 ^{L}	A	1	Matrix cracking
		1791.62 ^{NL}	A	1	Matrix cracking
	Tsai-Wu	1784.47 ^{L}	A	1	Matrix cracking
		1789.58 ^{NL}	A	1	Matrix cracking
	Hashin	1782.43 ^{L}	A	1	Matrix cracking
		1787.54 ^{NL}	A	1	Matrix cracking
	Puck	1782.43 ^{L}	A	1	Matrix cracking mode A
		1787.54 ^{NL}	A	1	Matrix cracking mode A
	Serviceability	280.90 ^{L}	A		
		276.81 ^{NL}	A		
ASAP	Maximum stress	674.16 ^{L}	A	1	Matrix cracking
		679.26 ^{NL}	A	1	Matrix cracking
	Maximum strain	*609.81* ^{L}	*A*	*1*	*Matrix cracking*
		613.89 ^{NL}	*A*	*1*	*Matrix cracking*
	Hoffman	668.03 ^{L}	A	1	Matrix cracking
		673.14 ^{NL}	A	1	Matrix cracking
	Tsai-Hill	694.59 ^{L}	A	1	Matrix cracking
		699.69 ^{NL}	A	1	Matrix cracking
	Tsai-Wu	650.66 ^{L}	A	1	Matrix cracking
		655.77 ^{NL}	A	1	Matrix cracking
	Hashin	670.07 ^{L}	A	1	Matrix cracking
		675.18 ^{NL}	A	1	Matrix cracking
	Puck	669.05 ^{L}	A	1	Matrix cracking mode A
		675.18 ^{NL}	A	1	Matrix cracking mode A
	Serviceability	113.38 ^{L}	A		
		112.36 ^{NL}	A		
SYAP	Maximum stress	825.33 ^{L}	A	1	Matrix cracking
		839.63 ^{NL}	A	1	Matrix cracking

Lamination	Failure theory	$\overline{\text{FPFL}}$	Failure zone	Failed ply	Failure mode / failure tendency
	Maximum strain	*740.55* ^{L}	*A*	*1*	*Matrix cracking*
		755.87 ^{NL}	*A*	*1*	*Matrix cracking*
	Hoffman	818.18 ^{L}	A	1	Matrix cracking
		832.48 ^{NL}	A	1	Matrix cracking
	Tsai-Hill	853.93 ^{L}	A	1	Matrix cracking
		866.19 ^{NL}	A	1	Matrix cracking
	Tsai-Wu	794.69 ^{L}	A	1	Matrix cracking
		808.99 ^{NL}	A	1	Matrix cracking
	Hashin	821.25 ^{L}	A	1	Matrix cracking
		834.53 ^{NL}	A	1	Matrix cracking
	Puck	820.22 ^{L}	A	1	Matrix cracking mode A
		833.50 ^{NL}	A	1	Matrix cracking mode A
	Serviceability	173.65 ^{L}	A		
		171.60 ^{NL}	A		

Note: "*L*" and "*NL*" indicate the linear and nonlinear failure pressures respectively
Note: $a/b = 1$, $a/h = 100$, $c/a = 0.2$

9.2.3 Behaviour of Skewed Hypar Shells for Different Boundary Conditions From Serviceability Point of View

Considering the permissible deflection limit of laminated composite skewed hypar shell as 0.004 times the shorter plan dimension, the author studies the FPF behaviour of skewed hypar shells from serviceability standpoint. The failure pressure values corresponding to permissible deflections are considered as the FPF pressures from a serviceability standpoint and the results are reported in Tables 9.2 and 9.3. It is noticed from these FPF pressure values from a serviceability point of view that the symmetric and anti-symmetric cross ply shells show higher values of failure pressure compared to those of angle ply shell options for both CFCF and CFFC edge conditions.

It is evident from the results furnished in Tables 9.2 and 9.3 that the FPF pressures considering serviceability conditions for all the shell options taken up here are lower than the failure pressures obtained from collapse criteria. This signifies the fact that all these hypar shells behave like ductile units as they do not undergo FPF up to serviceability limits. In Table

9.4, the ratios of collapse FPF pressure values to the failure pressure values from serviceability standpoint are furnished for each boundary condition. It is interestingly noted that for all the laminations, the ratios that come out for CFFC boundary condition are more than those obtained for CFCF boundary condition. So, CFFC shells shall be preferred to be used in high seismic zones as these units continue to withstand substantial over loading before failure even after the serviceability limits are exceeded. In other words, the engineers get a warning that a shell is approaching failure, when serviceability limits are exceeded, much ahead of actual failure.

Table 9.4 Ratio of collapse failure pressure to pressure corresponding to serviceability limit

Lamination	The ratio of collapse FPF pressure to a pressure corresponding to the permissible deflection	
	Boundary conditions	
	CFCF	CFFC
ASCP	1.834	8.301
SYCP	1.392	6.494
ASAP	2.061	5.581
SYAP	1.779	4.499

9.2.4 Effect of Boundary Conditions on First Ply Failure Characteristics of Composite Skewed Hypar Shells

The results that are reported here (Fig. 9.2) clearly establishes that cross ply shells exhibit better performances than angle ply ones in terms of FPF pressure. Naturally, in cases where a designer has a choice cross ply should always be selected.

It is interesting to observe that cross ply shells again, the CCFF boundary condition, where all of the fibres have at least one end clamped, performs better than the CFCF edge condition. Exactly in this line it is found that angle ply shells the CFCF boundary condition performs better than the CCFF one because for angle ply laminates, the one end of each fibre is always clamped for CFCF edges. Combining the two observations it may specifically be

concluded that for designing shells with free edges an engineer shall always try to ensure that at least one end of each fibre is clamped.

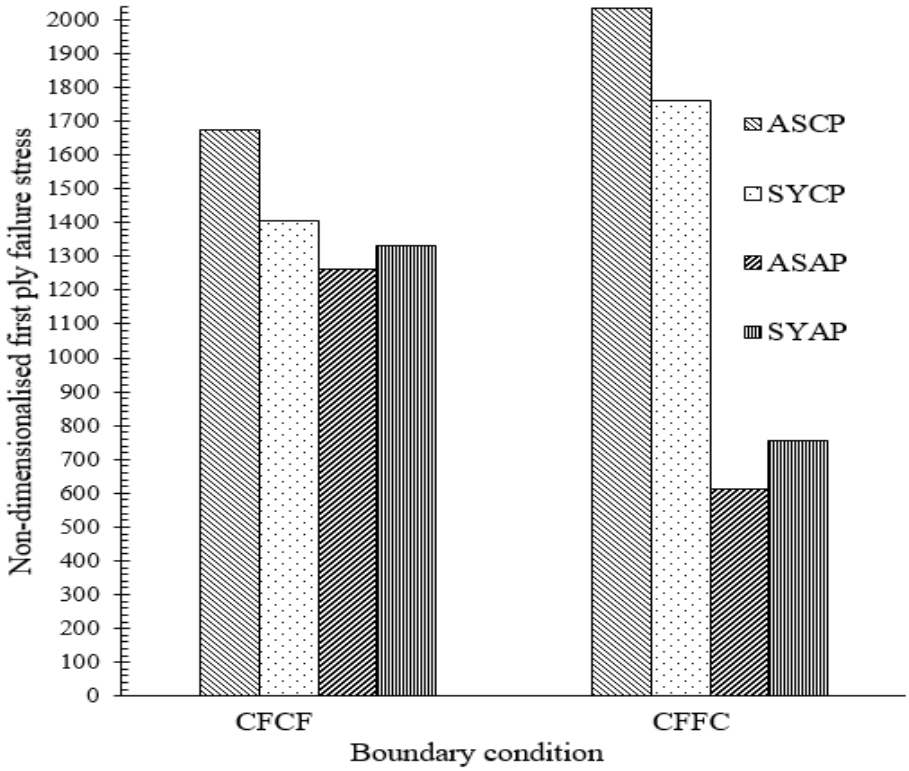

Fig. 9.2 Non-dimensionalised first ply failure collapse pressures for all boundary conditions

9.2.5 Guideline to Non-Destructive Test Monitoring Based on Failure Zones of Hypar Shells

For hidden flaw detection of a skewed hypar shell, it is necessary for practicing engineers to identify the zones of the shell surface prone to failure. The point where FPF possibly initiates is extremely important to be known for setting up any non-destructive instrumentation to monitor the structural health of the hypar shell. To fulfill this purpose, the author divides the hypar shell surface into four different zones in a plan such as zone – A, zone – B, zone – C and zone – D as shown in Fig. 7.6. The widths of each zones are equal to one-eighth of the corresponding plan dimensions. For all the cases taken up here, FPF always starts from a peripheral zone nearest to the edges i.e. zone – A for both collapse and serviceability failure points of view (refer Tables 9.2 to 9.3). It indicates that any non-destructive health

monitoring of a laminated composite skewed hypar shell should be started from this vulnerable zone only. These guidelines may be very helpful to the engineers for continuous health assessment of skewed hypar shells.

9.2.6 *Comparative Study Between Linear and Nonlinear Analysis for Adopting Design Approaches*

It is undoubtedly true that the geometrically nonlinear analysis gives more accurate results than the results that come out from the geometrically linear analysis. But linear analysis is easier than nonlinear analysis from the computer implementation point of view. So, a structural engineer should know the acceptable approach of analysis for the design of various hypar shell geometries. In cases where the linear approach yields a lower value of failure pressure compared to the nonlinear one, the easily implementable linear analysis may be recommended to be used. In fact, in practical design a factor of safety to the tune of 1.5 to 2.0 is applied on the failure load to obtain the working load values. Keeping this in mind the author may suggest a relaxation that even in cases where the failure pressure through linear analysis is not more than 5% of the nonlinear failure pressure, the linear approach is practically acceptable. Based on this logic the author proposes Table 9.5 which furnishes the preferred analysis approach that may be adopted for getting FPF pressure values considering the shell combinations taken up here. Hence, a practical recommendation on the design approach of analysis is suggested here in Table 9.5 for ready reference to the engineers. The table shows that the linear approach of analysis may be used for CFFC shells while for CFCF shells the geometrically nonlinear analysis must be adopted.

Table 9.5 Recommendation on design approaches

Lamination	Boundary condition	
	CFCF	CFFC
ASCP	Geometric nonlinear	Geometric linear
SYCP	Geometric nonlinear	Geometric linear
ASAP	Geometric nonlinear	Geometric linear
SYAP	Geometric nonlinear	Geometric linear

9.3 CONCLUDING REMARKS

The following conclusions are evident from the present investigation.

- The close agreement of the present results with the published ones as observed from the benchmark problems establishes the accuracy of the computer code used in this program.
- The Puck and maximum strain criteria may be recommended as the governing failure criteria for evaluation of uniformly distributed FPF pressures for almost all cases of CFCF and CFFC edge conditions respectively.
- The uniformly distributed FPF pressures of cross ply shells are significantly more than those of angle ply shells and among cross ply shells again the antisymmetric lamination turns out to be the best choice.
- CFFC shell options shall be preferred to be used compared to CFCF shell options in high seismic zones as the former yield higher ratios of collapse FPF pressure to the pressure corresponding to the permissible deflection.
- The linear approach of analysis may be used for prediction of uniformly distributed FPF pressure for CFFC shell options while for CFCF shells the geometrically nonlinear approach of analysis must be adopted for accurate prediction of FPF pressure.
- The failure behaviour of skewed hypar shells under non-uniform loads which may or may not be horizontal will be an interesting point for future studies.

Chapter 10

SCOPE FOR FUTURE RESEARCH

In the present research work, the author uses the geometrically linear and nonlinear strains to investigate the first ply and progressive failure of laminated composite thin skew plate and skewed hypar shell roofs. Despite the fact that the precise scope of current study is described in Chapter 3, the work is not claimed to be comprehensive in all respects. Several other areas where future research can be extended to and are still untouched and unattended have become obvious as a result of the literature analysis and the present research process. The following are some of the areas.

The frequency degradation at various stages of progressive failure can be studied considering geometric nonlinear strains. One may study the effect of various combinations of boundary conditions on first ply and progressive failure loads of laminated composite plates and shell roofs of varying shapes and geometry. The present research mainly considers the effect of uniformly distributed pressure on first and progressive failure behaviour of laminated composites skew plates and skewed hypar shells. Likewise, the present work may be extended to considering a non-uniform distribution of vertical load - e.g. due to an asymmetric accumulation of snow which may lead to failure with different mechanisms. One may include a three-dimensional failure criterion such as the Hashin's failure equations to trace failure in a laminate. The recently proposed North-Western (NU-Daniel) theory may be considered to investigate the lamina yielding and failure for multiaxial stress. Plates and shell configurations with cut-outs and concentric or eccentric stiffeners have received less attention and thus failure studies on such combinations are to be explored. Future research may focus on smart composite

shells and functionally graded materials which have recently drawn attentions of many researchers.

The areas listed above are only illustrative and not exhaustive. A more thorough examination of the literature is likely to reveal a spectrum of other issues that need to be addressed but are yet to be worked on and reported.

Appendix

REFERENCES

1. Aagaah, M.R., Mahinfalah, M., Jazar, G.N., 2006, 'Natural frequencies of laminated composite plates using third order shear deformation theory', Composite Structures, Vol. 72 (2006), pp. 273-279.
2. Abel, J.F. and Billington, D. P., 1972, 'Stability analysis of cooling towers – A review of current methods', Shell Structures and Climatic Influences, Proceedings of International Association for Shell Structures Symposium, July, University of Calgary, Alberta, Canada.
3. Adali, S. and Cagdas, I.U., 2011, 'Failure analysis of curved composite panels based on first-ply and buckling failures', Procedia Engineering, Vol. 10, pp. 1591-1596.
4. Ahmad, S., Irons, B. M. and Zienkiewicz, O. C., 1970, 'Analysis of thick and thin shell structures of curved finite elements', International Journal Numerical Methods in Engineering, Vol. 2, pp. 419-450.
5. Aksu, T., 1997, 'A finite element formulation for free vibration analysis of shells of general shape', Computers and Structures, Vol. 65, No. 5, pp. 687-694.
6. Ambartsumyan, S.A., 1953, 'Calculation of laminated anisotropic shells', Izvestiia Akademiia Nauk Armenskoi SSR, Ser. Fiz. Mat. Est. Tekh. Nauk., Vol. 6, No. 3, pp. 15.
7. Anish, Kumar, A. and Chakrabarti, A., 2019, 'Failure mode analysis of laminated composite sandwich plate', Engineering Failure Analysis, Vol. 104(2019), pp. 950-976.

8. Apeland, K., and Popov, E. P., September 1961, ‘Analysis of bending stresses in translational shells’, Proceedings of the Colloquim on Simplified calculation methods, Brussels, pp. 9-43.
9. Aron, H., 1874, ‘Das Gleichgewitcht und die Bewegund einer underlich dunner, beliebig, gekrummten, elastischen Schale’, J. fur reine und ang. Math., 78.
10. Anyfantis, K.N., and Tsouvalis, N.G., 2012, ‘Post buckling progressive failure analysis of composite laminated stiffened panels’, Applied Composite Material, Vol. 19 (2010), pp. 219-236.
11. Baharlou, B. and Leissa, A.W., 1987, ‘Vibration and buckling of generally laminated composite plates with arbitrary edge conditions’, International Journal of Mechanical Sciences, Vol. 29(8), pp. 545-555.
12. Bakshi, K. and Chakravorty, D., 2012, ‘Delamination and first ply failure study of composite conoidal shells’, Bonfring International Journal of Industrial Engineering and Management Science, Vol. 4, pp. 21-26.
13. Bakshi, K. and Chakravorty, D., 2013, ‘First ply failure study of composite conoidal shells used as roofing units in civil engineering’, Journal of Failure Analysis and Prevention, Vol. 13, No. 5, pp. 624-633.
14. Bakshi, K. and Chakravorty, D., 2014a, ‘First ply failure study of thin composite conoidal shells subjected to uniformly distributed loading’, Thin Walled Structures, Vol. 76, pp. 1-7.
15. Bakshi, K. and Chakravorty, D., 2014b, ‘Geometrically linear and nonlinear first ply failure loads of composite cylindrical shells’, ASCE Journal of Engineering Mechanics, Vol. 140, No. 12.

16. Bakshi, K. and Chakravorty, D., 2015, ‘First ply failure loads of composite conoidal shell roofs with varying lamination’, Mechanics of Advanced Materials and Structures, Vol. 22, pp. 978-987.
17. Bakshi, K. and Chakravorty, D., 2020, ‘Numerical study of thin composite conoidal shell roofs considering geometric nonlinearity’, KSCE Journal of Civil Engineering, Vol. 24(3), pp. 913-921.
18. Bakshi, K., 2021, ‘A numerical study on nonlinear vibrations of laminated composite singly curved stiffened shells’, Composite Structures, Vol. 278(114718), pp. 1-11.
19. Bandyopadhyay, J. N. and Ray, D. P., 1971-72, ‘Reinforced concrete hyperbolic paraboloid and cylindrical shells, Part-I, behavior of hyperbolic paraboloid shells in elastic and ultimate ranges’, Proceedings of Indian Society of Theoretical and Applied Mechanics, Allahabad, pp. 117-127.
20. Bandyopadhyay, J. N., 2000, ‘Thin shell structures- classical and modern analysis’, first ed., New Age International (P) Ltd., New Delhi.
21. Beltrami, E., 1881, ‘Sullequilibrio delle super ficite flessibilied in esterdibill’, Mem R. Acad. Sci. di Bologna.
22. Benveniste, Y. and Aboudi, J., 1975, ‘The dynamic response of a laminated plate under large deformations’, Journal of Sound and Vibration, Vol. 38(4), pp. 425-436.
23. Bert, C.W. and Kumar, M., 1982, ‘Vibration of cylindrical shells of bimodulus composite materials’, Journal of Sound and Vibration, Vol. 81, No.1, pp. 107-121.
24. Bert, C.W. and Reddy, V.S., 1982, ‘Cylindrical shells of bimodulus material’ Journal of Engineering Mechanics Division, ASCE, Vol. 8, No. EM 5, pp. 675-688.
25. Bhar, A., Phoenix, S.S. and Satsangi, S.K., 2010, ‘Finite element analysis of laminated composite stiffened plates using FSDT and HSDT: A comparative perspective’ Composite Structures, Vol. 92, pp. 312-321.

26. Bhaskar, K. and Varadan, T. K., 1993, ‘Interlaminar stresses in composite cylindrical shells under transient loads’, Journal of Sound and Vibration, Vol. 168, No.3, pp. 469-477.
27. Biswas, D. and Ray, C., 2019, ‘Effect of hybridisation in laminated composites on the first ply failure behaviour: Experimental and numerical studies’, International Journal of Mechanical Sciences, Vol. 161-162(2019), pp. 1-26.
28. Bogetti, T.A., Staniszewski, J., Burns, B.P., Hoppel, C.P.R., Jr Gillespie, J.W. and Tierney, J., 2012, ‘Predicting the nonlinear response and progressive failure of composite laminates under triaxial loading: Correlation with the experimental results’, Journal of Composite Materials, Vol. 46(19-20), pp. 2443-2459.
29. Burton, W. S. and Noor, A. K., 1995, ‘Assessment of computational models for sandwich panels and shells’, Computer Methods in Applied Mechanics and Engineering, Vol. 124, pp. 125-151.
30. Bongard, W., 1959, ‘Zurtheorite and berechnung von scalentragwerken in form gleichseltiger hyparbolischer paraboloide’, Bautechnik-Archiv, Vol. 15.
31. Brebbia, C. A., 1966, ‘An experimental and theoretical investigation into hyperbolic paraboloid shells’, University of Southampton, Civil Engineering, Report No. CE/2/66.
32. Brebbia, C. A. and Hadid, H. A., 1971, ‘Analysis of plates and shells using rectangular curved elements’, University of Southampton Civil Engineering, Report No. CE/5/71.
33. Budiansky, B. and Sanders, J.L., 1963, ‘On the best first-order linear shell theory’, Progress in Applied Mechanics, The Prager Anniversary Volume, Macmillan, pp. 129-140.

34. Cagdus, A.U. and Adali, S., 2013, 'Effect of fibre orientation on buckling and first ply failures of cylindrical shear deformable laminates', Journal of Engineering Mechanics, Vol. 139(8), pp. 967-978.
35. Chakravorty, D., Bandyopadhyay, J. N. and Sinha, P.K., 1995a, 'Free vibration analysis of point-supported laminated composite doubly curved shells – a finite element approach', Computers and Structures, Vol. 54, No. 2, pp. 191-198.
36. Chakravorty, D., Bandyopadhyay, J. N. and Sinha, P.K., 1995b, 'Finite element free vibration analysis of conoidal shells', Computers and Structures, Vol. 56, No. 6, pp. 975-978.
37. Chakravorty, D., Bandyopadhyay, J. N. and Sinha, P. K., 1996, 'Finite element free vibration analysis of doubly curved laminated composite shells', Journal of Sound and Vibration, Vol. 191, No. 4, pp. 491-504.
38. Chandrashekhara, K., 2001, 'Theory of plates', Universities Press, Hyderabad.
39. Chandrashekhara, K., 1989, 'Free vibrations of anisotropic laminated doubly curved shells', Computers and Structures, Vol. 33, No. 1-3, pp. 435-440.
40. Chandra, R. and Raju Basava, B., 1975a, 'Large amplitude flexural vibration of cross ply laminated composite plates', Fibre Science and Technology, Vol. 8, pp. 243-263.
41. Chandra, R. and Raju Basava, B., 1975b, 'Large deflection vibration of angle ply laminated plates', Journal of Sound and Vibration, Vol. 40(3), pp. 243-263.
42. Chang, J.S. and Huang, Y.P., 1991, 'Geometrically nonlinear static and transiently dynamic behavior of laminated composite plates based on a higher order displacement field ', Composite Structures, Vol. 18(1991), pp. 327-364.
43. Chang, R.R. and Chiang, T.H., 2010, 'Theoretical and experimental predictions of first ply failure of a laminated composite elevated floor plate', Proceedings IMECH E: Journal of Process Mechanical Engineering, Vol. 224(E), pp. 233-245.

44. Chang, R.R., 2000, ‘Experimental and theoretical analyses of first-ply failure of laminated composite pressure vessels ’, Composite Structures, Vol. 49(2000), pp. 237-243.
45. Chao, C.C. and Tung, T.P., 1989, ‘Step presence and blast response of clamped orthotropic hemispherical shells’, International Journal of Impact Engineering, Vol. 8, No. 3, pp. 191-207.
46. Chatterjee, D., Ghosh, A. and Chakravorty, D., 2021a, ‘First ply behaviour of laminated composite skew plates of various edge conditions’, Mechanics of Composite Materials, Vol. 57, No. 5, pp. 699-716.
47. Chatterjee, D., Ghosh, A. and Chakravorty, D., 2021b, ‘Nonlinear first ply failure study of laminated composite skew plates’, Materials Today: Proceedings, Vol. 45, No. P6, pp. 4925-4930.
48. Chatterjee, D., Ghosh, A. and Chakravorty, D., 2021c, ‘Finite element prediction of first ply failure loads of composite thin skewed hypar shells using nonlinear strains’, Thin-Walled Structures, Vol. 167(108159), pp. 1-13.
49. Chen, W.C. and Liu, W.H., 1990, ‘Deflections and free vibrations of laminated plates-Levy-type solutions’, International Journal of Mechanical Sciences, Vol. 32(9), pp. 779-793.
50. Chen, J.K. and Sun, C.T., 1985 a, ‘Nonlinear transient responses of initially stressed composite plates’, Computers and Structures, Vol. 21(3), pp. 513-520.
51. Chen, J.K. and Sun, C.T., 1985 b, ‘Dynamic large deflection response of composite laminates subjected to impact’, Composite Structures, Vol. 4(1985), pp. 59-73.
52. Chen, L.W. and Yang, J.Y., 1990, ‘Dynamic stability of laminated composite plates by the finite element method’, Computers and Structures, Vol. 36(5), pp. 845-851.

53. Chen, J., Dawe, D.J. and Wang, S., 2000, ‘Nonlinear transient analysis of rectangular composite laminated plates’, Composite Structures, Vol. 38 (2000), pp. 53-77.
54. Chetty, S. K. M. and Tottenham, H., 1964, ‘An investigation into the bending analysis of hyperbolic paraboloid shells’, Indian Concrete Journal, Vol. 38, pp.248-158.
55. Cheung, M.S., Akhras, G. and Li, W., 1995, ‘Progressive failure analysis of composite plates by the finite strip method’, Computer Methods in Applied Mechanics and Engineering, Vol. 124(1995), pp. 49-61.
56. Chia, C. Y. and Chia, D. S., 1992, ‘Nonlinear vibration of moderately thick antisymmetric angle-ply shallow spherical shell’, Computers and Structures, Vol. 44, No. 4, pp. 797-805.
57. Choi, C. K. and Schnobrich, W. C., 1970, ‘Finite element analysis of translation shells’, University of Illinois, Structural Research No. 368.
58. Chróścielewski J., Sabik, A., Sobczyk, B. and Witkowski, W., 2016, ‘Nonlinear FEM 2D failure onset prediction of composite shells based on 6-parameter shell theory’, Thin – Walled Structures, Vol. 105, pp. 207-219.
59. Coelho, A. M. G., Mottram, J. T. and Harries, K. A., 2015, ‘Finite element guidelines for simulation of fibre – tension dominated failures in composite materials validated by case studies’, Composite Structures, Vol. 126, pp. 299-313.
60. Coleby, J. R. and Majumdar, 1982, ‘Vibrations of simply supported shallow shells on elliptical bases’, Journal of Applied Mechanics, Transactions of ASME, Vol. 49, pp. 227-229.
61. Connor, J. J. and Brebbia, C. A., 1967, ‘Stiffness matrix for shallow rectangular shell element’, Journal of Engineering Mechanics Division, Proceedings of ASCE, Vol. 93, No. 5, pp. 43-66.

62. Crossland, J. A. and Dickinson, S.M., 1997, 'The free vibration of thin rectangular planform shallow shells with slits', Journal of Sound and Vibration, Vol. 199, No. 3, pp. 513-521.

63. Dai, K.Y., Liu, G.R., Lim, K.M. and Chen, X.L., 2004, 'A mesh free method for static and free vibration analysis of shear deformable laminated composite plates', Journal of Sound and Vibration, Vol. 269 (2004), pp. 633-652.

64. Das, D., Sahoo, P. and Saha, K., 2008, 'Large amplitude dynamic analysis of simply supported skew plates by a variational method', Journal of Sound and Vibration, Vol. 313, pp. 246-267.

65. Das, H.S. and Chakravorty, D., 2010, 'Bending analysis of stiffened composite conoidal shell roofs through finite element application', Journal of Composite Materials, Vol. 45(5), pp. 525-542.

66. Dash, P. and Singh, B.N., 2010, 'Geometrically nonlinear bending analysis of laminated composite plate', Communication in Nonlinear Science and Numerical Simulation, Vol. 15 (2010), pp. 3170-3181.

67. Dash, P. and Singh, B.N., 2012, 'Buckling and post buckling of laminated composite plates', Mechanics Research Communications, Vol. 46 (2012), pp. 1-7.

68. Dey, A., Bandyopadhyay, J. N. and Sinha, P. K., 1994, 'Behaviour of paraboloid of revolution shell using cross-ply and anti-symmetric angle-ply laminates', Computers and Structures, Vol. 52, No.6, pp. 1301-1308.

69. Dhatt, G. S., 1970, 'An efficient triangular finite element', AIAA Journal Vol. 8, No. 11, pp. 2100-2102.

70. Dong, S. B., 1968, 'Free vibrations of laminated orthotropic cylindrical shells', Journal of Acoustic Society, America, Vol. 44, No. 6, pp. 1628-1635.

71. Dong, S. B., Pister, K. S., and Taylor, R.L., 1962, ‘On the theory of laminated anisotropic shells and plates’, Journal of Aerospace Sciences, Vol. 29, pp. 969-975.
72. Donnell, L. H., 1933, ‘Stability of thin walled tubes in torsion’, NACA Report 479.
73. Dulaska, E., 1969, ‘Vibration and stability of anisotropic shallow shells’, Acta Tech., Vol. 65, No. 3/4 pp. 225-260.
74. Dym, C.L., 1974, ‘Introduction to the theory of shells’, Pergamon Press.
75. Ellul, B., Camilleri, D. and Betts, J.C., 2014, ‘A progressive failure analysis applied to fibre reinforced composite plates subject to out of plane bending’, Mechanics of Composite Materials, Vol. 49 (6), pp. 605- 620.
76. Ergatoudis, I., Irons, B. M. and Zienkiewicz, O. C., 1968, ‘Curved isoparametric quadrilateral elements for finite element analysis’, International Journal of Solids and Structures, Vol. 4, pp. 31-42.
77. Ferreira, G.F.O., Jr. Almeda, J.H.S., Ribeiro, M.L., Ferreira, A.J.M. and Tita, V., 2022, ‘A finite element unified formulation for composite laminates in bending considering progressive damage’, Thin Walled Structures, Vol. 172, pp. 1-13.
78. Fischer, L., 1960, ‘Determination of membrane stresses on elliptic paraboloid using polynomials’, Journal of American Concrete Institute, Vol. 32, No. 4, pp. 433-441.
79. Flügge, W. and Conrad, D. A., 1956, ‘Singular solution in the theory of shallow shells’, Tech. Report No. 101, Division of Engineering Mechanics, Stanford University.
80. Flügge, W. and Geyling, F. T., 1957, ‘A general theory of deformation of membrane shells’, International Association for Bridge and Structural Engineering, Vol. 17, pp. 23.

81. Falcó, O., Lopes, C.S., Sommer, D.E., Thomson, D., Ávila, R.L. and Tijs, B.H.A.H., 2022, 'Experimental analysis and simulation of low velocity impact damage of composite laminates', Composite Structures, Vol. 287, pp.1-9.
82. Falkowicz, K., Ferdynus, M. and Rozylo, P., 2021, 'Experimental and numerical analysis of stability and failure of compressed composite plates', Composite Structures, Vol. 263, pp.1-8.
83. Falkowicz, K., 2023, 'Experimental and numerical failure analysis of thin-walled composite plates using progressive failure analysis', Composite Structures, Vol. 305, 116474.
84. Ganapathi, M., Vardan, T. K. and Balamurugan, V., 1994, 'Dynamic instability of laminated composite curved panels using finite element method', Computers and Structures, Vol. 53, No. 2, pp. 335-342.
85. Ganeshan, R. and Liu, D.Y., 2008, 'Progressive failure and post buckling response of tapered composite plates under uniaxial compression', Composite Structures, Vol. 82 (2008), pp. 159-176.
86. Gallagher, R.H., 1969, 'Analysis of plate and shell structures – applications of finite element method in engineering', Vanderbilt University, ASCE Publication.
87. Gautham, B. P. and Ganesan, N., 1997, 'Free vibration characteristics of isotropic and laminated orthotropic spherical caps', Journal of Sound and Vibration, Vol. 204, No. 1, pp. 17-40.
88. Ge, X., Zhang, P., Zhao, F., Liu, M.,Liu, J. and Cheng, Y., 2022, 'Experimental and numerical investigations on the dynamic response of woven carbon fibre reinforced thick composite laminates under low velocity impact', Composite Structures, Vol. 279, pp. 1-41.

89. Gendy, A. S., Saleeb, A. F. and Mikhail, S. N., 1997, ‘Free vibrations and stability analysis of laminated composite plates and shells with hybrid/mixed formulation’, Computers and Structures, Vol. 63, No. 6, pp. 1149-1163.
90. Gergely, P., 1972, ‘Buckling of orthotropic hyperbolic paraboloid shells’, Journal of Structural Division, Proceedings of ASCE, Vol. 98, No. ST1, pp. 613-699.
91. Ghannadpour, S.A.M. and Abdollazadeh, N., 2021, ‘Progressive failure analysis of thick imperfect composite plates using nonlinear plate theory’, International Journal of Nonlinear Mechanics, Vol. 121 (2020), pp. 1-28.
92. Ghosh, B. and Bandyopadhyay, J.N., 1989, ‘Bending analysis of conoidal shells using curved quadratic isoparametric element’, Computers and Structures, Vol. 33, No. 3, pp. 717-728.
93. Ghosh, A. and Chakravorty, D., 2014, ‘Prediction of progressive failure behavior of composite skewed hypar shells using finite element method’, Journal of Structures, Vol. 2014, pp. 1-8.
94. Ghosh, A. and Chakravorty, D., 2018 a, ‘First ply failure analysis of laminated composite thin hypar shells using nonlinear finite element approach’, Thin-Walled Structures, Vol. 131, pp. 736-745.
95. Ghosh, A. and Chakravorty, D., 2018 b, ‘Nonlinear first ply failure analysis of composite skewed hypar shells using FEM, Structural Engineering and Mechanics, Vol. 68(1), pp. 81-94.
96. Giri, J. and Simitses, G.J., 1980, ‘Deflection response of general laminated composite plates to in-plane and transverse loads’, Fibre Science and Technology, Vol. 13, pp. 225-242.
97. Grafton, P. E. and Strome, D. R., 1963, ‘Analysis of axi-symmetric shells by the direct stiffness method’, AIAA Journal, Vol. 1, pp. 2342-2347.

98. Greene, B.E., Strome, D. R. and Weikel, R.C., 1961, ‘Application of the stiffness method of analysis of shell structures’, Proceedings Aviation Conference of ASME, Los Angeles, C.A.

99. Gohari, S., Sharifi, S., Vrcelj, Z. and Yahya, M.Y., 2015, ‘First-ply failure prediction of an unsymmetrical laminated ellipsoidal woven GFRP composite shell with incorporated surface-bounded sensor and internally pressurized’, Composites Part B , Vol. 77 (2015), pp. 502-518.

100. Goldenveizer, A. L., 1968, ‘Method for justifying and refining the theory of shells’, Applied Mathematics and Mechanics (Translation of Prikl. Mat. Mekh.), Vol. 32, pp. 704-718.

101. Gould, P.L., 1999, ‘Analysis of shells and plates’, Prentice Hall, New Jersey.

102. Gulati, S.T. and Essenberg, F., 1967, ‘Effects of anisotropy in axi-symmetric cylindrical shells’, Journal of Applied Mechanics, Vol. 34, pp. 650-666.

103. Gummadi, L.N.B. and Palazotto, A.N., 1998, ‘Progressive failure analysis of composite cylindrical shells considering large rotations’, Composites Part B, Vol. 29 B (1998), pp. 547-563.

104. Gupta, A. K., Patel, B. P. and Nath, Y., 2012, ‘Continuum damage mechanics approach to composite laminated shallow cylindrical/conical panels under static loading’, Composite Structures, Vol. 94, No. 5, pp. 1703-1713.

105. Gupta, A. K., Patel, B. P. and Nath, Y., 2013, ‘Nonlinear static analysis of composite laminated plates with evolving damage’, Acta Mechanica, Vol. 224, No. 6, pp. 1285-1298.

106. Gupta, A. K., Patel, B. P. and Nath, Y., 2015, ‘Progressive damage of laminated cylindrical/conical panels under meridional compression’, European Journal of Mechanics A/Solids, Vol. 53, pp. 329-341.

107. Gupta, A. and Pradyumna, S., 2022, ‘Geometrically nonlinear dynamic analysis of variable stiffness composite laminated and sandwich shell panels’, Thin-Walled Structures, Vol. 173, pp. 109021

108. Gurses, M., Civalek, O., Korkmaz, A.K. and Ersoy, H., 2009, ‘Finite element dynamic stability analysis of laminated composite skew plates containing cutouts based on HSDT’, Composite Science and Technology, Vol. 70, pp. 1249-1257.

109. Hildebrand, F. B., 1949, ‘Notes on the foundations of the theory of small displacements of orthotropic shells,’ NACA

110. Hochard, Ch., Payan, J., and Bordreuil, C., 2006, ‘A progressive first ply failure model for woven ply CFRP laminates under static and fatigue loads’, International Journal of Fatigue, Vol. 28(2006), pp. 1270-1276.

111. Hoppmann II, W.H., 1961, ‘Frequencies of vibration of shallow spherical shells’, Journal of Applied Mechanics, Transactions of ASME, Vol. 28, pp. 306-307.

112. Hu, C., Sang, L., Jiang, K., Xing, J., and Hou, W., 2022, ‘Experimental and numerical characterization of flexural properties and failure behaviour of CFRP/Al laminates’, Composite Structures, Vol. 281, pp. 1-7.

113. Hu, H.T. and Tzeng, W.L., 2000, ‘Buckling analysis of skew laminate plates subjected to uniaxial inplane loads’, Thin-Walled Structures, Vol. 38 (2000), pp. 53-77.

114. Hu, H.T, Yang, C.H., Lin, F.M., 2006, ‘Buckling analyses of composite laminate skew plates with material nonlinearity’, Composite Part B, Vol. 37 (2006), pp. 26-36.

115. Huang, J.H. and Shukla, K.K., 2005, ‘Post- buckling of cross-ply laminated rectangular plates containing short random fibers’, Composite Structures, Vol. 68 (2005), pp. 255-265.

116. Hussainy, S.A. and Srinivas, S., 1974, ‘Flexure of rectangular composite plates’, Fibre Science and Technology, Vol. 8, pp. 59-76.

117. Hwang, D. Y. and Foster Jr., W. A., 1992, ‘Analysis of axi-symmetric free vibration of isotropic shallow spherical shells with a circular hole’, Journal of Sound and Vibration, Vol. 157, No. 2, pp. 331-343.

118. Iyengar, K.T.S. and Srinivasan, R. S., 1967, ‘Clamped skew plate under uniform normal loading’, Journal of Royal Aeronautical Society, Vol. 71(674), pp. 139-140.

119. Iyengar, K.T.S. and Srinivasan, R. S., 1968, ‘Bending analysis of hyperbolic paraboloid shells’, The Structural Engineer, Vol. 46, No. 12, pp. 397-401.

120. Jing, H-S and Teng, K-G., 1995, ‘Analysis of thick laminated anisotropic cylindrical shells using a refined shell theory’, International Journal of Solids and Structures, Vol. 32, No. 10, pp. 1459-1476.

121. Johnson, M. W., and Reissner, E., 1958, ‘On transverse vibrations of shallow spherical shells’, Quarterly of Applied Mathematics, Vol. 15, No. 4, pp. 365-380.

122. Jr. Knight, N.F., Rankin, C.C. and Brogan, F.A., 2002, ‘STAGS computational procedure for progressive failure analysis of laminated composite structures’, International Journal of Nonlinear Mechanics, Vol. 37(2002), pp. 833-849.

123. Joshi, R. and Duggal, S.K., 2020, ‘Free vibration analysis of laminated composite plates during progressive failure’, European Journal of Mechanics/ A solids, Vol. 83 (2020), pp. 1-13.

124. Kalnins, A. and Naghdi, P. M., 1960, ‘Axi-symmetric vibrations of shallow elastic spherical shells’, Journal of Acoustic Society, America, Vol. 32, pp. 342-347.

125. Kam, T.Y. and Lai, F.M., 1999, ‘Experimental and theoretical predictions of first ply failure strength of laminated composite plates’, International Journal of Solids and Structures, Vol. 36, pp. 2379-2395.

126. Kam, T.Y., Sher, H.F., Chao, T.N. and Chang, R.R., 1996, 'Predictions of deflection and first-ply failure load of thin laminated composite plates via the finite element approach', International Journal of Solids and Structures, Vol. 33, pp. 375-398. https://doi.org/10.1016/0020-7683(95)00042-9.

127. Kant, T., Kumar, S. and Singh, U. P., 1994, 'Shell dynamics with three-dimensional degenerate finite elements', Computers and Structures, Vol. 50, No. 1, pp. 135-146.

128. Kant, T. and Swaminathan, K., 2002, 'Analytical solutions for the static analysis of laminated composite and sandwich plates based on a higher order refined theory', Composite Structures, Vol. 56 (2002), pp. 329-344.

129. Kapania, R. K. and Raciti, S., 1989 a, 'Recent advances in analysis of laminated beams and plates part I: shear effects and buckling', AIAA Journal, Vol. 27, No. 7, pp. 923-934.

130. Kapania, R. K. and Raciti, S., 1989 b, 'Recent advances in analysis of laminated beams and plates part II: vibration and wave propagation', AIAA Journal, Vol. 27, No. 7, pp. 935-946.

131. Karsh, P.K., Mukhopadhyay, T. and Dey, S., 2018, 'Spatial vulnerability analysis for the first ply failure strength of composite laminates including effect of delamination', Composite Structures, Vol. 184 (2018), pp. 554-567.

132. Kelly, G. and Hallstrom, S., 2005, 'Spatial vulnerability analysis for the first ply failure strength of composite laminates including effect of delamination', Composite Structures, Vol. 184 (2018), pp. 554-567.

133. Kermanidis, T.B. and Labeas, G.N., 1995, 'Static and stability analysis of composite plates by a semi-analytical method ', Computers and Structures, Vol. 57(4), pp. 673-679.

134. Khatri, K. N. and Asnani, N. T., 1996, 'Vibration and damping analysis of fibre reinforced composite material conical shells', Journal of Sound and Vibration, Vol. 193, No. 3, pp. 581-595.

135. Kharghani, N., and Guedes Soares, C., 2019, 'Analytical and experimental study of the ultimate strength of delaminated composite laminates under compressive loading', Composite Structures, Vol. 228 (2019), pp. 1-18.

136. Kirchhoff, G., 1876, 'Vor elesungen Uber Mathematische Physik', Vol. 1, Mechanik.

137. Koiter, W.T., 1960, 'A consistent first-approximation in the general theory of thin elastic shells', Proc. Symposium on Theory of Thin Elastic Shells, IUTAM Delft, 24-28, Aug. 1953, North Holland Publishing Co., Amsterdam, pp. 12-33.

138. Kolli, M. and Chandrashekhara, K., 1997, 'Nonlinear static and dynamic analysis of stiffened laminated plates', International Journal of Nonlinear Mechanics, Vol. 32(1), pp.89-101.

139. Kouchakzadeh, M.A. and Sekine, H., 2000, 'Compressive buckling analysis of rectangular composite laminates containing multiple delaminations', Composite Structures, Vol. 50 (2000), pp. 249-255.

140. Kraus, H., 1967, 'Thin elastic shells', Wiley, New York.

141. Kumar, A., Chakrabarty, A., Bhargava, P. and Prakash, V., 2015, 'Efficient failure analysis of laminated composites and sandwich cylindrical shells based on higher-order zigzag theory', Journal of Aerospace Engineering, Vol. 28 (4), pp. 1-14.

142. Kumar, A., Chakrabarty, A., 2017, 'Failure analysis of laminated composite skew laminates', Procedia Engineering, Vol. 173, pp. 1560-1566.

143. Kumar, Y.V.S. and Srivastava, A., 2003, 'First ply failure analysis of laminated stiffened plates', Composite Structures, Vol. 60, pp. 307-315

144. Lai, S.K., Zhou, L., Zhang, Y.Y. and Xiang, Y., 2011, 'Application of DSC element method to flexural vibration of skew plates with continuous and discontinuous boundaries', Thin Walled Structures, Vol. 49, pp. 1080-1090.

145. Lal, A., Singh, B.N. and Patel, D., 2012, 'Stochastic nonlinear failure analysis of laminated composite plates under compressive transverse loading', Composite Structures, Vol. 94(2012), pp. 1211-1223.

146. Lakshminarayana, H. V. and Viswanath, S., 1976, 'A high precision triangular laminated anisotropic cylindrical shell finite element', Computers and Structures, Vol. 8, pp. 633-640.

147. Lame, G. and Clapeyron, B.P.E., 1833, 'Memoire Sur I'equilibre interieur des corps solids', Mem. Pres. Par. Div. Savants 4.

148. Laxminarayana, A., Vijayakumar, R. and Rao, G.K., 2016, 'Progressive failure analysis of laminated composite plates with elliptical or circular cutouts using finite element method', IOP Conference Series: Material Science and Engineering, Vol. 149, pp. 1-14.

149. Lee, J.D., 1982, 'Three-dimensional finite element analysis of damage accumulation in composite laminate', Computer Structures, Vol. 15, pp. 335-350.

150. Lee, S.Y., 2010, 'Finite element dynamic stability analysis of laminated composite skew plates containing cutouts based on HSDT', Composites Science and Technology, Vol. 70 (2010), pp. 1249-1257.

151. Leissa, A.W., Lee, J.K. and Wang, A.J., 1981, 'Vibrations of cantilevered shallow cylindrical shells of rectangular planform', Journal of Sound and Vibration, Vol. 78, No. 3, pp. 311-328.

152. Leissa, A.W., Lee, J.K. and Wang, A.J., 1983, ‘Vibrations of cantilevered doubly-curved shallow shells’, International Journal of Solids and Structures, Vol. 19, No. 5, pp. 411-424.

153. Li, H., Yu, Z., Tao, Z. and Liu, K., 2023, ‘Experimental investigations on the repeated low velocity impact and compression-after-impact behaviours of woven glass fiber reinforced composite laminates’, Polymer Composites, https://doi.org/10.1002/pc.27896

154. Librescu, L. and Stein, M., 1991, ‘A geometrically nonlinear theory of transversely isotropic laminated composite plates and its use in the post buckling analysis’, Thin-Walled Structures, Vol. 11(1991), pp. 177-201.

155. Liew, K. M. and Lim, C. W., 1994, ‘Vibration of perforated doubly curved shallow shells with rounded corners’, International Journal of Solids and Structures, Vol. 31, No. 11, pp. 1519-1536.

156. Lim, C. W. and Liew, K. M., 1995, ‘A higher order theory for vibration of shear deformable cylindrical shallow shells’, International Journal of Mechanical Sciences, Vol. 37, No. 3, pp. 277-295.

157. Lin, S.C., Kam, T.Y. and Chu, K.H., 1998, ‘Evaluation of buckling and first ply failure probabilities of composite laminates ’, International Journal of Solids Structures, Vol. 35(13), pp. 1395-1410.

158. Lin, S.C., 2000, ‘Buckling failure analysis of random composite laminates subjected to random loads’, International Journal of Solids and Structures, Vol. 37 (2000), pp. 7563-7576.

159. Liu, T., Li, Z.M., Qiao, P. and Jin, S., 2021, ‘A novel C1 continuity finite element based on Mindlin theory for doubly curved laminated composite shells’, Thin Walled Structures, Vol. 167, pp. 1-14.

160. Liu, B., Wang, W. and Sutherland, L., 2023, ‘Experimental and numerical response and failure of laterally impacted of carbon/glass fibre-reinforced hybrid composite laminates’, International Journal of Impact Engineering, Vol. 179, 104654.

161. Lopes, C.S., Camanho, P.P., Gurdal, Z. and Tatting, B.F., 2007, ‘Progressive failure analysis of tow-placed, variable stiffness composite panels’, International Journal of Solids and Structures, Vol. 44 (2007), pp. 8493-8516.

162. Lopes, C.S., Gurdal, Z. and Camanho, P.P., 2008, ‘Variable-stiffness composite panels: Buckling and first-ply failure improvements over straight fibre laminates’, Computers and Structures, Vol. 86(2008), pp. 897-907.

163. Love, A.E.H., 1888, ‘On the small free vibrations and deformations of thin elastic shells’, Phil. Trans. Royal Society, 179(A).

164. Lu, X. and Guo, X.M., 2022, ‘An interactive orthotropic non-local damage model for progressive failure analysis of composite laminates’, Composite Structures, Vol. 295, 115841.

165. Mahdy, W.M., Zhao, L., Liu, F., Pian, R., Wang, H. and Zhang, J., 2021, ‘Buckling and stress- competitive failure analyses of composite laminated cylindrical shell under axial compression and torsional loads’, Composite Structures, Vol. 255, pp. 1-8.

166. Malekzadeh, P., 2008, ‘Differential quadrature large amplitude free vibration analysis of laminated skew plates based on FSDT’, Composite Structure, Vol. 83 (2008), pp. 189-200.

167. Marguerre, K., 1938, ‘Zurtheorie der gekrummten platte grossen formanderung’, Proceedings of Fifth International Congress of Applied Mechanics.

168. Michael Spottswood, S. and Palazotto, A.N., 2001, ‘Progressive failure analysis of a composite shell’, Composite Structures, Vol. 53 (2001), pp. 117-131.

169. Mizusawa, T. and Kito, H., 1995, ‘Vibration of antisymmetric angle-ply laminated cylindrical panels by the spline finite strip method’, Computers and Structures, Vol. 56, No.4, pp. 589-604.

170. Mohd, S. and Dawe, D. J., 1993, ‘Finite strip vibration analysis of composite prismatic shell structures with diaphragm ends’, Computers and Structures, Vol. 49, No. 5, pp. 753-765.

171. Mohammadrezazadeh S. and Jafari, A.A., 2021, ‘Nonlinear vibration analysis of laminated composite angle ply cylindrical and conical shells’, Composite Structures, Vol. 255, pp. 1-13.

172. Mondal, S., and Ramachandra, L.S., 2018, ‘Stability and failure analyses of delaminated composite plates subjected to localized heating’, Composite Structures, Vol. 209 (2017), pp. 258-267.

173. Mukherjee, A., 1991, ‘Free vibration of laminated plates using a high order element’, Computers and Structures, Vol. 40(6), pp. 1387-1393.

174. Mukhopadhyay, M. and Sheikh, A.H., 2004, ‘Matrix and finite element analyses of structures’, Anne books pvt. Limited.

175. Munro, J., 1961, ‘The linear analysis of thin shallow shells’, The Institute of Civil Engineering, Proceedings, Vol. 19, pp. 291-306.

176. Nanda, N. and Bandyopadhyay, J.N., 2009, ‘Geometrically nonlinear transient analysis of laminated composite shells using the finite element method’, Journal of Sound and Vibration, Vol. 325, pp. 174-185.

177. Nazarov, A. A., 1949 (English Translation in NASA TN 1426, 1956), ‘On the theory of thin shells’, Prikl. Mat. Mek., Vol. 13, pp. 547-550.

178. Noor, A.K. and Burton, W.S., 1989, ‘Assessment of shear deformation theories for multilayered composite plates’, Applied Mechanics Reviews, Vol. 42, No. 1, pp. 1-12.

179. Noor, A.K. and Burton, W.S., 1990, ‘Assessment of computational models for multi-layered composite shells’, Applied Mechanics Reviews, Vol. 43, No. 4, pp. 67-97.

180. Olson, M.D. and Lindberg, G. M., 1968, ‘Vibration analysis of cantilevered curved-plates using a new cylindrical shell finite element’, Proceedings 2nd Conference on Matrix Methods Structural Mechanics, AFFDL-TR-68-150, pp. 247-270.

181. Potluri, R. and Rao, S., 2019, ‘Buckling analysis of thin FRP cross ply laminated composite panel with circular cutout subjected to transverse compressive loading’, Materials Today: Proceedings, Vol. 18, pp.375-383.

182. Reinoso, J. and Blázquez, A., 2016, ‘Application and finite element implementation of 7-parameter shell element for geometrically nonlinear analysis of layered CFRP composites’, Composite Structures, Vol. 139, pp. 263-276.

183. Wang, C. T., 1953, ‘Applied elasticity’, McGraw-Hill Book Company, New York.

184. Martinez, J.R. and Bishay, P.L., 2021, ‘On the stochastic first ply failure analysis of laminated composite plates under in plane tensile loading’, Composites Part C, Vol. 4 (2021), pp. 1-15.

185. Naghdi, P.M., 1963, ‘Foundations of elastic shell theory’, Progress in Solid Mechanics, Vol. IV, North Holland Publishing Co., Amsterdam.

186. Naghsh, A. and Azhari, M., 2014, ‘Nonlinear free vibration analysis of point supported laminated composite skew plates ’, International Journal of Nonlinear Mechanics, Vol. 15 (2014), pp. 1-46.

187. Nagaraj, M.H., Carrera, E. and Petrolo, M., 2020, 'Progressive damage analysis of composite laminates subjected to low-velocity impact using 2D layer-wise structural models', International Journal of Non Linear Mechanics, Vol. 127 (2020), pp. 1-9.

188. Namdar, O. and Darendeliler, H., 2017, 'Buckling, postbuckling and progressive failure analyses of composite laminated plates under compressive loading', Composites Part B, Vol. 120 (6), pp. 143-151.

189. Narita, Y. and Leissa, A.W., 1984, 'Vibrations of corner supported shallow shells of rectangular planform', Earthquake Engineering and Structural Dynamics, Vol. 12, pp. 651-661.

190. Narwariya, M., Sharma, A.K., Patidar, V. and Chauhan, P.S., 2019, 'Harmonic analysis of symmetric and antisymmetric laminated skew plate using finite element method', IOP Conference Series: Material Science and Engineering, Vol. 691, pp. 1-12.

191. Novozhilov, V.V., and Radok, J.M.R., 1964, 'Thin shell theory', Springer.

192. Onkar, A.K., Upadhyay, C.S. and Yadav, D., 2007, 'Probabilistic failure of laminated composite plates using the stochastic finite element method', Composite Structures, Vol. 77 (2007), pp. 79-91.

193. Owen, D.R.J and Li, Z.H., 1987a, 'A refined analysis of laminated plates by finite element displacement methods-I. Fundamentals and static analysis', Computers and Structures, Vol. 26(6), pp. 907-914.

194. Owen, D.R.J and Li, Z.H., 1987b, 'A refined analysis of laminated plates by finite element displacement methods-II. Vibration and Stability', Computers and Structures, Vol. 26(6), pp. 915-923.

195. Palazotto, A.N. and Dennis, S.T., 1992, 'Nonlinear analysis of shell structures. AIAA Education Series', American Institute of Aeronautics and Astronautics (AIAA), Washington, DC, (1992), pp. 195-232.

196. Padhi, G.S., Shenoi, R.A., Moi, S.S.J. and Hawkins, G.L., 1998, 'Progressive failure and ultimate collapse of laminated composite plates in bending', Composite Structures, Vol. 40(3-4), pp. 277-291.

197. Pal, P. and Bhattacharyya, S.K., 2007, 'Progressive failure analysis of cross ply laminated composite plates by finite element method', Journal of Reinforced Plastics and composites, Vol. 26 (5), pp. 465-477.

198. Parme, A. L., 1956, 'Hyperbolic paraboloid and other shells of double curvatures', Journal of Structural Division, Proceedings of ASCE, Vol. 82, No. ST5, pp. 1057-1m to 32.

199. Pavan, G.S. and Nanjunda Rao, K.S., 2017, 'Bending analysis of laminated composite plates using isogeometric collocation method ', Composite Structures, Vol. 17 (2017), pp. 1-40.

200. Petit, P.H., and Waddoups, M.E., 1969, 'A Method of Predicting the Nonlinear Behavior of Laminated Composites," Journal of Composite Material, Vol. 3, No. 1, pp. 2-19.

201. Pica, A., Wood, R.D. and Hinton, E., 1980, 'Finite element analysis of geometrically nonlinear plate behavior using a Mindlin formulation', Computers and Structures, Vol. 11, pp. 203-215.

202. Piskunov, V. G., Verijenko, V. E., Adali, S. and Tabakov, P. Y., 1994, 'Transverse shear and normal deformation higher-order theory for the solution of dynamic problems of laminated plates and shells', Computers and Structures, Vol. 31, No. 24, pp. 3345-3374.

203. Priyadharshani, S. A., Prasad A. M. and Sundaravadivelu R., 2017, 'Analysis of GFRP stiffened composite plates with rectangular cutout', Composite Structures, Vol. 169, pp. 42-51.

204. Provan, J. W. and Koeller, R. C., 1970, 'On the theory of elastic plates', International Journal Solids Structures, Vol. 6, pp. 993-950.

205. Prusty, B.G., 2005, 'Progressive failure analysis of laminated unstiffened and stiffened composite panels', Journal of Reinforced Plastics and Composites, Vol. 24(6), pp. 633-642.

206. Prusty, B.G., Satsangi, S.K. and Ray, C., 2001a, 'First ply failure analysis of laminated panels under transverse loading', Journal of Reinforced Plastics and Composites, Vol. 20(8), pp. 671-684.

207. Prusty, B.G., Ray, C. and Satsangi, S.K., 2001b, 'First ply failure analysis of stiffened panels- a finite element approach', Composite Structures, Vol. 51(2001), pp. 73-81.

208. Qatu, M.S., 1989, 'Free vibration and static analysis of laminated composite shallow shells', Ph.D. Dissertation, Ohio State Univ.

209. Qatu, M. S. and Leissa, A. W., 1991a, 'Natural frequencies for cantilevered doubly-curved laminated composite shallow shells', Computers and Structures, Vol. 17, No.3, pp. 227-256.

210. Qatu, M. S. and Leissa, A. W., 1991b, 'Vibration studies for laminated composite twisted cantilever plates', International Journal of Mechanical Sciences, Vol. 33, No. 11, pp. 927-940.

211. Qatu, M. S., 1992, 'Review of shallow shell vibration research', Shock and Vibration Digest, Vol. 24, No.9, pp. 3-15.

212. Qatu, M. S. and Leissa, A. W., 1993, 'Vibrations of shallow shells with two adjacent edges clamped and others free', Journal of Mechanics of Structural Machines, Vol. 21, No. 3, pp. 285-301.

213. Qatu, M. S., 1996, 'Vibration analysis of cantilevered shallow shells with triangular and trapezoidal planforms', Journal of Sound and Vibration, Vol. 191, No. 2, pp. 219-231.

214. Ramaswamy, G. S. and Rao, K., 1961, 'The membrane theory applied to hyperbolic paraboloid shells', Indian Concrete Journal, Vol. 35, pp. 156-171.

215. Ramaswamy, G. S., 1971, 'Design and construction of concrete shell roofs', Tata McGraw-Hill, New Delhi.

216. Rao, K.P., 1978, 'A rectangular laminated anisotropic shallow thin shell finite element', Computer Methods in Applied Mechanics and Engineering, Vol. 15, pp. 13-33.

217. Reddy, J. N. and Chao, W. C., 1981, 'Large deflection and large amplitude free vibrations of laminated composite material plates', Computers and Structures, Vol. 13, No. 1-3, pp. 341-347.

218. Reddy, J.N., 1999, 'Theory and analysis of elastic plates', Taylor and Francis, Philadelphia.

219. Reddy, J.N., 2004, 'Mechanics of laminated composite plates and shells', 2nd. ed., CRC Press, Boca Raton.

220. Reddy, J. N., 1984, 'Exact solutions of moderately thick laminated shells', Journal of Engineering Mechanics, Vol. 110, No. 5, pp. 794-809.

221. Reddy, J.N. and Chao, W.C., 1980, 'Finite element analysis of laminated bimodulus composite material plates', Computers and Structures, Vol. 12, pp. 245-251.

222. Reddy, J.N. and Pandey, A.K., 1987, 'A first ply failure analysis of composite laminates', Computers and Structures, Vol. 25(3), pp. 371-393.

223. Reddy, Y.S.N. and Reddy, J. N., 1992, 'Linear and nonlinear failure analysis of composite laminates with transverse shear', Composite Science and Technology, Vol. 44(1992), pp. 227-255.

224. Reddy, Y.S.N., Dakshina Moorthy, C.M. and Reddy, J. N., 1995, 'Nonlinear progressive failure analysis of laminated composite plates', International Journal of Nonlinear Mechanics, Vol. 30(5), pp. 629-649.

225. Reisman, H. and Culowski, P. M., 1968, 'Forced axi-symmetric motion of shallow spherical shells', Journal of Engineering Mechanics Division, Vol. 94, pp. 653-670.

226. Reissner, E., 1946, 'On vibrations of shallow spherical shells', Journal of Applied Physics, Vol. 17, pp. 1038-1042.

227. Reissner, E., 1955, 'On transverse vibrations of thin shallow elastic shells', Quarterly of Applied Mathematics, Vol. 13, pp. 169-176.

228. Russel, R. R. and Gerstle, K. H., 1967, 'Bending of hyperbolic paraboloid structures', Journal of Structural Division, Proceedings of ASCE, Vol. 93, No. ST3, pp. 181-199.

229. Russel, R. R. and Gerstle, K. H., 1968, 'Hyperbolic paraboloid structures on four supports', Journal of Structural Division, Proceedings of ASCE., Vol. 94, No. ST4.

230. Sabik, A., 2018, 'Progressive failure analysis of laminates in the framework of 6 field nonlinear shell theory', Composite Structure, Vol. 200 (2018), pp. 195-203.

231. Sadek, E.A., 1998, 'Some serendipity finite elements for the analysis of laminated plates ', Computers and Structures, Vol. 69(1998), pp. 37-51.

232. Sanders, J.L.(Jr.), 1959, 'An improved first approximation theory for thin shells, NASA TR-R24

233. Sathyamoorthy, M., 1994, ‘Vibrations of moderately thick shallow spherical shells at large amplitudes’, Journal of Sound and Vibration, Vol. 172, No. 1, pp. 63-70.

234. Sathyamoorthy, M., 1995, ‘Nonlinear vibrations of moderately thick orthotropic shallow spherical shells’, Computers and Structures, Vol. 57, No. 1, pp. 59-65.

235. Sathyamoorthy, M. and Chia, C.Y., 1980, ‘Nonlinear vibration of anisotropic rectangular plates including shear and rotary inertia’, Fibre Science and Technology, Vol. 13, pp. 337-361.

236. Schokker, A., Sridharan, S. and Kasagi, A., 1996, ‘Dynamic buckling of composite shells’, Computers and Structures, Vol. 59, No. 1, pp. 43-53.

237. Satish Kumar, Y.V. and Srivastava, A., 2003, ‘First ply failure analysis of laminated stiffened plates’, Composite Structures, Vol. 60, pp. 307-315.

238. Serna Moreno, M.C., Romero Gutiérrez, A. and Martínez Vicente, J.L., 2016, ‘First flexural and interlaminar shear failure in symmetric cross ply carbon fibre laminates with different response under tension and compression’, Composite Structures, Vol. 146(2016), pp. 62-68.

239. Sheikh, A.H., Haldar, S. and Sengupta, D., 2002, ‘A high precision shear deformable element for the analysis of laminated composite plates of different shapes’, Composite Structures, Vol. 55 (2002), pp. 329-336.

240. Sheinman, I. and Reichman, Y., 1992, ‘A study of buckling and vibration of laminated shallow curved panels’, International Journal Solids and Structures, Vol. 29, No. 11, pp. 1329-1338.

241. Shin, D. K., 1997, ‘Large amplitude free vibration behaviour of doubly curved shallow open shells with simply-supported edges’, Computers and Structures, Vol. 62, No. 1, pp. 35-49.

242. Singh, G. and Sadasiva Rao, Y.V.K., 1987, ‘Large deflection behavior of thick composite plates’, Composite Structures, Vol. 8, pp. 13-29.

243. Sinha, L., Mishra, S.S, Nayak, A.N. and Sahu, S.K., 2020, ‘Free vibration characteristics of laminated composite stiffened plates: Experimental and numerical investigation’, Composite Structures, Vol. 233, pp. 1-40.

244. Singha, M.K. and Ganapathy, M., 2004, ‘Large amplitude free flexural vibrations of laminated composite skew plates’, International Journal of Nonlinear Mechanics, Vol. 39 (2004), pp. 1709-1720.

245. Singha, M.K. and Daripa, R., 2007, ‘Nonlinear vibration of symmetrically laminated composite skew plates by finite element method’, International Journal of Nonlinear Mechanics, Vol. 42, pp. 1144-1152.

246. Sivasubramonian, B., Kulkarni, A. M., Rao, G. V. and Krishnan, A., 1997, ‘Free vibration of curved panels with cutouts’, Journal of Sound and Vibration, Vol. 200, No. 2, pp. 227-234.

247. Soare, M., 1966, ‘A numerical approach to the bending theory of hyperbolic shells – 1 and 2’, Indian Concrete Journal, pp. 63-69 and pp. 113-119.

248. Sridhar, C. and Rao, K.P., 1995, ‘Large deformation finite element analysis of laminated circular composite plates’, Computers and Structures, Vol. 54(1), pp. 59-64.

249. Srinivas, S., Joga Rao, C.V. and Rao, A. K., 1970 a, ‘An exact analysis for vibration of simply supported homogenous and laminated thick rectangular plates’, Journal of Sound and Vibration, Vol. 12(2), pp. 187-199.

250. Srinivas, S. and Rao, A. K., 1970 b, ‘Bending, vibration and buckling of simply supported thick orthotropic rectangular plates and laminates’, International Journal Solids Structures, Vol. 6, pp. 1463-1481.

251. Srinivasa, C. V., Suresh, Y.J. and Prema Kumar, W. P., 2014, 'Experimental and finite element studies on free vibration of skew plates', International Journal of Advanced Structural Engineering, Vol. 6 (48), pp. 1-11.

252. Srinivasa, C. V., Suresh, Y.J. and Prema Kumar, W. P., 2012, 'Free flexural vibration studies on laminated composite skew plates', International Journal of Engineering, Science and Technology, Vol. 4 (4), pp. 13-24.

253. Srinivasan, R.S. and Munaswamy, K., 1975, 'Frequency analysis of skew orthotropic point support plates', Journal of Sound and Vibration, Vol. 39(2), pp. 207-216.

254. Stavsky, Y., 1963, 'Thermoelasticity of heterogeneous aelotropic plates', Journal of Engineering Mechanics Division, ASCE, Vol. 89, No. EM2, pp. 89-105.

255. Sundara Raja Iyenger, K.T. and Srinivasan, R.S., 1967, 'Clamped skew plate under uniform normal loading', Journal of the Royal Aeronautical Society, Vol. 71(3), pp. 139-140.

256. Suzuki, K., Shikanai, G. and Leissa, A.W., 1996, 'Free vibrations of laminated composite non-circular thick cylindrical shells', International Journal of Solids and Structures, Vol. 33, No. 27, pp. 4079-4100.

257. Tanriover, H. and Senocak, E., 2004, 'Large deflection analysis of unsymmetrically laminated composite plates: analytical-numerical type approach', International Journal of Nonlinear Mechanics, Vol. 39 (2004), pp. 1385-1392.

258. Taetragool, U., Shah, P.H., Halls, V.A., Zheng, J.Q. and Batra, R.C., 2017, 'Stacking sequence optimization for maximizing the first failure initiation load followed by progressive failure analysis until the ultimate load', Composite Structures, Vol. 180 (2017), pp. 1007-1021.

259. Tessler, A., Tsui, T. and Saether, E., 1995, 'A(1,2) – order theory for elasto dynamic analysis of thick orthotropic shells', Computers and Structures, Vol. 32, No. 22. pp. 3237-3260.

260. Thakur, B.R., Verma, S., Singh, B.N. and Maiti, D.K., 2020, 'Dynamic analysis of folded laminated composite plate using nonpolynomial shear deformation theory ', Aerospace Science and Technology, Vol. 106, pp. 1-20.

261. Timoshenko, S.P., and Woinowsky - Krieger, S., 1959, 'Theory of plates and shells', 2nd. ed., McGraw-Hill, New York.

262. Tolson, S. and Zabaras, N., 1991, 'Finite element analysis of progressive failure in laminated composite plates', Computers and Structures, Vol. 38 (3), pp. 361-376.

263. Touratier, M., 1992, 'A refined theory of laminated shallow shells', International Journal of Solids and Structures, Vol. 29, No. 11, pp. 1401-1415.

264. Tsai, C. T. and Palazotto, A. N., 1991, 'On the finite element analysis of non-linear vibration for cylindrical shells with high order shear deformation theory', International Journal of Non-linear Mechanics, Vol. 26, No. 3/4, pp. 379-388.

265. Upadhyay, A.K. and Shukla, K.K., 2012, 'Large deformation flexural behavior of laminated composite skew plates: An analytical approach ', Composite Structures, Vol. 94 (2012), pp. 3722-3735.

266. Vinson, J. R. and Sierakowski, R. L., 1986, 'The behaviour of structures composed of composite materials', Nijhoff, The Hague, Springer Netherlands.

267. Vlasov, V.Z., 1958, 'Allegemeine Schalen theorie und ihre anwendung in dar technik', Akademie-Verlag GmBH, Berlin.

268. Vlasov, V.Z., 1947, 'Membrane theory of thin shells formed by second order surfaces', Prikl. Mat. Mekh., Akademiya Nauk., S.S.S.R., XI, 4.

269. Vlasov, V.Z., 1964, ‘General theory of shells and its application in engineering’, English translation of 1949 Russian Edition, NASA, USA, No. N64-19883.

270. Wang, Y.Y., Lam, K.Y. and Liu, G.R., 2000, ‘The effect of rotary inertia on the dynamic response of laminated composite plate’, Composite Structures, Vol. 48(2000), pp.265-273.

271. Wang, S., 1997, ‘Free vibration analysis of skew fibre-reinforced composite laminates based on first order shear deformation plate theory’, Computers and Structures, Vol. 63(3), pp. 525-538.

272. Wang, J. and Schweizerhof, K., 1997, ‘Free vibration of laminated anisotropic shallow shells including transverse shear deformation by the boundary-domain element method’, Computers and Structures, Vol. 62, No. 1, pp. 151-156.

273. Wang, X. Jia, P. and Wang, B., 2022, ‘Progressive failure model of high strength glass fibre composite structure in hygrothermal environment’, Composite Structure, Vol. 280, pp. 1-8.

274. Whitney, J. M. and Sun, C. T., 1973, ‘A higher order theory for extensional motion of laminated isotropic shells and plates’, Journal of Sound and Vibration, Vol. 30, pp. 85.

275. Whitney, J. M. and Sun, C.T., 1974, ‘A refined theory for laminated anisotropic cylindrical shells’, Journal of Applied Mechanics, Vol. 41, pp. 471-476.

276. Widera, G.E.O. and Chung, S.W., 1970, ‘A theory for non-homogeneous isotropic cylindrical shells’, Journal of Applied Mathematics and Physics (JAMP), Vol. 21, pp. 378-399,.

277. Widera, G.E.O. and Logan, D.L., 1980, ‘Refined theories for non-homogeneous anisotropic cylindrical shells: Part I – Derivation’, Journal of Engineering Mechanics Division, ASCE, Vol. 106, No. EM6, pp. 1053-1074.

278. Witt, M. and Sobczyk, K., 1980, ‘Dynamic response of laminated plates to random loading’, International Journal of Solids and Structures, Vol. 16, pp. 231-238.

279. Xiang-Sheng, C., 1985, ‘Forced vibrations of elastic shallow shells due to moving loads’, Applied Mathematics and Mechanics, Vol. 6, No. 3, pp. 233-240.

280. Xiao-ping, S., 1996, ‘An improved simple higher-order theory for laminated composite shells’, Computers and Structures, Vol. 60, No. 3, pp. 343-350.

281. Xie, F., Liu, T. and Wang, Q.S., 2019, ‘Free vibration analysis of parallelogram laminated thin plates under multipoints supported elastic boundary conditions’, Thin Walled Structures, Vol. 144, pp. 1-13.

282. Xu, Y., Jung, J., Nojavan, S. and Yang, Q., 2019, ‘An orthotropic augmented finite element method (A-FEM) for high-fidelity progressive damage analyses of laminated composites’, Composite Structures, Vol. 229 (2019), pp. 1-19.

283. Ye, Z. and Han, R. P. S., 1995, ‘On the nonlinear analysis of orthotropic shallow shells of revolution’, Computers and Structures, Vol. 55, No. 2, pp. 325-331.

284. Ye, Jianqiao and Soldatos, K. P., 1995, ‘Three dimensional buckling analysis of laminated composite hollow cylinders and cylindrical panels’, International Journal of Solids and Structures, Vol. 32, No. 13, pp. 1949-1962.

285. Yuan, Y., Yao, X., Liu, B.,Yang, H. and Imtiaz, H., 2017, ‘Failure modes and strength prediction of thin ply CFRP angle-ply laminates’, Composite Structures, Vol. 176 (2017), pp. 729-735.

286. Zahari, R. and Zafrany, A.E., 2009, ‘ Progressive failure analysis of composite laminated stiffened plates using finite strip method’, Composite Structures, Vol. 87, pp. 63-70.

287. Zhang, Y., Zhu, P. and Lai, X., 2006, 'Finite element analysis of low velocity impact damage in composite laminated plates', Materials and Design, Vol. 27 (2006), pp. 513-519.

288. Zhang, X., Wang, S. and Zhang, Y., 2010, 'Stress and failure analysis of laminated composites based on layerwise B-spline finite strip method', Composite Structures, Vol. 92 (2010), pp. 3020-3030.

289. Zukas, J. A. and Vinson, J. R., 1971, 'Laminated transversely isotropic cylindrical shells', Journal of Applied Mechanics, Vol. 38, pp. 400-407.

****

Dona Chatterjee
18.06.2024